Aus der II. Medizinische Klinik
der Medizinischen Fakultät Mannheim
(Direktor: Prof. Dr. med. Matthias Ebert)

FXR and FOXA2 govern two complementary regulatory mechanisms to maintain apical BSEP expression in hepatocytes

Inauguraldissertation
zur Erlangung des Doctor scientiarum humanarun (Dr. sc. hum)
der
Medizinischen Fakultät Mannheim
der Ruprecht-Karls-Universität
zu
Heidelberg

vorgelegt von
Sai Wang

aus
Shandong, China
2020

Dekan: Prof. Dr. med. Sergij Goerdt

Referent: Prof. Dr. rer. nat. Steven Dooley

CONTENTS

Page

LIST OF ABRREVIATIONS.....1

1 INTRODUCTION.....4

1.1 Bile acid metabolism..... 4

1.1.1 Bile acid synthesis..... 4

1.1.2 Bile canaliculi..... 6

1.1.3 Bile acid transport and enterohepatic circulation..... 9

1.1.4 Regulation of bile acid synthesis 10

1.2 Bile salt export pump (BSEP)..... 11

1.2.1 Structure and function of BSEP..... 11

1.2.2 Localization of BSEP..... 12

1.2.3 transcription regulation of BSEP..... 12

1.2.4 BSEP mutations and diseases..... 13

1.3 FXR: the nuclear farnesoid X receptor..... 13

1.3.1 FXR in bile acid homeostasis..... 14

1.3.2 Role of FXR in regulating hepatocyte membrane transporters..... 14

1.3.3 FXR in glucose metabolism..... 16

1.4 Acute on chronic liver failure..... 17

1.4.1 Pathophysiology of systemic inflammation in ACLF..... 17

1.4.2 Glucose homeostasis in ACLF..... 18

1.4.3 FXR in ACLF 19
1.4.4 Cholestasis in ACLF 20
1.5 Foxa2: Forkhead box protein A2 20
1.5.1 Structure and activity of Foxa2 20
1.5.2 Foxa2 in liver development 21
1.5.3 Foxa2 in glucose metabolism 21
1.5.4 Foxa2 in bile acid regulation 22
1.6 Aims of this study 22

2 MATERIALS AND METHODS 23

2.1 Materials 23
2.1.1 Chemicals and reagents 23
2.1.2 Antibodies 24
2.1.3 Buffer preparation 26
2.1.4 Cell culture materials 29
2.1.5 Liver tissue apecimens of patients 30
2.1.6 Instruments and software 30

2.2 Methods 31
2.2.1 Cells and cell culture medium used in this study 31
2.2.2 Cell culture and treatment 31
2.2.3 Primary hepatocytes isolation from mice and patients 32
2.2.4 Collagen sandwich hepatocytes culture 33
2.2.5 RNA interference 33
2.2.6 Plasmid transfection 34
2.2.7 Cell protein extraction 34

2.2.8 Subcellular fraction 35
2.2.9 Protein concentration measurement 35
2.2.10 Western blot 35
2.2.11 mRNA isolation, cDNA synthesis and Realtime PCR 36
2.2.12 ChIP assay 38
2.2.13 immunofluorescence and confocal microscopy 39
2.2.14 Immunohistochemical staining 40

3 RESULTS 42

3.1 FXR determines BSEP expression in hepatocytes 42
3.1.1 In HBV patients, both FXR and BSEP are expressed in hepatocytes 42
3.1.2 Fxr promotes Bsep expression in AML12 cells and MPHs 42
3.1.3 Fxr knockdown reduces Bsep expression in AML12 cells and MPHs 44
3.2 Lack of BSEP is associated with high cholestasis and poor prognosis in ACLF patients 45
3.3 Hepatocytes of ACLF patients maintain BSEP on bile canaliculi regardless of FXR expression 47
3.4 FOXA2 expression in hepatocytes of ACLF patients 47
3.5 FOXA2 is required for BSEP expression in hepatocytes 49
3.5.1 FOXA2 overexpression promotes BSEP expression in hepatocytes 49
3.5.2 FOXA2 knockdown reduces BSEP expression in hepatocytes 50
3.6 Ectopic Foxa2 expression rescues Bsep expression on bile canaliculi when Fxr is disrupted in vitro 52
3.7 Ectopic Foxa2 expression restores Bsep expression in *fxr* knockout mice 55
3.7.1 Bsep expression is remarkably decreased in *fxr* knockout mice 55
3.7.2 Ectopic Foxa2 expression restores Bsep expression in primary hepatocytes of *fxr* knockout mice. 56

3.7.3 Ectopic Foxa2 expression restores Bsep expression in *fxr* knockout mice. 58

3.8 Foxa2 up-regulating bsep through binding to its prmoter 59

3.9 Balance between insulin and glucagon influences Foxa2-dependent Bsep expression 61

3.9.1 Glucagon induces Bsep expression through up-regulating Foxa2..... 61

3.9.2 Insulin inhibits Foxa2 activation via insulin-Akt signaling-mediated phosphorylation at Ther156 and nuclear exclusion 63

3.9.3 Glucagon restored insulin-mediated inhibition to Foxa2 and Bsep 64

3.10 Inflammation inhibits Fxr while induces Foxa2 in hepatocytes 65

3.10.1 TNFα and LPS induce Foxa2-dependent Bsep expression 65

3.10.2 TNFα administration induces insulin resistance in hepatocytes 67

3.10.3 LPS induces Foxa2-dependent bsep expression through NFκB signaling 68

3.10.4 High concentration of LPS induces Foxa2 nuclear exclusion 70

4 DISCUSSION 72

4.1 Significance of BSEP maintanence in hepatocytes of ACLF patients 72

4.2 FXR and FOXA2 in physiological condition or chronic liver disease 73

4.3 FXR and FOXA2 in ACLF..... 74

4.4 Clinical significance 76

5 SUMMARY 77

6 REFERENCES 79

7 LIST OF FIGURES AND TABLES 96

8 CURRICULUM VITAE 98

9 ACKNOWLEDGEMENT 100

LIST OF ABBREVIATIONS

°C	Celsius
ABC	ATP-binding cassette
ACLF	Acute-on-chronic liver failure
AF1	Activation function domain 1
AF2	Activation function domain 2
AKT	Protein kinase B
ASBT	Apical sodium-dependent bile salt transporter
BC	Bile canaliculi
BRIC2	Benign recurrent intrahepatic cholestasis type 2
BSA	Bovine serum albumin
BSEP	Bile salt export pump
CA	Cholic acid
CDCA	Chenodeoxycholic acid
CYP7A1	Cholesterol 7α-hydroxylase
CYP8B1	Cytpchrome P450 family 8 subfamily B member 1
DBD	DNA binding domain
DCA	Deoxycholic acid
DMEM	Dulbecco's modified eagle medium
DMSO	Dimethylsulfoxide
DNA	Deoxyribonucleic acid
FBS	Fetal bovine serum
FOXA1	Forkhead box protein A1
FOXA2	Forkhead box protein A2
FOXA3	Forkhead box protein A3
FXR	Farnesoid X receptor
GAPDH	Glyceraldehyde 3-phosphate dehydrogenase
GCA	Glycocholic acid
GSK3β	Glycogen synthase kinase 3β
HBV	Hepatitis B virus
HCC	Hepatocellular carcinoma
HNF4α	Hepatocyte nuclear factor 4α

HPH	Human primary hepatocytes
HRP	Horseradish peroxidase
I-BABP	Intestinal bile acid binding protein
IL	Interleukin
IRS-1	Insulin receptor substrate 1
IRS-2	Insulin receptor substrate 2
IST	Insulin-Transferrin-Selenium
JNK	c-Jun N-terminal kinase
kg	kilo gram
KO	Knockout
LBD	Ligand binding domain
LCA	Lithocholic acid
LM	lateral membrane
LPS	lipopolysaccharide
LRH-1	liver-related homologue-1
LTx	liver transplantation
M	Molar (mol/l)
MDR1	Multidrug resistance protein 1
MDR3	Multidrug resistance protein 3
MPH	Mouse primary hepatocytes
MRP2	Multidrug resistance-associated protein 2
NRF2	Nuclear erythroid 2 P45-regulated fator 2
NTCP	Na^+-taurocholate cotransporting polypeptide
OATPs	Organic-anion-transporting polypeptides
OST	Organic solute transporter
PBS	Phosphate buffered saline
PBC	Primary biliary cirrhosis
PCR	Polymerase chain reaction
PEPCK	Phosphoenolpyruvate carboxykinase
PFIC2	Progressive familial intrahepatic cholestasis type 2
PPIA	Peptidylprolyl isomerase A
PSC	Primary sclerosing cholangitis
RNA	Ribonucleic acid
RXR	Retinoid X receptor

SDS	Sodium dodecyl sulfate
siRNA	Small interfering RNA
SHP	Small heterodimer partner
shRNA	Short hairpin RNA
TBST	Tris buffered saline with Tween-20
TEMED	N,N,N´,N´-Tetramethylethylenediamine
TNF	Tumor necrotic factor
Tris	Tris (hydroxymethyl)-aminoethane
TUTCA	Tauroursodeoxycholic acid
WT	Wild type
ZO-1	Zonula occludens-1
ZO-2	Zonula occludens-2

1. INTRODUCTION

The liver is an organ with a wide range of physiological functions. One of its multiple functions is to produce, secrete and recycle bile, normally between 600 and 1000 ml/day. Bile has two important functions in fat digestion and absorption: (1) bile acids help to emulsify large fat particles in the food into many small particles, and (2) they aid in absorption of the digested fat end products through the intestinal mucosal membrane by making it soluble in water. In addition, bile serves as a means of excretion of water insoluble waste products from the blood, including drugs, xenobiotics, bilirubin, an end product of hemoglobin destruction, and excesses of cholesterol (John E. Hall. Guyton and Hall Textbook of Medical Physiology. 12th ed. 2011. ISBN: 978-1-4160-4574-8. International Edition: 978-0-8089-2400-5).

Bile is synthesized in hepatocytes and is secreted into the tiny canaliculi of the biliary tree through specific transporters on the apical membranes. Impairment of the delivery system leads to intrahepatic cholestasis, which impairs liver function and may even cause to hepatocyte death. To date, the detailed mechanisms of how mammals maintain bile synthesis and transport under conditions of severe liver stress remain largely unknown. The current study focuses on one aspect of these complex mechanisms: how is bile acid transporter maintained in a liver suffering from severe inflammation?

1.1 Bile acid metabolism

1.1.1 Bile acid synthesis

Bile acids are the end product of cholesterol catabolism (Russell and Setchell, 1992). In humans, the bile acids pool consists of primary bile acids cholic acid (CA) and chenodeoxycholic acid (CDCA), and the secondary bile acids deoxycholic acid (DCA), and lithocholic acid (LCA) (Vlahcevic et al., 1992). Primary bile acids are synthesized from cholesterol through two general pathways, the classic pathway and the alternative pathway (**Figure 1**) (Pikuleva et al., 1998; Vlahcevic et al., 1992). The classic pathway is responsible for more than 90% of the total bile acid production. Cholesterol 7α-hydroxylase (CYP7A1) catalyzes the first and rate-limiting step in the classic pathway (Myant and Mitropoulos, 1977). The intermediate product in the classic pathway 7α-hydroxy-4-cholestene-3-one serves as the common precursor for both CA and CDCA,

which can be hydroxylated at C-12 position by microsomal sterol 12α-hydroxylase (CYP8B1) and eventually be converted to CA. Without CYP8B1, 7α-hydroxy-4-cholestene-3-one is converted to CDCA. Thus, CYP7A1 controls the overall rate of bile acid production, while CYP8B1 controls the CA: CDCA ratio in the bile acid pool.

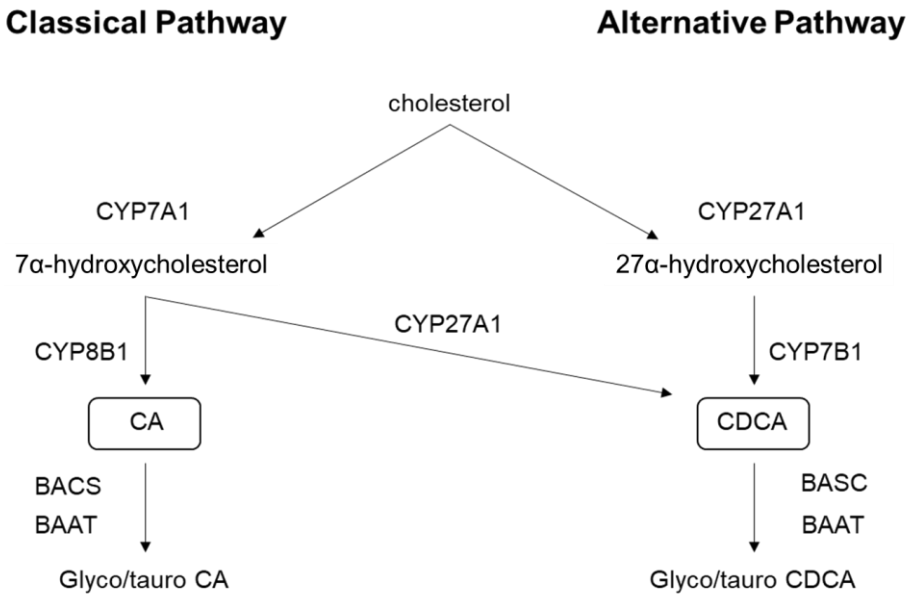

Figure 1. Classic and alternative pathways of bile acid synthesis. The human liver produces two primary bile acids, cholic acid (CA), and chenodeoxycholic acid (CDCA), are produced. Key regulatory enzymes in both pathways are shown. Microsomal cholesterol 7α-hydroxylase (CYP7A1) catalyzes the first the rate-limiting step in the classic pathway converting cholesterol into 7-hydroxycholesterol, whereas mitochondrial sterol 27-hydroxylase (CYP27A1) initiates the alternative pathway by converting cholesterol into 27-hydroxycholesterol, which is then 7-hydroxylated by microsomal oxysterol 7-hydroxylase (CYP7B1). CYP8B1 regulates cholic acid synthesis in the classic pathway.

1.1.2 Bile canaliculi

Bile canaliculi of hepatocytes are formed by extracellular matrix, adherens, tight junctions, cytoskeleton and apical plasma membranes with their microvilli. It is formed by adjoining apical membranes of two adjacent hepatocytes and is sealed by tight junction proteins zonula occludens ((Anderson, 1996)(**Figure 2A**). A freeze fracture replicas elegantly reveals a series of four to five cross-linked parallel strands inside the tight junction structure (**Figure 2B**). These strands are primarily composed of globular proteins occludins and claudins, which are connected to cytoskeletal proteins (ZO-1 and ZO-2) on the cytoplasmic side of the membrane (**Figure 2C**). Tight junctions hold the neighboring hepatocytes together and provide a barrier that prevents leakage of bile acids and other large solutes from bile, however, allow pass of small ions. Ca^{2+} is needed to maintain this seal.

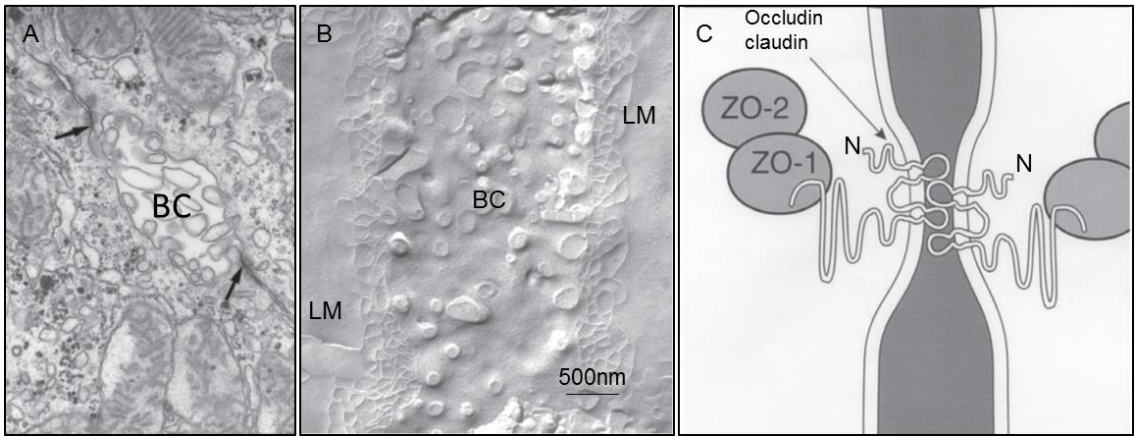

Figure 2. The hepatocyte tight junction complex (Boyer, 2013). (**A**) Electron microscopy depicts a bile canaliculus sealed by tight junctions (arrows). The lumen is filled by microvilli. (**B**) Freeze fracture replica of the bile canaliculus. The tight junctions elements represent the only anatomical barrier between bile and the intercellular space lined by the lateral membrane (LM) of the hepatocytes. (**C**) A schema showing that transmembrane proteins occludin and claudin form the tight junction seal, whereas zonula occluden proteins 1 and 2 (ZO-1 and ZO-2) are cytoplasmic proteins that serves as anchors for occludin.

Bile canaliculi are the location of multiple pivotal molecues involved in substance transport, including BSEP, MRP2, MDR1, NTCP, OATPs (**Figure 3**; **Table 1**) (Boyer J. 2013; Aleksandr Treyer et al.,2013). Maintaining these molecules on bile canaliculi requires intracellular protein trafficking machinery and energy production. The apical canalicular membrane surface area is amplified by microvilli where a number of transport proteins including members of the ATP-binding cassette (ABC) super family export various constituents from hepatocyte into the biliary tree (**Figure 3**).

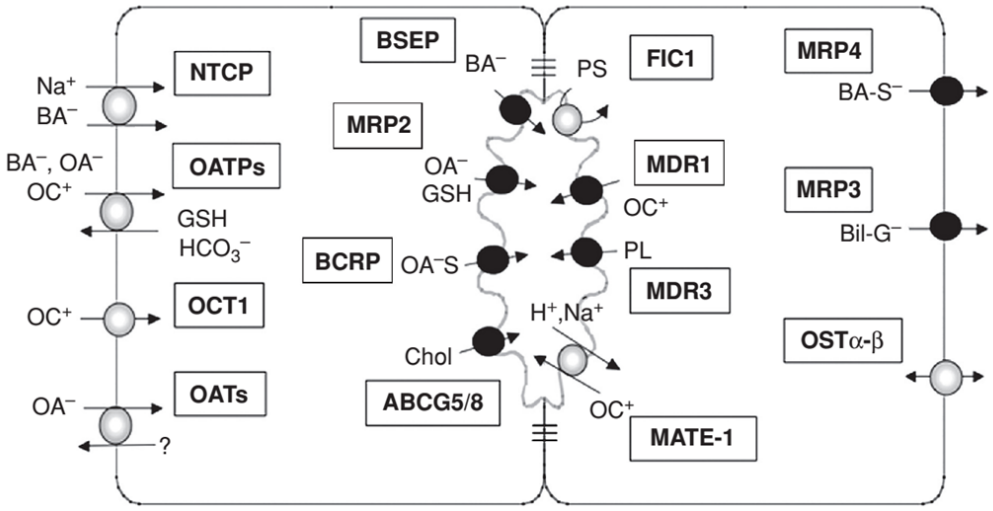

Figure 3. Membrane transporters in hepatocytes (Boyer J.2013)

Abbreviation	Name	Function
Basolaterally targeted and simusoidal membrane proteins		
NTCP	Sodium-taurocholate cotransporter	Principal carrier for bile salt uptake from portal vein
OATPs	Organic anion transporting proteins	Uptake of organic solutes from portal vein
OCT-1	Organic cation transporter-1	Uptake of small organic cations
OCT-2	Organic cation transporter-2	Uptake of drugs and prostaglandins
MRP6	Multidrug-resistance-associated protein-6	ATP-dependent transport of small peptides and organic anions
MRP3	Multidrug-resistance-associated protein-3	ATP-dependent transport of small peptides and organic
Na+/K+ATPase	Sodium-potassium ATPase	Pumps out Na+ and exchange for K+
NHE-1	Na+/H+-exchanger isoform1	Regulates intracellular pH
ASOR	Asialoglycoprotein receptor	Lectin that removes glycoprotein without sialic acid from the circulation via receptor-mediated endocytosis
pIgR	Polymeric immunoglobulin receptor	Transcellular transport of IgA and IgM from the bood into the bile
Tf-R	Transferrin receptor	Iron import via receptor-mediated endocytosis
LDL-R	Low-density lipoprotein receptor	Endocytosis of cholesterol-rich LDL
HA321	HA321	Lateral membrane protein of unknown functior
CE9/EMMPRIN/CD147	Rat CE-9, cluster of differentiation 147, EMMPR	Matrix metalloprotein inducer
Apical/limunal membrane proteins		
MDR1	Multidrug-resistance-1 P-glycoprotein	ATP-dependent excretion of organic cations, xenobiotics, and cytotoxins into bile
MDR3	Multidrug-resistance-3 Phospholipid transporter	Canalicular phospholipid flippase that mediates excretion of phospholipids
BSEP	Bile salt export pump/sister of P-glycoprotein	ATP-dependent bile salt transport into bile, stimulates bile salt-dependent bile flow
MRP2	Multidrug-resistance-associated protein 2	ATP-dependent multispecific organic anion transport (e.g., bilirubin and diglycoronide) into bile
BRCP	Breast cancer resistance protein	ATP-dependent multispecific drug transporter
ABCG5/G8	Sterolin-1/2	Heteromeric ATP-dependent cholesterol transporter
AE-2	Anion exchanger-2	Sodium-independent chloride-bicarbonate anion exchanger; generates hydroionic fluxes into secretion
MATE-1	Multidrug and toxin extrusion protein-1	Organic cation/H+ exchanger, excretes xenobiotics
HA4/cCAM105	Cell-cell adhesion molecule 105 kD	Homophilic cell-cell adhesion molecule and ecto-ATPase
DPPIV/CD26	Dipeptidyl peptidase IV	Ectopeptidase; regulates extracellular concentration of biologically active peptides, function at the BC not clear
APN/CD13	Amino peptidase N	Metallo exoprotease, function at BC not clear
LAP	Leucine aminopeptidase	Metallo exopeptidase, function at BC not clea
GGT	Gamma-glutamyltranspeptidase	gamma-glutamyl moiety to an acceptor; drug and xenobiotic detoxification, elevated in HCC and alcoholic liver disease
5'-NT	5′-ribonucleotide phosphohydrolase	GPI-anchored ectonucleotidase; catalyzes the hydrolysis of nucleotides; mediates extracellular adenosine formation from AMP in injured cells, which promotes fibrosis
ALP	Liver alkaline phosphatase	GPI-anchored ectophosphatase; dephosphorylates nucleotides, proteins, alkaloids

Table 1. List of selected membrane proteins targeted to either the canalicular or sinusoidal membrane of hepatocytes.

1.1.3 Bile acid transport and enterohepatic circulation

Once produced, bile acids are transported from hepatocytes to the bile canaliculi and stored in the gallbladder. After a meal, bile acids stored in the gallbladder are released into the intestinal tract to aid the digestion and absorption of fat. The remaining bile acids are absorbed by the ileum, transported back to the liver via portal blood and reabsorbed by hepatocytes. This process is defined as enterohepatic circulation of bile acids (**Figure 4**) (Chiang, 1998). Several ATP-binding cassette (ABC) transporters on the canalicular membranes of hepatocytes are responsible for transporting bile acids and other organic compounds into the bile canaliculus against a steep concentration gradients (**Table 1**) (Trauner and Boyer, 2003). The bile salt export pump (BSEP, ABCB11) is the exclusive transporter of bile acids (**Figure 5**) (Childs et al., 1995; Strautnieks et al., 1997). Phospholipids, mainly phosphatidylcholine, are excreted by the phospholipid flippase MDR2 (ABCB4) (**Figure 5**) (Smit et al., 1993). Biliary-free cholesterol secretion medicated by ABCG5/G8 transporters is an important route for hepatic cholesterol elimination (Langheim et al., 2005). Bile acids, phospholipids, and cholesterol are three major organic solutes of the bile. Once secreted, they form mixed micelles to increase cholesterol solubility and reduce their toxicity. Bile acids are conjugated with taurine or glycine in the peroxisomes and present as bile salts. Bile salts from intestine cannot cross the hepatocyte membrane and need special transporters for cellular uptake (Meier, 1995). Two bile acid transporters, Na^+-dependent taurocholate transporter (NTCP) (**Figure 5**) and organic anion transporter (OATPs) are in charge of bile acid transport into hepatocytes across the basolateral membrane (Trauner and Boyer, 2003). In the intestine, bile salts are deconjugated by bacterial 7α-dehydroxylase that converts CA and CDCA to DCA and LCA, respectively. These secondary bile acids are highly toxic. In the intestinal lumen, bile acids are re-absorbed mostly at the terminal ileum, mainly by the apical sodium-dependent bile salt transporter (ASBT) (**Figure 5**) (Shneider et al., 1995). Once absorbed into the enterocytes, bile acids bind the intestinal bile acid binding protein (I-BABP) and are transported to the basolateral membrane for secretion (Gong et al., 1994). Heterodimeric organic solute transporters OSTα and OSTβ are the major basolateral bile acid transporters in the intestine (**Figure 5**) (Dawson et al., 2005).

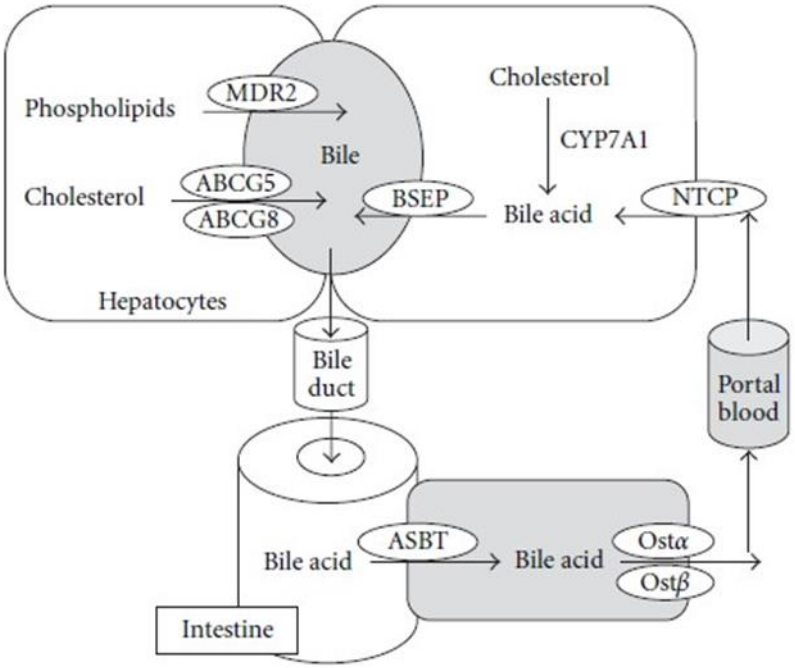

Figure 4. Enterohepatic circulation of the bile acids (Tiangang Li et al., 2011). Bile acids are synthesized from cholesterol in the hepatocytes. CYP7A1 performs the rate-limiting step in the classic bile acid biosynthetic pathway. Bile acids are secreted into the gallbladder by BSEP. Phospholipids are transported via MDR3 (MDR2 in mice), and cholesterol is transported by the ABCG5/G8 transporters into bile. In the canaliculi, bile acids, phospholipids, and cholesterol from mixed micelles to solubilize cholesterol and to reduce bile acid toxicity. After meal intake, gall bladder releases bile into the small intestine where bile acids facilitate the absorption of dietary lipids and vitamins. At the terminal ileum, most of the bile acids are reabsorbed by ASBT into the enterocytes, and secreted into the portal circulation via basolateral bile acid transporters Ostα/Ostβ. At the basolateral membrane of the hepatocytes, bile acids are taken up by the NTCP transporter for re-secretion into the gallbladder.

1.1.4 Regulation of bile acid synthesis

Bile acid synthesis is mainly performed by rate-limiting enzyme *CYP7A1*, which is regulated by bile acids via multiple nuclear receptors (Chiang, 2009). This bile acid feedback mechanism allows the liver to efficiently increase or decrease bile acid synthesis and thus to maintain bile acid homeostasis in responce to physiological alterations. Bile acid induced feedback inhibition of *CYP7A1* is mediated by the bile acid-activated nuclear receptor farnesoid X receptor (FXR) in both hepatocytes and enterocytes. Bile acid-dependent FXR expression induces another nuclear receptor small heterodimer partner (SHP), which interacts with and represses the transcriptional activator liver-related homologue-1 (LRH-1). Given that LRH-1 binds to the CYP7A1 gene promoter, its silencing by SHP inhibits CYP7A1 transcription (Goodwin et al., 2000). It is worth to note that FXR-SHP-LRH-1 cascade is not the only pathway

regulating CYP7A1 (Kerr et al., 2002; Wang et al., 2002). Nutrition directly regulates bile acid synthesis. In humans, CYP7A1 activity is increased postprandially and is decreased during fasting and at night (Galman et al., 2005). Bile acids are markedly elevated in sera of patients with normal glucose tolerance after an oral glucose challenge, but not in patients with impaired glucose tolerance (Shaham et al., 2008). In addition, insulin rapidly induces while glucagon represses CYP7A1 mRNA expression (Li et al., 2006). These data suggest that bile acid synthesis is closely associated with glucose metabolism.

1.2 The bile salt export pump (BSEP)

The bile salt export pump (BSEP, ABCB11), a member of the B subfamily of ABC transporters, is the primary transporter deliverying bile acids from hepatocytes to the biliary system, a rate-limiting step determining bile salt dependent bile flow, the enterohepatic circulation of bile acids, and the digestion of dietary fats. Mutations in BSEP lead to cholestatic diseases such as progressive familial intrahepatic cholestasis type2 (PFIC2), benign recurrent intrahepatic cholestasis type 2 (BRIC2), drug-induced cholestasis, and intrahepatic cholestasis of pregnancy.

1.2.1 Structure and function of BSEP

BSEP was first described in 1991. Nishida et al found an ATP dependent bile salt transporter in canalicular membrane vesicles (Nishida et al., 1991), which was confirmed by 3 other groups (Adachi et al., 1991; Muller et al., 1991; Stieger et al., 1992). Given its similarity to the multidrug resistance protein, P-glycoprotein (MDR1, *ABCB1*), it was named sister of P-glycoprotein (spgp). The full-length coding region was identified in 1998 in rat liver (Gerloff et al., 1998). It was named as the bile salt export pump (BSEP), encoded by ABCB11 gene. Human BSEP is a protein with a molecular weight of ~160kDa and consists of 1321 amino acids (Strautnieks et al., 1997). Mouse *Bsep* is located in a region of chromosome 2 syntenic to 2q24-31 (Lecureur et al., 2000). Rodent Bseps are ~80% identical to human BSEP (Cai et al., 2001). A molecular model of BSEP structure was proposed based on the crystal structure of the multidrug transporter of S. aureus, Sav1866 (Kubitz et al., 2012). Both the N- and C- terminal portions of the molecule are located to the cytoplasmic face of the plasma membrane. The first extracellular loop contains four N-glycosylation sites which act in the stability, trafficking and function of BSEP (Mochizuki et al., 2007).

Besides, BSEP is modified by phosphorylation and ubiquitinylation (Hayashi and Sugiyama, 2009; Kubitz et al., 2004; Noe et al., 2001; Wang et al., 2008a).
BSEP-mediated transport of bile salts is dependent on ATP hydrolysis. BSEP mainly transports monovalent bile salt species, including taurine and glycine conjugates of primary bile salts (CA and CDCA), and the secondary bile salts (DCA and UDCA) (Stieger, 2011). The affinity of conjugated bile salts in human and rodent BSEP is TCDCA = TCA > TDCA > tauroursodeoxycholic acid (TUDCA) ~glycocholic acid (GCA) (Byrne et al., 2002; Gerloff et al., 1998; Green et al., 2000; Noe et al., 2002).

1.2.2 Localization of BSEP

BSEP is expressed on the hepatocyte canalicular membrane (Cai et al., 2013). It is still unclear how BSEP traffics to the canalicular membrane after its synthesis and post-translational modification in the Golgi. Biosynthetic labeling analysis in rat showed that BSEP initially traffics from the Golgi to the subapical compartment before moving to the apical membrane (Kipp and Arias, 2000). This subapical compartment consists of rab11-positive endosomes (Wakabayashi et al., 2004). The half-life of BSEP in the canalicular membrane is about 4-6 days. BSEP protein is constitutively recycled between the plasma membrane and subapical vesicles containing Rab11. The process requires myosin Vb (Lam et al., 2007; Wakabayashi et al., 2005).

1.2.3 Transcriptional regulation of BSEP

The main transcriptional regulator of BSEP is the nuclear receptor farnesoid X receptor (FXR, NR1H4) (Trauner and Boyer, 2003). FXR can transactivate the proximal promoter of BSEP in humans and rodents (Ananthanarayanan et al., 2001; Gerloff et al., 2002). Bile acids are the physiologic ligand of FXR and can regulate the transcription of their own transporter (Makishima et al., 1999). Among bile salts, CDCA is the major endogenous physiological ligand of FXR (Wang et al., 1999). The role of FXR in BSEP expression was identified in FXR-/- mice. In these mice, the lack of FXR leads to hepatocyte weakly responding to bile acids (Marschall et al., 2006). FXR regulates bsep gene transcription by forming a heterodimer with retinoid X receptor, RXRα (Forman et al., 1995; Mangelsdorf and Evans, 1995). In addition to FXR, the BSEP transcription can also be induced by the hepatocyte-specific liver receptor homologue-1 (LRH-1, *NR5A2*) and the nuclear erythroid 2 P45-regulated factor 2 (NRF2) (Song et al., 2008).

1.2.4 BSEP mutations and diseases

BSEP gene mutations cause hereditary liver diseases, including progressive familial intrahepatic cholestasis type II (PFIC2) and the bengin recurrent intrahepatic cholestasis type II (BRIC2) (Lam et al., 2006; Pauli-Magnus et al., 2005). In these syndromes impaired bile salt secretion caused by lack of functional BSEP on the canalicular membrane leads to intrahepatic cholestasis characterized as diminished bile production, reduced bile flow and intrahepatic accumulation of toxic bile salts, concomitant with high plasma levels of bile salts and bilirubin, resulting in early development of hepatocellular carcinoma (HCC) and cholangiocarcinoma (Knisely et al., 2006; Scheimann et al., 2007; Strautnieks et al., 2008). Numerous BSEP variants are associated with several other liver diseases including primary intrahepatic stones, gallstone disease and neonatal cholestasis (Pauli-Magnus et al., 2004). Although the association of BSEP mutations and polymorphisms with the related liver disease is clearly identified, the mechanism how these mutations lead to the syndromes are diverse and controversial. Further studies are needed to clarify the underlying mechanisms of BSEP in diseases.

1.3 FXR: the nuclear farnesoid X receptor

FXR has typical nuclear receptor structure, including the activation function domain 1 (AF1) at the N-terminus, a conserved DNA binding domain (DBD), a ligand binding domain (LBD) that contains the activation function domain 2 (AF2) at the C-terminus, and a hinge region that links the DBD and LBD (Forman et al., 1995). FXR is abundant in liver, kidney, intestine and adrenal gland. It is also expressed at lower levels in other organs, including lung, heart, vessel, stomach, thymus, spleen, adipose, ovary and testes (Bishop-Bailey et al., 2004; Forman et al., 1995; Huber et al., 2002). The role of FXR in the liver and intestine is to maintain bile salt homeostasis. The physiological function of FXR in other organs remains to be determined. It is not clear how FXR expression is regulated in liver. CDCA and FXR agonist GW4064 can induce FXR mRNA and protein expression in HepG2 cells (Lew et al., 2004). TNF-α and IL-1β repress FXR mRNA expression in Hep3B cells (Kim et al., 2003). In mouse model, lipopolysaccharide induced acute phase response in the liver. But in WT mice receiving LPS with simultaneous GW4064 administration compared with those receiving LPS alone, Tool-loke receptor 4 (TLR4) and p38 mitogen-activated protein kinase (MAPK) were decreased, while this was not observed in FXR-KO mice, suggesting that LPS-

TLR4-NFκB signaling and MAPKs might be involved in FXR expression (Kim et al., 2003).

1.3.1 FXR in bile acid homeostasis

FXR plays a pivotal role in maintaining bile acid homeostasis by regulating key genes of bile acid synthesis, metabolism and transport, including CYP7A1, UGT2B4, BSEP, MDR3, MRP2, ASBT, I-BABP, NTCP and OSTα-OSTβ (Ananthanarayanan et al., 2001; Craddock et al., 1998; Dawson et al., 2005; Gong et al., 1994; Huang et al., 2003; Kast et al., 2002; Wong et al., 1994).

Bile acids inhibit their own biosynthesis by downregulating expression of cytochrome P450 (CYP) hydroxylase enzymes, including CYP7A1 and CYP8B1 (Chiang, 2002). CYP7A1 is the rate-limiting enzyme that catalyzes cholesterol into bile acids. Bile acids repress CYP7A1 through the FXR - SHP pathway. Bile acids-activated FXR induces SHP through binding to IR-1 FXR expression element (FXRE) and thus inhibits CYP7A1 and CYP8B1 expression (Chiang, 2002). In addition to depending on SHP, FXR also suppress the CYP7A1 expression through a c-Jun N-terminal kinase (JNK)-dependent pathway in primary human hepatocytes and mouse liver (Gupta et al., 2001; Inagaki et al., 2005; Kerr et al., 2002; Wang et al., 2002).

1.3.2 Role of FXR in regulating hepatocyte membrane transporters

FXR directly regulates the expression of canalicular bile transporters BSEP, MRP2 and MDR3 (**Figure 5**) (Ananthanarayanan et al., 2001; Huang et al., 2003; Kast et al., 2002). These ATP-binding cassette transporters play an essential role in bile formation by secreting bile salts, xenobiotics, bilirubin and phospholipids from hepatocyte into bile (Kullak-Ublick et al., 2004). BSEP is the major bile salt export pump, which has been described in section *part 1.2*. MRP2 is a multi-drug conjugate export pump that excretes divalent bile acid conjugates (Keppler and Konig, 1997). In addition to the function in hepatocytes, it is expressed in biliary, renal and intestinal cells for secretion of numerous organic anions, including endogenous compounds such as bilirubin and several organic anions, and exogenous compounds such as drugs and toxic chemicals (Paulusma et al., 1997; Paulusma and Oude Elferink, 1997). Multiple nuclear receptors are capable of regulating MRP2 expression. It is increased in human hepatocytes and rat hepatocytes by FXR agonists, such as CDCA and GW4064 (Downes et al., 2003;

Guo et al., 2003; Kast et al., 2002). A FXRE (ER8) has been identified in the MRP2 promoter by luciferase reporter assays in HepG2 cells (Kast et al., 2002). MDR3 (MDR2 in mouse) functions as a phospholipid translocator or flippase for biliary phosphatidylcholine excretion (Jacquemin et al., 2001; Oude Elferink et al., 1995; Smit et al., 1993). Mdr2-/- mice develop bile duct injury relevant to the inability of hepatocytes to secrete phospholipid into bile. The lack of phospholipids in bile results in toxic injury to the biliary epithelium becausee bile acids are unable to form lipid micelles. Therefore, functional MDR3 is essential to avoid cholestatic liver injury (Jacquemin et al., 2001). FXR directly upregulate MDR3 expression in human hepatocytes. An IR-1 FXRE in the promoter of MDR3 gene has been identified to be responsible for gene transcription (Huang et al., 2003).

FXR also regulates intestinal bile acid absorption, a process requires membrane transporters ASBR, I-BABP and OSTα-OSTβ. FXR regulates expression of these membrane protein (**Figure 5**) (Cai and Boyer, 2006). As a major transporter for bile salt reabsorption, ASBT is expressed in the ileum, caecum, cholangiocyte and kidney (Lazaridis et al., 1997; Wong et al., 1994). Bile salts repress ASBT expression through activating the FXR/SHP axis *in vitro* and *in vivo* (Neimark et al., 2004). I-BABP is a cytosolic bile acid binding protein, which is mainly expressed in ileum. A typical IR-1 FXRE in the human I-BABP promoter was also identified (Grober et al., 1999). OSTα-OSTβ localizing in the basolateral membrane transport bile acids and a variety of other organic solutes and sterols (Boyer et al., 2006). Promoter analysis revealed two and one FXRE in the human OSTα and OSTβ promoter, indicating that the two genes is directly regulated by FXR (Landrier et al., 2006).

In addition, FXR regulates hepatic bile acid uptake and basolateral sinusoidal membrane excretion by controlling NTCP and OATPs (**Figure 5**) (Hagenbuch and Meier, 2003; Tirona and Kim, 2002). NTCP and OATP1B1 are the major hepatocellular basolateral sinusoidal membrane transporters for the uptake of bile salts and organic solutes (Hagenbuch and Meier, 1994; Stieger et al., 1994). NTCP is responsible for the single pass clearance of conjugated bile acids, whereas OATPs uptake unconjugated bile acids. NTCP and OATP1B1 are downregulated in cholestatic livers of patients and animals, in order to protect the liver from toxic bile salt injury by minimizing the hepatic uptake of these compounds from portal blood (Gartung et al.,

1996; Green et al., 1996; Kakyo et al., 1999; Oswald et al., 2001; Shneider et al., 1997; Simon et al., 1996; Zollner et al., 2001). Promoter analysis indicates that the basal expression of these two genes is activated by HNF1 and suppressed by SHP (Denson et al., 2001).

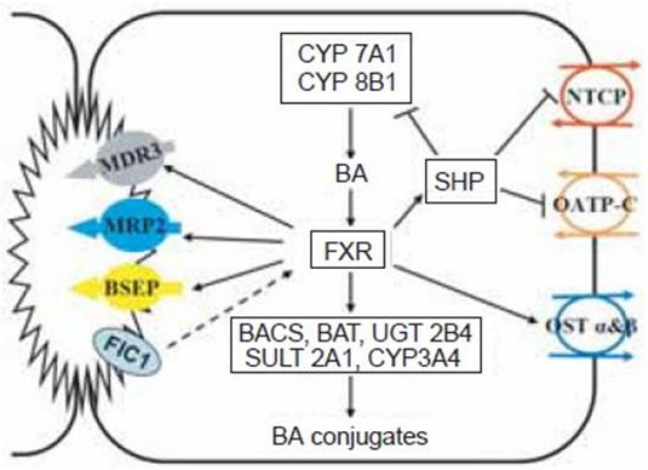

Figure 5. FXR regulates the expression of key genes acting in bile acid synthesis, conjugation and transport in hepatocyte (Cai and Boyer, 2006). BA: Bile acid; BACS: Bile acid-CoA synthesis; BAT: Bile acid-CoA: amino acid N-acetyltransferase; BSEP: Bile salt export pump; CYP: Cytochrome P450; FIC1: Familial intrahepatic cholestasis type 1; FXR: Fernesoid X receptor; MDR3: Multidrug resistance protein 3; MRP2: Multidrug resistance protein 2; NTCP: Sodium-dependent taurocholate cotransporting polypeptite; OATP: Organic anion transporting polypeptide; OST: Organic solute transporter; SHP: Short heterodimeric protein; SULT: Sulfotransferase; UGT: UDP-glucuronosyltransferase.

1.3.3 FXR in glucose metabolism

FXR plays an important role in glucose homeostasis through regulating serum glucose levels and insulin tolerance (Ma et al., 2006; Zhang et al., 2006). Hypoglycemic effects of FXR activation rely on repression of gluconeogenesis and induction of glycogen synthesis (Zhang et al., 2006). Different studies have shown that BAs repressed gluconeogenesis by FXR-dependent repression of PEPCK and G6PAse and SHP-dependent repression of HNF4α and FOXO1 (Ma et al., 2006; Yamagata et al., 2004). The latter two transcription factors inhibit PEPCK (Yamagata et al., 2004). However, PEPCK expression was reduced in FXR knockout mice after fasting and refeeding (Duran-Sandoval et al., 2005). In rat primary hepatocytes and hepatoma cell lines, GW4064 and CDCA induce PEPCK expression (Stayrook et al., 2005). Zhang et al. investigated FXR effects on glycogen synthesis in diabetic mice (Zhang et al., 2006). They found that GW4064 administration increases hepatic glycogen synthesis and

glycogen content in db/db mice. It revealed that incorporation of glucose into glycogen is increased in murine primary hepatocytes upon GW4064 treatment. In addition, GW4064 induces phosphorylation of GSK3β, IRS-1, IRS-2 and AKT, suggesting that FXR increase glycogen synthesis by enhancing insulin sensitivity. Another mechanism underlying FXR-mediated glycogen synthesis is through inhibiting glucose oxidation. In the setting of high blood glucose concentrations, FXR decreases transcription of liver pyruvate kinase (LPK) by releasing ChREBP (Caron et al., 2013). Suppression of LPK results in shifting glucose metabolites towards glycogen synthesis (Duran-Sandoval et al., 2005). Another study identified that FXR deactivation by BA sequestrants improve glucose homeostasis by increasing GLP-1 synthesis and secretion, decreasing intestinal glucose absorption, and enhancing hepatic glycolysis and lipogenesis in diabetes type 2 patients (Smushkin et al., 2013). A recent study suggested that inhibition of intestinal FXR downregulates hepatic gluconeogenesis through modulation of the ceramide pathway and the attenuation of hepatic mitochondria acetyl-CoA levels (Xie et al., 2017). Intestinal FXR-induced FGF19 promotes hepatic glycogen synthesis, which is important for glucose homeostasis (Kir et al., 2011). Taken together, FXR is a transcriptional regulator coordinating glucose metabolism. Whether interfering with FXR benefits glucose homeostasis needs further studies.

1.4 Acute-on-chronic liver failure (ACLF)

Acute-on-chronic liver failure (ACLF) is a sepsis-like syndrome characterized by acute deterioration of liver function in an individual with pre-existing chronic liver disease. The disease usually progresses to multiple organ failure and has a high short-term mortality. Alcoholic liver disease and chronic viral hepatitis are the most common underlying liver diseases. Infection, active alcoholism and relapse of chronic viral hepatitis are major precipitating factors, although up to 40%-50% of ACLF patients do not have identifiable precipitating event. Systemic inflammatory response plays a crucial role in the progression of ACLF (Hernaez et al., 2017).

1.4.1 Pathophysiology of systemic inflammation in ACLF

Systemic inflammation is a hallmark of ACLF, white cell count and plasma levels of C reactive protein (CRP) and pro-inflammatory molecules such as IL-6, IL1β, IL-8 are

higher in patients with ACLF (Bernsmeier et al., 2015; Claria et al., 2016; Moreau, 2016; Moreau et al., 2013). The inflammatory response develops when inducers of inflammation are recognized by sensors that engage effectors of the response (Arroyo et al., 2016; Medzhitov, 2008; Moreau, 2016). The most common inducers of inflammation are microbial organisms, which includes bacterial, viruses and fungi (Hernaez et al., 2017; Medzhitov, 2008; Moreau, 2016). Bacterial trigger inflammation by two distinct classes of molecules: pathogen-associated molecular patterns (PAMPs) and virulence factors (Arroyo et al., 2016; Medzhitov, 2008; Moreau, 2016; Takeuchi and Akira, 2010). PAMPs are recognized by pattern-recognition receptors (PRRs), which are expressed in innate immune cells and epithelial cells (Iwasaki and Medzhitov, 2015). PRRs include toll-like receptors (TLRs), nucleotide-binding oligomerization domain-like receptors (NLRs), retinoic acid-inducible gene (RIG)-1, cytosolic DNA sensors, inflammatory caspase-4/5 in humans and caspase-11 in mice (Arroyo and Moreau, 2017; Gustot et al., 2009; Moreau, 2016; Takeuchi and Akira, 2010). PRR engagement by PAMPs stimulates intracellular signaling cascades that activate core transcription factors, e.g. NF-κB, which activate gene expression of cytokines and chemokines (Gustot et al., 2009; Takeuchi and Akira, 2010). The primary purpose of the inflammatory response to bacterial infection is to promote host resistance by reducing bacterial burden and virulence. When local defenses are insufficient to contain the infection, a systemic response is initiated to fight against the spreading microbe. In some cases, the early systemic inflammatory response to bacteria is excessive and may cause organ damage (Medzhitov, 2010). Inflammation is a protective response to infection and injury, but it operates at the expense of normal tissue function (Okin and Medzhitov, 2012).

1.4.2 Glucose homeostasis in ACLF

In healthy humans, energy supply and expenditure are in homeostasis balance. However, the energy homeostasis in ACLF patients is disturbed. ACLF is a highly lethal disease, which is the result of a complex interplay of pathophysiological alterations, including inflammation, hypoxia, and metabolic reprogramming. Sustained inflammation results in elevated plasma glucose due to increased hepatic glucose production (Okin and Medzhitov, 2016). Furthermore, there is a high energy need, but patients are unwilling or incapable of eating and thus develops a starvation response. Due to this complex condition, high levels of blood glucose are urgently required for

the protection of priority organs or tissues, e.g. the brain and immune system (Rui, 2014). To sustain blood glucose levels, a large amount of glucagon is produced and released from pancreatic α cell (Rui, 2014). Patients with sepsis and ACLF usually maintain high levels of circulation glucagon (Van Wyngene et al., 2018). On the other hand, hyperglycemia induces hyperinsulinemia (Van Wyngene et al., 2018). To inhibit insulin-dependent glycogen deposition, insulin resistance occurs in major metabolic organs, including skeletal muscle, adipose tissue and hepatocytes (Jenniskens et al., 2016). As a result, both glucagon and insulin are present at high levels in ACLF patients.

1.4.3 FXR in ACLF

Nutrient sensing and inflammatory response are closely itertwined. Immune defense is energy demanding. Malnutrition or starvation impair immune function, however, excessive nutrient induce inflammation (Demas et al., 1997; Marti et al., 2001). Nutrient sensing nuclear receptor, FXR, represses inflammation and plays a role in metabolism and immunity signaling pathways (Bensinger and Tontonoz, 2008; Cave et al., 2016; Venteclef et al., 2011). The livers of FXR null mice show increased pro-inflammatory cytokines and monocyte/macrophage infiltration. (Kim et al., 2007; Liu et al., 2012). FXR activation inhibits NF-κB transcriptional activation of pro-inflammatory genes in hepatocytes (Wang et al., 2008b). In addition, FXR activation inhibits gluconeogenesis and improves insulin sensitivity (Hotamisligil, 2006; Shoelson et al., 2006). On the other side, expression of FXR is negatively impacted by inflammation, particularly in serious infection and inflammatory response, e.g. sepsis and ACLF (Jenniskens et al., 2016). The liver plays a central role in the response to sepsis and other critical illnesses by releasing acute-phase proteins, cytokines, and coagulants and by facilitating clearance of pathogenic organisms and toxins. In condtions of critical illness, FXR expression is inhibited rapidly (Vanwijngaerden et al., 2011). *In vitro* and *in vivo* studies show that FXR nuclear exclusion is regulated by c-Jun N-terminal kinases which are activated by inflammatory mediators (Zimmerman et al., 2006). Inhibition of FXR leads to compromised FXR/SHP-CYP7A1 regulatory feedback response, causing severe cholestasis (Geier et al., 2006). Whether these pathophysiological alterations are maladaptive or adaptive response requires further investigations.

1.4.4 Cholestasis in ACLF

Sepsis and extrahepatic bacterial infection with inflammation are often accompanied by cholestasis (Geier et al., 2006). There is severe cholestasis in ACLF, in which situation bile acid levels increase in the liver and serum, followed by hepatocyte injury and bile duct proliferation. There are three main reasons leading to cholestasis in ACLF: (1) due to submassive hepatic necrosis, bile acids in hepatocytes are secreted into the blood; (2) in remaining hepatocytes, bile acids are over-produced because of the disturbed FXR/SHP-CYP7A1 feedback regulation; (3) due to functional impairment of the bile acid transporting system, bile acids cannot be exported into the bile canaliculi (Woznica et al., 2018). Without treatment, cholestasis will cause more severe liver injury in ACLF (Hofmann and Hagey, 2008). Bile acids induce liver injury directly or by inflammatory response (Attili et al., 1986; Galle et al., 1990; Scholmerich et al., 1984). Exposure of cultured mouse primary hepatocytes to 200μM of TCA, significantly stimulated the expression of a series of cytokines, including MCP1, MIP-2 and ICM-1 (Li et al., 2017). The cholestasis-induced inflammatory response resulted in ER stress and mitochondrial damage in hepatocytes (Li et al., 2017). Therefore, controlling the inflammatory response and cholestasis are important for the treatment of ACLF.

1.5 Foxa2: Forkhead box protein A2

The hepatocyte nuclear factor 3 (HNF-3)/forkhead family of transcription factor in mammals comprises three genes, Foxa1(Hnf-3α), Foxa2(Hnf-3β), and Foxa3 (Hnf-3γ) (Kaestner et al., 1994). These genes all possess a common highly conserved 100-aa winged-helix motif in common that is responsible for binding specific DNA target sites (Brennan, 1993; Lai et al., 1990; Weigel and Jackle, 1990; Weigel et al., 1989). Foxa2 is a transcriptional activator for liver-specific genes such as albumin and transthyretin. In addition, Foxa2 is essential for the development of the foregut endoderm and subsequent liver development.

1.5.1 Structure and activity of Foxa2

The Foxa protein family was initially discovered on the basis of DNA binding activity in liver nuclear extract which is specific for the promoters of the *transthyretin*, *α1-antitrypsin* and *albumin* gene (Herbst et al., 1991; Lai et al., 1990). The sequence of Foxa1, Foxa2 and Foxa3 forkhead box protein are 95% indentical. Their flanking

sequences are required for nuclear localization (Clark et al., 1993). Among the family, Foxa2 is unique because it contains an AKT2/PKB phosphorylation site at the N terminus of the forkhead domain (**Figure 6**) (Pani et al., 1992; Qian and Costa, 1995).

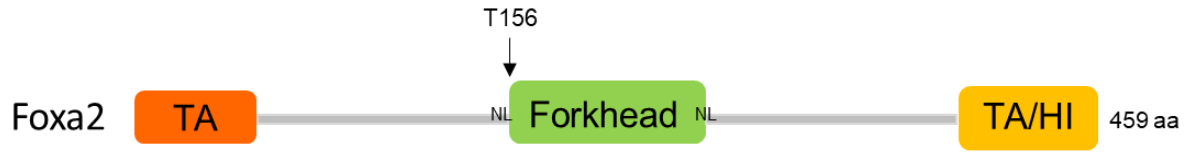

Figure 6. Structure of the forkhead domain. Within helix 3 (H3) and wing/loop 2 (W2), multiple residues make direct and water-mediated contacts with the DNA. H3 interacts within the major groove, while W2 straddles the DNA backbone and makes contacts in both the major and minor grooves.

1.5.2 Foxa2 in liver development

The Foxa subfamily of winged helix/forkhead box (Fox) transcription factors, Foxa1, Foxa2, Foxa3, have been found to play important roles in mammalian development (Carlsson and Mahlapuu, 2002). Foxa2 is required for the formation of the node and notochord, given that its absence results in severe defects in gastrulation, neural tube patterning, and gut morphogenesis, and even embryonic lethality (Monaghan et al., 1993). Foxa1 and Foxa2 cooperate to establish competence in foregut endoderm and are required for normal development of endoderm-derived organs such as liver, pancreas, lungs and prostate (Kaestner et al., 1993; Sasaki and Hogan, 1993). Foxa2 protein has been identified as ‘pioneer factors’ whose binding to promoters and enhancers of genes, such as albumin, alpha-fetoprotein and transthyretin, enable chromatin access for other liver-specific transcription factors (Lee et al., 2005; Sund et al., 2000).

1.5.3 Foxa2 in glucose metabolism

Foxa2 plays a significant role in maintaining normal glucose homeostasis by regulating rate-limiting enzymes relevant to gluconeogenesis and glycogenolysis, including phosphoenol-pyruvate carboxy kinase (PEPCK) and glucose-6-phosphatase (G6pc) (Gerrish et al., 2000; O'Brien et al., 1995; Shih et al., 1999). Insulin induces Foxa2 phosphorylation and nuclear exclusion, and thus inhibiting Foxa2-dependent transcriptional activity. In addition, Foxa2 physically interacts with Akt and is phosphorylated at a single conserved site (T156) (Wolfrum et al., 2003). Opposimg the

effects of insulin, high glucagon concentrations induce glycogen breakdown and gluconeogenesis to maintain high levels of circulation glucose during starvation or hypoglycemia (Habegger et al., 2010). Foxa2 is acetylated at the conserved residue Lys259 and the cofactors p300 and SirT1 are involved in Foxa2 acetylation and deacetylation respectively. Physiologically, fasting state and glucagon are sufficient to induce Foxa2 acetylation, which promotes Foxa2 activity (von Meyenn et al., 2013). In conclusion, the the balance between insulin and glucagon regulate glucose metabolism through controlling Foxa2 activation.

1.5.4 Foxa2 in bile acid regulation

There are few studies to date investigating the role of Foxa2 in regulating bile acid homeostasis. Foxa2 overexpression in the liver impacts lipid metabolism. Bochkis et al. used a Foxa2 knockout mouse model to study the role of Foxa2 in the adult liver. They found that silencing of Foxa2 decreases the transcription of genes encoding bile acid transporters on both basolateral and canalicular membranes, thus resulting in intrahepatic cholestasis, liver injury and ER stress. This study suggests an important role for Foxa2 in hepatic bile acid homeostasis and in the prevention of cholestatic liver injury (Bochkis et al., 2008).

1.6 Aims of this study

This study aims to investigate the regulatory mechanisms of how the host maintains hepatic BSEP expression in physiological and pathophysiological circumstances, particularlt in an acute inflammatory condition such as ACLF.

Aim 1: To detect the correlation between FXR, FOXA2 and BSEP expression in ACLF patients;
Aim 2: To compare the clinical outcome of ACLF patients with or without BSEP expression on bile canaliculi;
Aim 3: To clarify wheather and how FOXA2 regulates BSEP expression in ACLF;
Aim 4: To investigate the regulatory mechanism of FXR- and FOXA2- dependent BSEP expression.

2. MATERIALS AND METHODS

2.1 Materials

2.1.1 Chemicals and reagents

Table 2. Chemicals and reagents

Chemicals	**Cat. No.**	**Company**
Acetic acid	338826	Sigma-Aldrich (USA)
Albumin standard (BSA)	12659	Merck (Germany)
Ammonium persulfate (APS)	A3678	Sigma-Aldrich (USA)
Dexamethasone	D1159-100MG	Sigma-Aldrich (USA)
3.3'-diaminobenzidine (DAB)	D-5905	Sigma-Aldrich (USA)
DMEM	BE12-709F	Lonza (Germany)
DMEM/F12	12634-010	Life Technology (Canada)
Dimethyl sulfoxide (DMSO)	41639	Sigma-Aldrich (USA)
DRAQ5 dye	4084	Cell Signaling Technology (USA)
EDTA	324503	Calbiochem (Germany)
Ethanol	K928.4	Carl Roth
Fetal Bovine Serum (FBS)	10270-098	Invitrogen
Formaldehyde	F1635	Sigma-Aldrich (USA)
GW4064	G5172-5MG	Sigma-Aldrich (USA)
Hematoxylin	HX69715174	Carl Roth (Germany)
Hydrogen peroxide (H2O2)	H1009	Sigma-Aldrich (USA)
Insulin	HI0210	Lilly (Germany)
Glucagon	G2044-5MG	Sigma-Aldrich (USA)
Insulin-Transferrin Selenium	41400045	Thermo Scientific
L-glutamine	BE17-605E	Lonza (Germany)
Laemmli-buffer	161-0737	BioRad (USA)
Lipofectamine 3000 reagent	L3000008	Thermo Fisher
Lipofectamine RNAiMAX	13778-075	Thermo Fisher
Malinol mounting medium	3C-242	Waldeck (Germany)
2-β-Mercaptoethanol	516732	Sigma-Aldrich (USA)
Mounting medium	S3023	DAKO

Methanol	8388	Carl Roth (Germany)
Penicillin/Streptomycin	A2210	Biochrom KG
Phosphatase Inhibitor Cocktail 2	P5726	Sigma-Aldrich (USA)
Protease Inhibitor Cocktail Tables	S8820	Sigma-Aldrich (USA)
RNase A	19101	Qiagen (Germany)
Sodium dodecyl sulfate (SDS)	L3771	Sigma-Aldrich (USA)
TEMED	T9821	Sigma-Aldrich (USA)
TRIS	4855	Carl Roth (Germany)
Triton X-100	T-9284	Sigma-Aldrich (USA)
Trypsin/EDTA) 10X	T4174	Sigma-Aldrich (USA)
Tween 20	9127.2	Carl Roth (Germany)
Type I collagen	40231	Corning
Collagenase II	C2-28	Merck

2.1.2 Antibodies

Table 3. Primary antibodies used for immunoblotting

Antibody	**Company**	**Cat. No.**	**Predicted molecular weight**
BSEP	Santa Cruz	sc-74500	160kDa
CYP7A1	Abcam	ab65596	58kDa
FOXA2	Santa Cruz	sc-101060	54kDa
FXR	R&D system	PP-A9033A-00	56kDa
GAPDH	Santa Cruz	sc-32233	36kDa
HistoneH1	Santa Cruz	sc-8030	31kDa
SHP	Abcam	ab96605	28kDa

Table 4. Primary antibodies used for immunohistochemistry

Antibody	**Company**	**Cat. No.**	**Dilution**
BSEP	Santa Cruz	sc-74500	1:50
CYP7A1	Abcam	ab65596	1.100
FOXA1	Abcam	ab170933	1:100
FOXA2	Santa Cruz	sc-101060	1.100

FXR	R&D system	PP-A9033A-00	1:100
HNF4α	Cell signaling	C11F12	1:100
RXRα	Santa Cruz	sc-515929	1:100
SHP	Abcam	ab96605	1.100

Table 5. Primary antibodies used for immunofluorescence

Antibody	**Company**	**Cat. No.**	**Dilution**
FXR	R&D system	PP-A9033A-00	1:100
FOXA2	Santa Cruz	sc-101060	1.100
BSEP	Santa Cruz	sc-74500	1:50

Table 6. Primary antibodies used for ChIP

Antibody	**Company**	**Cat. No.**	**Dilution**
FOXA2	Sigma-Aldrich	17-10258	2µg antibody/10 6 cells

Table 7. Second antibodies

Antibody	**Company**	**Dilution in WB**	**Dilution in IHC**	**Dilution in IF**
Goat anti mouse IgG HRP	Santa Cruz	1:5000	------	------
Goat anti rabbit IgG HRP	Santa Cruz	1:5000	------	------
Goat anti mouse IgG HRP	DAKO	------	1:200	
Goat anti tabbit IgG HRP	DAKO	------	1:200	
Goat anti-mouse FITC	Merck/Millipore	------	------	1:200
Goat anti-rabbit Rhodamine	Merck/Millipore	------	------	1:200
Alexa Fluor 488 Donkey Anti-Mouse	Jackson Immuno Research	------	------	1:200
Cy3 Donkey Anti-Mouse	Jackson Immuno Research	------	------	1:200
DRAQ5	Cell signaling technology	------	------	1:1000

2.1.3 Buffer preparation

Table 8. Buffers

Chemicals	**Ingredients**
10% APS	1g APS
	add to 10ml H2O
RIPA buffer stock	50 mM Tris-HCL PH 7.2-7.6
	150 mM NaCl
	2 mM EDTA
	0.1% SDS
	0.5% Sodium-Desoxycholate
	1% Nonidet P-40
	10% v/v Glycerol
Lysis buffer for WB	90 µl RIPA buffer
	1 µl Phosphatase Inhibitor
	15 µl Protease Inhibitor
Subcellular fraction	250 mM Sucrose
	20 mM HEPES (PH 7.4)
	10 mM KCl
	1.5 mM MgCl2
	1 mM EDTA
	1 mM EGTA
	1 mM DTT
	PI cocktail
Nuclear lysis buffer	50 mM Tris HCL (PH 8)
	150 mM NaCl
	1%Nonidet P-40
	0.5 % sodium deoxycholate
	0.1 % SDS
	10% glycerol
	PI cocktail
TBST 10X	0.2 M Tris
	1 M NaCl

	10 ml Tween 20
	adjust PH value to 7.4
SDS running buffer 10X	144 g Glycin
	30.34 Tris
	10g SDS
	add to 1L ddH2O
	adjust PH value to 8.3
SDS running buffer 1X	100ml SDS running buffer 10X
	900 ml ddH2O
Transfer buffer 10X	144g Glycin
	30.2 Tris
	add to 1L ddH2O
Transfer buffer 1X	100ml Transfer buffer 10X
	200 ml Methanol
	700 ml ddH2O
Glucose solution	9 g D-Glucose
	add to 1L ddH2O
KH buffer	60 g NaCl
	1.75 g KCl
	1.6 g KH2PO4
	add to 1L H2O
	adjust PH value to 7.6
HEPES buffer 8.5	60 g HEPES
	1L H2O
	adjust PH value to 8.5
HEPES buffer 7.6	60 g HEPES
	1L H2O
	adjust PH value to 7.6
EGTA solution	475 mg EGTA
	add ddH2O to 10ml
	add NaOH for dissolving
	adjust PH value to 7.6
CaCl2·2 H2O solution	1.9 g CaCl2·2 H2O

	add ddH2O to 100 ml
MgSO4·7 H2O solution	1.23 g MgSO4·7 H2O
	add ddH2O to 50 ml
Amino acid solution	0.27 g L-Alanine
	0.14 g L-Aspartic
	0.4 g L-Asparagine
	0.27 g L-Citrulin
	0.14 g L-Cysteine hydrochloride monohydrate
	1 g L-Histidine monohydrochloride monohydrate
	1 g L-Glutamic acid
	1 g L-Glycine
	0.4 g L-Lsoleucine
	0.8 g L-Leucine
	1.3 g L-Lysine monohydrochloride
	0.55 g L-Methionine
	0.65 g L-Ornithine monohydrochloride
	0.55 g L-Phenylalanine
	0.55 g L-Proline
	0.65 g L-serine
	1.35 g L-Threonine
	0.65 g L-Tryptophane
	0.55 g L-Tyrosine
	0.8 g L-Valine
	Dissolve amino acids in 800 ml ddH2O
	Add naOH to dissolve amino acids
	adjust PH value to 7.6
	Add ddH2O to 1 L
	Sterile-filter (0.22 µm filter)
Glutamine solution	0.07 g Glutamine
	add ddH2O to 10 ml
	Sterile-filter (0.22 µm filter)

EGTA buffer for cell isolation	124 ml Glucose solution
	20 ml KH buffer
	20 ml HEPES PH 8.5
	30 ml Amino acid solution
	2 ml Glutamine solution
	0.8 ml EGTA
Collagenase buffer for cell isolation	77.5 ml Glucose solution
	12.5 ml KH buffer
	12.5 ml HEPES PH 8.5
	19 ml Amino acid solution
	1.25 ml Glutamine solution
	5 ml CaCl2
	7176 units per 50 ml collagenase buffer
Suspension buffer for cell isolation	310 ml Glucose solution
	50 ml HK buffer
	75 ml amino acid solution
	5 ml Glutamine solution
	4 ml CaCl2·2 H2O solution
	50 ml HEPES PH 7.6
	2 ml MgSO4·7 H2O solution
	1g BSA

2.1.4 Cell culture materials

Table 9. Cell culture materials

Material	**Company**
Cell culture flasks 25 cm2/ 75 cm2/ 175 cm2	Greiner Bio-one (Germany)
Cell scraper	Falcon (Germany)
Conical centrifuge tubes 15 ml / 50ml	Falcon (Germany)
Cell culture plate 96 well	Greiner Bio-one (Germany)
Cell culture plate 12 well	Greiner Bio-one (Germany)
Cell culture plate 6 well	Greiner Bio-one (Germany)

0.5 or 1.5 ml tubes	Eppendorf, Germany
Eppendorf epT.I.P.S	Eppendorf, Germany
Microscope slide	Carl Roth (Germany)
PCR-Tubes 0.2m	Life Technology
Petri dishes	Falcon (Germany)
Sterile pipette	Greiner Bio-one (Germany)

2.1.5 Liver tissue specimens of patients

Fifteen liver tissues were collected from 5 HBV infected and 10 ACLF patients in the Department of Gastroenterology and Hepatology, Beijing You'an Hospital, Affiliated with Capital Medical University. Five HBV infected patients received liver biopsy while the 10 ACLF patients received liver transplantation. ACLF was identified in patients hospitalized for at least 1 day who suffered from acute decompensation of cirrhosis. Acute decompensation was defined by the development of one or more major complications of liver diseases: (i) development of grade 2 to 3 ascites within <2 weeks; (ii) hepatic encephalopathy; (iii) gastrointestinal hemorrhage; (iv) bacterial infections (spontaneous bacterial peritonitis, spontaneous bacteremia, urinary tract infection, pneumonia, cellulitis) (Li et al., 2015)

The study protocol was approved by three local ethics committees. Written informed consent was obtained from patients or their representatives. In Beijing, allocation and timing of LTx was governed by the China Liver Transplant Registry (CLTR) (Wan et al., 2016), an official organization for scientific registry authorized by the Chinese Health Ministry, according to the Model for End-Stage Liver Disease (MELD) score of the patient.

2.1.6 Instruments and software

Table 10. Instruments and software

Instruments or software	**Company**
Centrifugation	Eppendorf (Germany)
TCS SP2 Confocal microscope	Leica (Germany)
Immunofluorescence optical microscope	Olympus (Germany)
Light Microscope	Leica (Germany)
Inverted Microscope	Zeiss (Germany)

Step-one real-time PCR machine	Biosystems
Western-Blot imaging system chemismart 5100	PEQLAB (Germany)
Incubator for cell culture	Haraeus GmbH (Germany)
Incubator for bacterial	Haraeus GmbH (Germany)
Microwave oven	Sharp (USA)
Bioruptor Plus sonication device	Diagenode (Germany)
PH-Meter 538 mutical	WTW (Germany)
Weight balance	Sartorius (Germany)
Image J	National institute of Health
GraphPad prism 5.0	Graphpad Software (USA)
Primer 5.0 input	Premier (Canada)

2.2 Methods

2.2.1 Cells and cell culture medium used in this study

Table 11. Cells and cell culture medium

Cell	Culture medium
AML12	DMEM/F12, 10% FBS, 1% P/S, 1% L-glutamine, 0.5% ITS, 0.1% Dexamethasone
MPH*	William's E medium, 10% FBS, 1% P/S, 1% L-glutamine, 0.5% ITS, 0.1% Dexamethasone
HPH*	William's E medium, 10% FBS, 1% P/S, 1% L-glutamine, 0.5% ITS, 0.1% Dexamethasone

*: MPH: Mouse primary hepatocyte

*: HPH: Human primary hepatocyte

2.2.2 Cell culture and treatment

All the cells were cultured in a humidified incubator at 37°C and 5% CO2 atmosphere. For FXR agonist GW4064 treatment, GW4064 was dissolved in DMSO to make a 10 mM stock solution and diluted with cell culture medium into 10 µM. DMSO was diluted in the same manner as control. The cells were cultured in 6-well or 12-well plate overnight and treated with 10 µM GW4064 or DMSO for 48h. For transient transfection

of SiRNA, FOXA2 over-expression plasmid, cells were treated with indicated culture medium without penicillin/streptomycin, and were collected 24h or 48h later after transfection.

2.2.3 Primary hepatocytes isolation from mice and patients

FVB wild type and *fxr* knockout mice (B6-129X1(FVB)-Nr1h4tm1Gonz/J; Stock: #007214, purchased from Jackson Lab) were used for primary hepatocyte isolation. All animal protocols were performed in full compliance with the guidelines for animal care and approved by the local Animal Care Committee.

Isolation of hepatocytes from mouse livers was performed as described previously (Godoy et al., 2009). Six to twelve weeks old B6 mice were used for isolation of primary hepatocytes. The use of mice for hepatocyte isolation has been approved by the local animal experimental committees and animals were handled and housed according to specific pathogen free (SPF) conditions. Anaesthesia was achieved by intraperitoneal injection of 5mg/100mg body weight ketamine hydrochloride 10% and 1mg /100 mg body weight xylazine hydrochloride 2%. Perfusion buffer and collagenase buffer were pre-warmed in 37°C water bath. Collagenase was added immediately prior perfusion. After shaving and sterilization of the abdomen, the abdominal cavity was opened and the portal vein was cannulised with a 24G catheter. A silicon tube (diameter 2.4 mm) was connected to the catheter and perfusion buffer using a peristaltic pump at a flow rate of 6 ml per minute. After starting the infusion, the vena cava and the right heart ventricle were incised to permit sufficient outflow. The liver was perfused with perfusion buffer for 5 minutes, followed by collagenase buffer for 5 to 7 minutes. Successful perfusion was evidenced by the steady and constant change from dark red-brown to a light brown color in all liver lobes. After perfusion, the liver was transferred to a sterile 10cm dish and the gall bladder was removed. From this step, all the following procedures were performed in a sterile hood. The liver capsule was carefully removed with forceps. Gentle shaking disintegrated the perfused liver which resulted in a suspension of single of cells, some cell clumps and cell debris. The suspension was placed onto a 100 µm cell strainer and allowed to filter through the mesh by gravity flow. The cell suspension was transferred to a 50 ml Falcon tube and washed twice with Williams E medium. Cells were centrifuged at room temperature at 28g for 2 minutes. To remove the dead cells, hepatocytes were mixed with balanced Percoll solution followed by centrifugation at 50g/10min/4°C. The cell pellet was resuspended

in culture medium and the percentage of viable cells was determined by counting of staining (with trypan blue) and unstained cells. On average, viability was around 85%-95%.

Primary human hepatocytes were isolated by the Cell Isolation Core Facility of the Biobank Großhadern, University Hospital, LMU Munich, using a two-step collagenase perfusion technique with modifications (Lee et al., 2013).

2.2.4 Collagen sandwich hepatocytes culture

Mouse and human primary hepatocytes were cultured in William's E medium as indicated. 4 x 10 5 freshly isolated hepatocytes were seeded in 6-well plate pre-coated with type I collagen (250 µg/ml). After overnight growth, hepatocytes were overlaid with collagen (0.83 mg/ml) and cultured in a humidified 37°C incubator.

For the pre-coated collagen preparation, a solution of 250 µg/ml of rat tail collagen-I was prepared with 0.2% acetic acid and allowed to dry for 2 h in the humidified 37°C incubator. After solidification, the gel was washed with PBS for three times, added 1 ml William's E medium per well and put in incubator for use. For up-layer collagen preparation, a solution of 0.83 mg/ml rat tail collagen-I dissolved by 0.2% acetic acid and DMEM was neutralized on ice with 1M NaOH, and adjusted the PH value to 7.4. 300 µl of the collagen solution was added to each well (6-well plate) and allowed to polymerize at 37 °C for 30 minutes. After solidification, the cells and gels were washed with PBS for three times, added culture medium as indicated and cultured in the humidified 37°C incubator.

2.2.5 RNA interference

Small interfering RNA (SiRNA) targeting mouse FOXA2 was purchased from Santa Cruz (HNF3β SiRNA mouse sc-35570).

3.5 x 10^{5} AML12 cells or 4 x 10^{5} mouse primary hepatocytes were seeded in 6-well plate with 2 ml culture medium as indicated. After overnight culture, the cells were transfected with FOXA2 SiRNA using RNAiMAX. A detailed protocol in the following:

(1) Dilute 3µl (30 pmol) FOXA2 SiRNA in 150µl Opti-MEM medium; mix gently by pipetting.

(2) Dilute 6µl RNAiMAX in 150 µl Opti-MEM medium; mix gently by pipetting.

(3) Add diluted SiRNA to diluted RNAiMAX reagent with a ratio of 1 to 1, and incubate the mixture in room temperature for 15 minutes.

(4) Add 300 µl RNA-lipid complexes to each well.
(5) Incubate overnight.
(6) Change to the culture medium as indicated.
RNA and protein were extracted 48 hours after transfection for measuring the knockdown efficiency and the expression of related genes.

2.2.6 Plasmid transfection

ShRNA targeting mouse FOXA2 was purchased from Dharmacon. (Gene set: TCR Nr1h4 ShRNA, RMM4534-EG20186 glycerol set.)
FOXA2 overexpression plasmid was purchased from Addgene. (pGCDNsam-Foxa2-IRES-GFP, Plasmid #33008.)
3.5 x 10 5 AML12 cells or 4 x 10 5 mouse primary hepatocytes were seeded in 6-well plate with 2 ml culture medium as indicated. After overnight culture, the cells were transfected with plasmid using Lipofectamine 3000 reagent. A detailed protocol in the following:
(1) Dilute 2.5µg plasmid into 125µl Opti-MEM medium; mix gently by pipetting.
(2) Dilute 3.75 µl Lipofectamine 3000 reagent into 125 µl Opti-MEM medium, mix gently by pipetting.
(3) Add diluted plasmid to diluted lipofectamine 3000 reagent with a ratio of 1 to 1, and incubate the mixture in room temperature for 15 minutes.
(4) Add 250µl DNA-lipid complexes to each well.
(5) Incubate overnight.
(6) Change to the culture medium as indicated.
RNA and protein were extracted 48 hours after transfection for measuring the knockdown efficiency and the expression of related genes.

2.2.7 Cell protein extraction

The cells were washed twice with ice-cold PBS and immediately added 80 µl RIPA buffer to per well of 6-well plate and put on ice. Then the cells were scraped to collect lysate and transferred to 1.5 ml Eppendorf tube. The supernatant was collected in a new 1.5 ml Eppendorf tube after centrifuge at 13000 rpm at 4°C. The protein concentration was determined using the Bio-Rad protein assay. For SDS/PAGE, 20-40 µg protein was prepared and supplemented with reducing loading buffer.

2.2.8 Subcellular fractionation

Subcellular fraction was performed following the detailed protocol below:

(1) Wash the cells twice with ice-cold PBS and immediately add 100 µl SF buffer to each well (6-well plate) and put on ice, use cell scraper to collect lysate and transfer to a 1.5 ml Eppendorf tube. (If multiple samples are collected, process one specimen at a time.)
(2) Agitate the lysates at 4 °C for 30 minutes at around 30-50 rpm on the tube roller.
(3) Centrifuge at 720 x g 4 °C for 5 minutes.
(4) Carefully transfer the supernatant to anew 1.5 ml tube for future use. Keep th pellet for next step.
(5) Wash the pellet with 500 µl of SF buffer and disperse the pellet with a pipette.
(6) Centrifuge the pellet at 720 x g at 4 °C for 10 minutes.
(7) Remove the supernatant and resuspend the pellet in 80 µl NL buffer. Agitate and incubate at 4 °C for 15 minutes. Optional: Sonicate the pellet on ice (2 x 3 sec sonication, separated by 3 sec resting, under 30% full amplitude power). This is the nuclear fraction including nuclear membranes.
(8) Centrifuge the supernatant from step 4 at 10,000 x g at 4 °C for 10 minutes.
(9) Carefully transfer the supernatant to a new 1.5 ml tube. This is the cytosolic and membrane fraction.

2.2.9 Protein concentration measurement

The protein concentration was determined with a Bio-Rad protein assay. After getting the protein lysates, 20 µl mixture of Reagent S and Reagent A (The ratio of Reagent S to reagent A is 1:50) was added into a 96-well plate followed by 2 µl of each sample and mixed with 200 µl Reagent B. The plate was incubated for 10 minutes at room temperature on the shaker. Then the protein concentrations were quantified by infinite M200 at 595 nm. A standard curve was produced by quantifying BSA samples of standard concentration (0, 0.125, 0.25, 0.5, 1, 1.5, 2 mg/ml.)

2.2.10 Western blot

2.2.10.1 Sample preparation for Western Blot

20-40 µg of protein was pipetted into a 1.5 ml tube, the mixed with 4X NuPage LDS Sample Buffer and 10 X DTT. Protein samples were adjusted to a volume with 1X

loading buffer. After incubation at 99 °C for 5 minutes, the protein samples were briefly centrifuged and loaded onto SDS/PAGE gels.

2.2.10.2 SDS-PAGE gel preparation

10% sodium dodecyl sulfate polyacrylamide electrophoresis (SDS-PAGE) gel was prepared as below:

2.2.10.3 Protein electrophoresis

After loading the protein samples, the gel was run in a Bio-Rad chamber at constant voltage of 120 V in SDS running buffer.

2.2.10.4 Western transfer

After the protein electrophoresis was finished, the gel was transferred to a nitrocellulose membrane. Chromatography paper and nitrocellulose membrane were used to prepare the gel-membrane sandwich. Blotting pads and the gel-membrane sandwich were placed in the Bio-Rad chamber with transfer buffer. Blotting was performed for 90 minutes at a constant current of 200 mM for one gel and 400 mM for two gels.

2.2.10.5 Immunodetection of proteins

The blotting nitrocellulose membrane was incubated with Ponceau Red solution to determine equal loading. After washing the membrane with TBST for 3 times, the membrane was block for 1 h at room temperature with 5 % milk (in TBST) on the shaker, followed by incubation with first antibody overnight at 4 °C. Next day, the membrane was washed for 5 minutes / 4 times in TBST buffer, and incubated with the second antibody for 1 h at room temperature, then washed for 5 minutes / 4 times in TBST. To achieve detection, the membrane was incubated with ECL solution. Chemiluminescence was detected using a Fujifilm LAS 1000 image detection system.

2.2.11 mRNA isolation, cDNA synthesis and real time PCR

2.2.11.1 RNA isolation

RNA isolation was performed using TRIZOL. Cells grows in 6-well plate were lysed with 300 µl TRIZOL and pipetted into Eppendorf tubes. Samples were added with 200 µl $CHCl_3$, mixed gently and stayed at room temperature for 3 minutes. After centrifugation at 4°C 13,000 rpm for 15 minutes, the supernatant was collected to a

new Eppendorf tube. The samples were added the same volume of isopropanol, mixed gently and stayed at room temperature for 10 minutes. After centrifugation at 4°C 13,000 rpm for 10 minutes, the supernatant was discarded and the precipitation was washed by 1 ml 70% ethanol. After centrifugation at 4°C 13,000 rpm for 10 minutes, the precipitation was dissolved in 75 µl DEPC water. RNA concentration was photometric determined by measuring the RNA solution in a nanocrystalline plate at 260 nm with Tecan infinite M200. The integrity of the isolated RNA was examined by formaldehyde agarose gel electrophoresis.

2.2.11.2 RNA electrophoresis

1 g agarose added into 100 ml TAE buffer was boiled and cooled down to allow polymerization. 200 ng RNA was separated for 1-2 hours to prove the integrity of the RNA samples and to demonstrate accuracy of the quantity-determination.

2.2.11.3 Reverse transcription

For cDNA synthesis, reverse transcription of 500 ng RNA was performed with Random Primer (Thermo Scientific), RevertAid H Minus M-MuLV reverse transcriptase (Thermo Scientific) and RNase inhibitor (Thermo Scientific) according to the manufacture instructions. 500 ng total RNA was reverse transcribed into 10 µl cDNA and used for quantitative real-time PCR and conventional PCR. For Real-Time PCR, cDNA samples were diluted 1:10 with DEPC water.

2.2.11.4 Quantitative real time PCR

20 µl mixture for real time PCR contained 5 µl cDNA, 4 µl SYBR Green, 0.5 µl forward primer, 0.5 µl reverse primer and 10 µl ddH2O was performed on a StepOnePlus Real-Time PCR (Applied Biosystem). PCR amplification cycling conditions comprised 10 minutes polymerase activation at 95 °C and 40 cycles at 95 °C for 15s and 60 °C 1 minutes. A melting curve analysis was performed for each PCR analysis. Relative quantification of target genes was normalized against the house keeping gene PPIA. The reverse and forward primers used for the current study are listed in Table 12.

Table 12. primers used for qRT-PCR in this study

Primer	Forward	Reverse
mBSEP	GGGAGCAGTGGGTGTGGTAAAAG	TCCTGGGAGACAATCCCAATGTT
mCYP7A1	GCTTGTAGAGAGCCACACCAA	AGTGGTGGCAAAATTCCCA
mFOXA2	CCCTACGCCAACATGAACTCG	GTTCTGCCGGTAGAAAGGGA

mFXR	GGCAGAATCTGGATTTGGAATCG	GCTGAACTTGAGGAAACGGG
mPPIA	GAGCTGTTTGCAGACAAAGTT	CCCTGGCACATGAATCCTGG
mRXR	CTGCCGAGACAACAAGGACT	TTCTCATTCCGGTCCTTGCC
mSHP	GTACCTGAAGGGCACGATCC	AGCCTCCTGTTGCAGGTGT
ChIP-mBSEP 1170-1625	CATTCATAGTTCAACCCAC	ATACCAACAGCCTACACC
ChIP-hBSEP 1114-1807	AGGTTGCAACTGTGGAGGTC	GGATGCTGACGAGTGTGAGA
ChIP-mFoxa2 567-963	GGCTGCAGACACTTCCTACT	CCTGAAGTGTGGTGGCTACT

2.2.12 Chromatine immunoprecipitation

Chromatin Immunoprecipitation was performed according to previous description (Nelson et al., 2006). After treatments as planned, approximately 1×10^6 cells were washed with ice cold PBS for two times. Chromatin was cross-linked by 1% formaldehyde for 10 minutes in 37 °C incubator. After removing the formaldehyde, cells were washed with cold PBS for two times. Subsequently, cells were scraped in cold PBS following centrifuge at 7000 rpm, 4°C for 5 minutes. After removing the supernatant, the pellet was resuspended in 100µl lysis buffer and was put on ice for 10 minutes. Sonication was performed using a Bioruptor plus (Diagenode SA, Liège, Belgium) with low power setting for 50 cycles of alternating pulses and pauses for 30 seconds each. Following centrifugation at 12,000 rpm, 4°C for 10 minutes, 10% of chromatin was diluted to 1:10 by dilution buffer and saved as input. The rest was also diluted to 1:10 by dilution buffer and separated in different groups according to the experimental setting. They were incubated with 45-50 µl Protein A/G Plus Agarose (Santa Cruz), 2µg salmon DNA for 2h at 4°C. After centrifugation at 2000 rpm, 4°C for 5 minutes, the supernatant was incubated with 2 µg of FOXA2 antibody or normal mouse IgG for 16h at 4°C. Next, antibody-protein complexes were added 45 µl of Protein A/G Plus Agarose and 2µg salmon DNA, and incubated for 1h at 4°C. After centrifugation at 2000 rpm for 5 minutes, the supernatant was removed. The pellets were washed by 1ml TSEI, TSEII, BufferIII and TE buffer for 10 minutes at 4°C one by one. After centrifugation at 2000 rpm for 10 minutes, the beads were washed by 100µl Elution buffer for 10 minutes at room temperature. Immunoprecipitated complexes

were reverse-crosslinked by heating at 65°C for 6h. Samples were cooled and treated with ddH_2O, phenol and chloroform, and then were centrifuged at 10,000 rpm for 5 minutes. The chromatin was precipitated with 1/10 volume of 1M sodium acetate (PH5.2) and 2 times volume of ethanol and put at -20°C for 10 minutes. After centrifugation at 10,000 rpm for 5 minutes, the eluted DNA was used for PCR analysis.

2.2.13 Immunofluorescence and confocal microscopy

2.2.13.1 Sample fixation

Cells were washed three times with ice cold PBS and fixed by 4% PFA/PBS for 10 minutes, followed by permeabilization and block with 0.5% Triton X-100/1% BSA for 1 h at room temperature on the shaker.

2.2.13.2 BSEP immunostaining

Cells were incubated with BSEP antibody (1:50 in PBS) overnight at 4 °C. Then the cells were washed 3 times with PBS, and incubated with Alexa-555-goat anti-mouse IgG (1:200 in PBS) and DRAQ5 for nuclei staining (1:1000 in PBS) for 1h at room temperature on the shaker. From this step, all procedures were protected from light. The samples were then washed 3 times with PBS and mounted on glass slides with fluorescent mounting medium. Samples were mounted on glass slides using Dakocytomation Fluorescent Mounting Medium (DakoCytotamation, hamburg, geermany).

2.2.13.3 Phase contrast and fluorescent microscopy

Phase contrast and conventional epi-fluorescence images were obtained with the Leica IPB microscope equipped with a Leica DC500 camera (Leica Microsystem, Wetzlar, Germany). For conventional epi-fluorescent images, excitation was performed with an EQB 100 isolated fluorescent lamp. Image acquisition was done with Leica IM50 software.

2.2.13.4 Confocal microscopy

Confocal images were obtained by using a Leica laser scanning spectral confocal microscope, model DM IRE2, with an HCX PL Apo 63 x/ 1 numeric aperture oil objective (Leica Microsystems, Wetzar, Germany). Excitation was performed with an argon laser emitting at 488 nm, a krypton laser emitting at 568 nm, and a helium/neon laser emitting at 633 nm. Images were acquired with a TCS SP2 scanner and Leica Confocal software, version 2.5 (Leica Microsystem).

2.2.14 Immunohistochemical staining

The Immunohistochemical staining protocol was used for formalin-fixed, paraffim-embedded tissue specimens. Do not allow slides to dry at any time during this procedure. This is the detailed protocol below:

1. Deparaffinization and rehydration
   (1) Incubate sections in 3 times xylene for 5 minutes each time;
   (2) Incubate sections in 1 time wash of 100% ethanol for 10 minutes;
   (3) Incubate sections in 1 time wash of 100% ethanol for 5 minutes;
   (4) Incubate sections in 1 time wash of 96% ethanol for 5 minutes;
   (5) Wash sections 3 times in PBS for 5 minutes each time;
2. Antigen unmasking
   Heat-induced epitope retrieval using a microwave with 1mM EDTA solution, pH 8.4.
   Total 10 minutes: 15 seconds boiling, 45 seconds waiting.
   Cool slides on bench to room temperature;
3. Blocking
   (1) Wash sections in PBS 3 times for 5 minutes each time;
   (2) Blocking: incubate sections in DAKO Blocking Peroxide for 30 minutes;
4. Staining primary antibody
   (1) Wash sections in PBS 3 times for 5 minutes each;
   (2) Dilute the primary antibody to the indicated concentration and adds the diluted antibody to the sections.
   (3) Incubate the sections overnight at 4°C;
5. Staining secondary antibody
   (1) Remove primary antibody and wash sections in PBS 3 times for 10 minutes each time;
   (2) Add corresponding secondary antibody diluted to the indicated concentration in PBS to each section and incubate for 45 minutes at room temperature;
   (3) Remove secondary antibody and rinse sections 3 times with PBS for 10 minutes;
6. Staining to detect horse radish peroxidase (HRP)
   (1) Prepare DAB solution: add 10mg DAB in 15mM Tris (hydroxymethyl)-aminomethean solution (pH 7.6), and then filter the clumps;

(2) Add 12ul H_2O_2 to the DAB solution to activate DAB, and then add the activated DAB to each section and monitor staining under a microscope;
Note: Let the sections develop 10 minutes but do not exceed 10 minutes and immerse slides in ddH_2O;
(3) Counterstain sections in hematoxylin for 10 to 30 seconds;
(4) Wash sections using tap water for 10 minutes;

7. Dehydrate sections
   (1) Incubate sections in 95% ethanol 2 times for 10 seconds each time;
   (2) Repeat in 100% ethanol, incubating sections 2 times for 10 seconds each time;
   (3) Repeat in xylene, incubating sections 2 times for 10 seconds each time;
   (4) Mounted the sections with malinol mounting medium;
8. Record the staining results using Leica upright research microscope.

3. RESULTS

3.1 FXR determines BSEP expression in hepatocytes

3.1.1 In HBV patients, both FXR and BSEP are expressed in hepatocytes

It is well recognized that FXR controls BSEP expression in normal hepatocytes (Ananthanarayanan et al., 2001). In this study, we observed the same phenomena in HBV patients and *in vitro*. In patients with chronic HBV infection, IHC staining for FXR and BSEP showed that hepatocytes expressed both FXR and BSEP (**Figure 7**). FXR resided in nuclei of hepatocytes, while BSEP was localized on bile canaliculi.

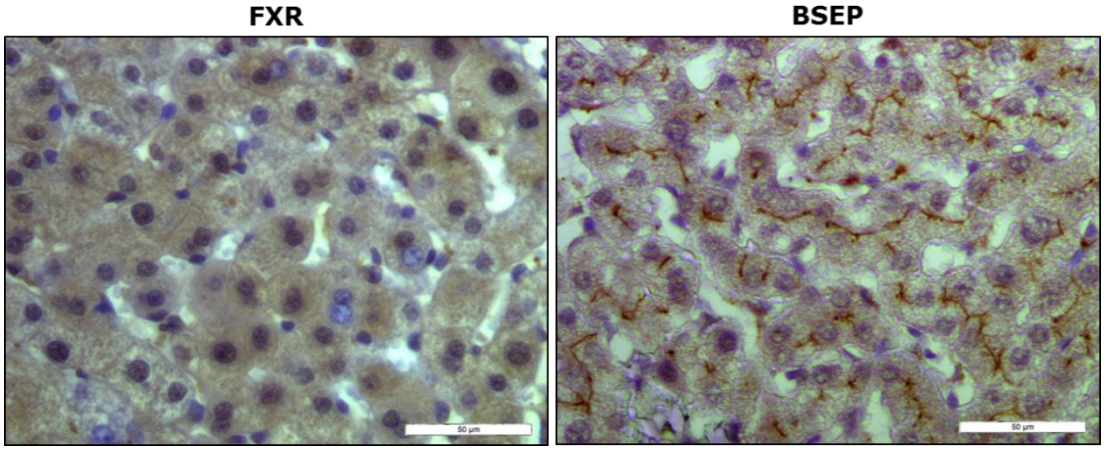

Figure 7. Immunohistochemistry staining depicts expression of FXR and BSEP in HBV infected patients.

3.1.2 Fxr promotes Bsep expression in AML12 cells and mouse primary hepatocytes

To confirm the role of Fxr in regulating Bsep expression, we treated hepatocytes with Fxr agonist GW4064. In AMl12 cells and collagen-sandwich cultured mouse primary hepatocytes, incubation with 5µM or 10 µM GW4064 for 48h induced high levels of mRNA and protein expression of Bsep (**Figure 8A-B**). GW4064 treatment did not alter the morphological profile of bile canaliculi (**Figure 8C**), however, it promoted Bsep expression on bile canaliculi in mouse primary hepatocytes (immunofluorescence staining in **Figure 8D**).

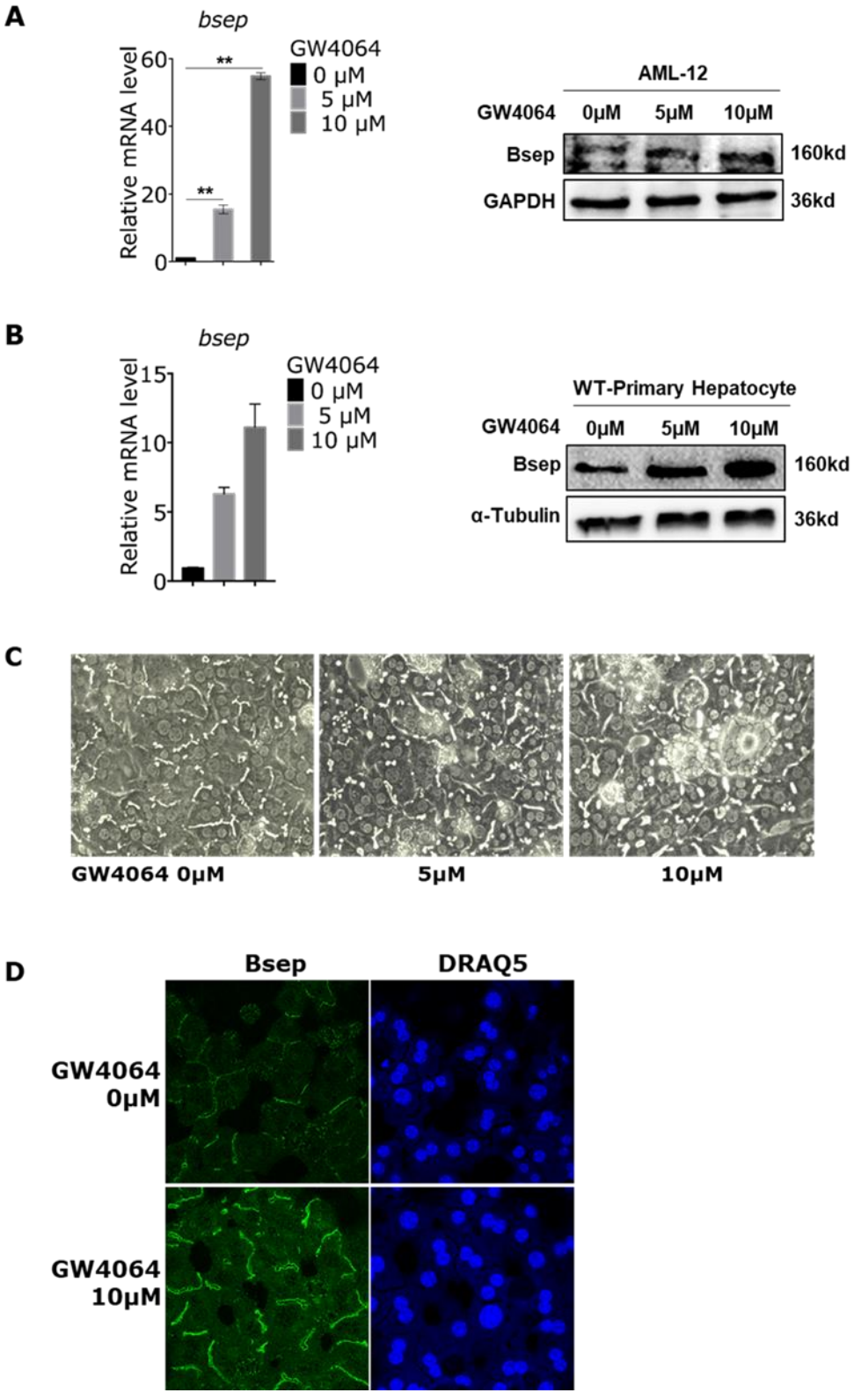

Figure 8. Fxr agonist GW4064 promotes Bsep expression on bile canaliculi. (**A-B**) qPCR and Western blotting were performed to analyze mRNA and protein expression of Bsep in AML-12 cells and mouse primary hepatocytes (MPHs) with different dosage of GW4064 treatment. (**C**) Polarized microscopy showed bile canaliculi in MPHs with or without GW4064 treatment. (**D**) Immunofluorescence staining showed Bsep in sandwich-collagen cultured MPHs with or without GW4064 treatment.

3.1.3 Fxr knock-down reduces Bsep expression in AML12 cells and mouse primary hepatocytes.

In contrary, knockdown of Fxr with shRNA significantly reduced mRNA and protein expression of Bsep in both AML12 cells (**Figure 9A**) and mouse primary hepatocytes (**Figure 9B**).

These results confirmed the key role of Fxr in the regulation of Bsep expression in normal hepatocytes.

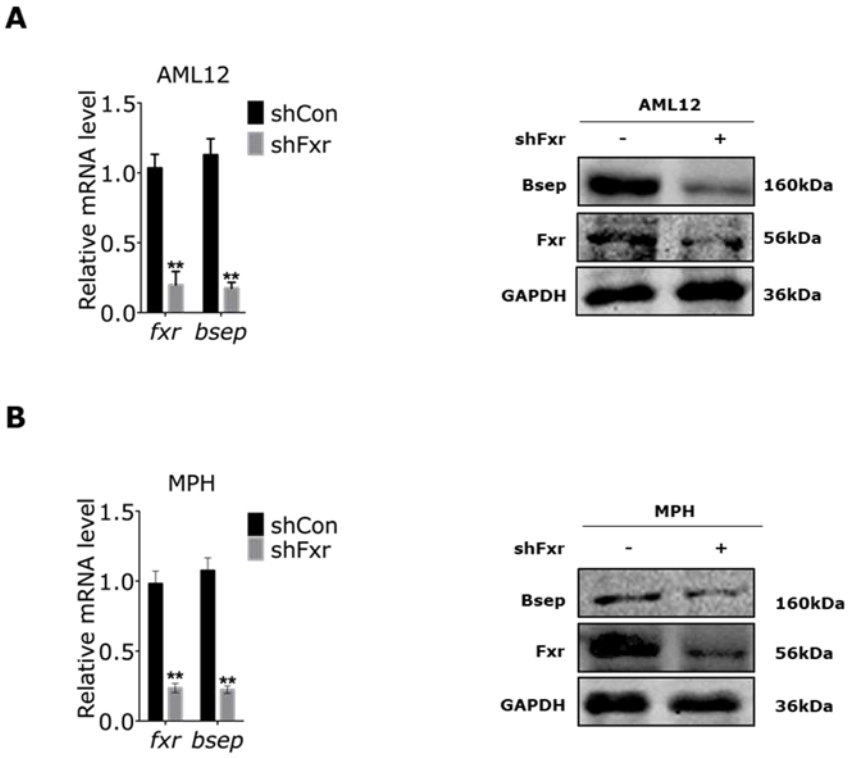

Figure 9. Fxr impacts Bsep expression in hepatocytes. (**A-B**) qPCR and Western blotting were performed to analyze mRNA and protein expression of Bsep in AML-12 cells and MPHs with or without shFxr treatment. For Western blotting, GAPDH was used as loading control.

3.2 Lack of BSEP is associated with high cholestasis and poor prognosis in ACLF patients

Firstly, we used immunohistochemical staining (IHC) to examine BSEP expression in 26 liver tissues (3 controlled, 5 chronic HBV infected, and 18 ACLF patients). IHC analysis showed intact BSEP apical expression in controlled (data not shown), chronic HBV infected and recovered ACLF patients (**Figure 10A**). In irreversible ACLF patients, 10 displayed BSEP expression in most hepatocytes while 3 did not have detectable BSEP expression in most areas of the specimens (**Figure 10A**).

We compared clinical parameters between ACLF patients possessing and lacking BSEP expression. There were no differences in age, and serum levels of alanine aminotransferase (ALT), aspartate aminotransferase (AST), albumin, and creatinine between the recovered and irreversible ACLF patients (**Figure 10B**). Compared to the irreversible patients, the recovered patients displayed longer clinical duration defined as the interval between acute decompensation and receiving histological examination although there was no statistically difference ($p>0.05$, **Figure 10B**). The recovered patients showed significant remarkably improved serum total bilirubin, international normalized ratio (INR) and Model for End-stage Liver Disease (MELD) score ($p<0.01$ for all parameters, **Figure 10B**). In addition, serum total bilirubin levels in the irreversible ACLF patients possessing or losing BSEP were also significantly different. Compared to the irreversible patients possessing BSEP, the patients who lost apical BSEP demonstrated higher serum total bilirubin concentration ($p<0.05$, **Figure 10B**). These results suggested that the maintenance of BSEP in hepatocytes was important for the recovery of ACLF.

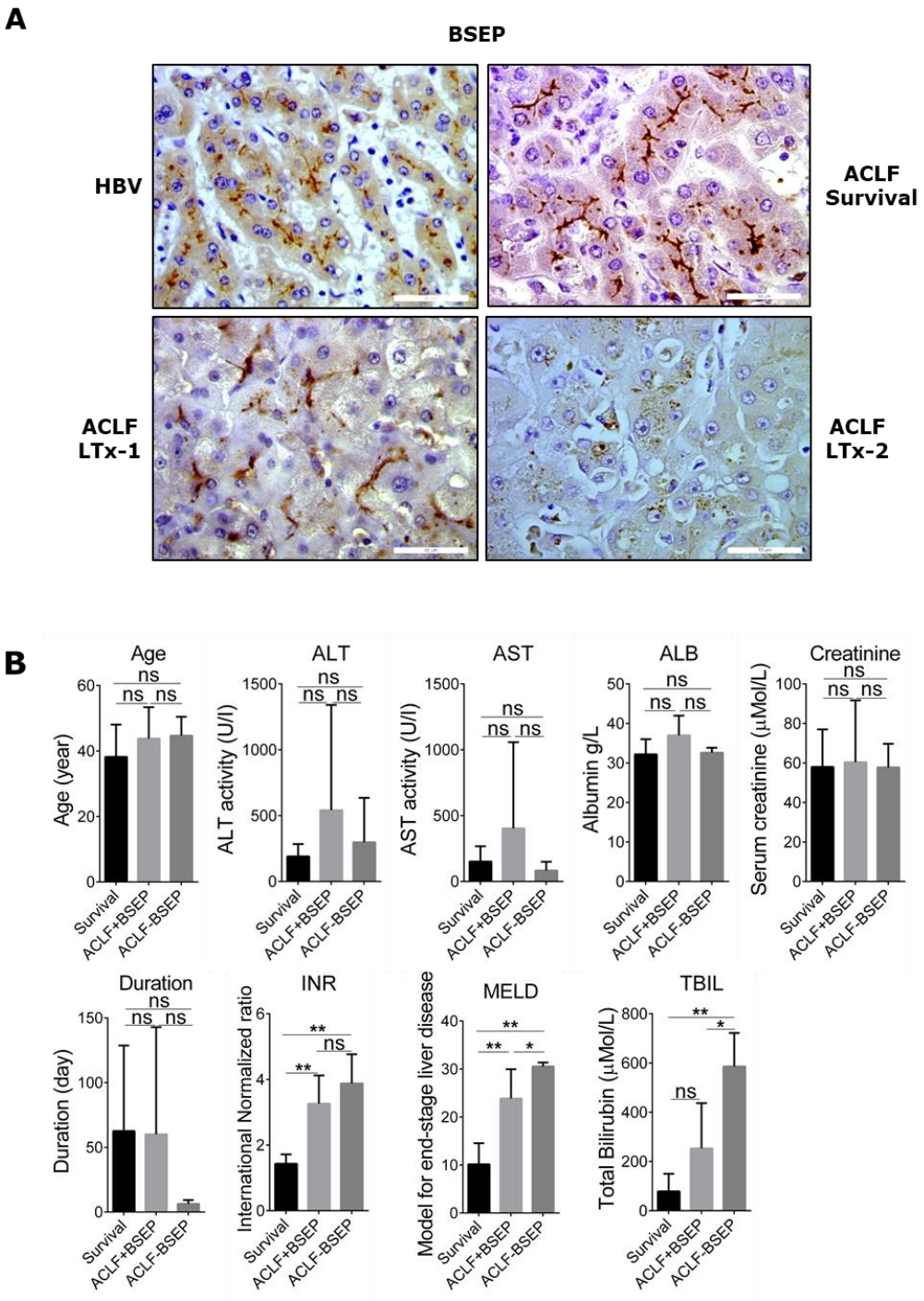

Figure 10. Immunohistochemistry staining depicts expression of BSEP in HBV infection and ACLF. (**A**) Immunohistochemistry staining of BSEP in HBV-infected patients, ACLF-recovered patients and ACLF-LTx patients. (**B**) Age, ALT, AST, ALB, Creatinine, Duration, INR, MELD and total bilirubin were compared between survival ACLF patients, irreversible ACLF patients maintaining BSEP and irreversible ACLF patients lacking BSEP.

3.3 Hepatocytes of ACLF patients maintain BSEP on bile canaliculi regardless of FXR expression

In end-stage of liver disease such as ACLF, the maintenance of BSEP on bile canaliculi plays a crucial role in disease recovery (Soroka and Boyer, 2014). Therefore, we measured expression of BSEP and FXR by IHC staining in 26 liver tissues (3 controlled, 5 chronic HBV infected, and 18 ACLF patients) and did the statistical analysis of the IHC statings. Only in controlled (data not shown) and HBV patients, FXR was in the nuclei of hepatocytes (**Figure 11A-B**). In ACLF-Survival and 10 ACLF-LTx patients, BSEP was located on the bile canaliculi of hepatocytes, while FXR was not detectable in the nuclei. 3 ACLF-LTx patients didn't display BSEP expression on bile canaliculi (**Figure 11A-B**). Next we performed real-time PCR to measure mRNA level of FXR and BSEP in ACLF livers. Compared to control group, FXR was decreased while BSEP was increased in ACLF liver tissue (**Figure 11C**). These results implied that BSEP expression in these ACLF patients seemed to be FXR independent.

3.4 FOXA2 expression in hepatocytes of ACLF patients

To clarify which transcription factor is replacing FXR for controlling BSEP expression in ACLF, we focused on transcription factors FOXA1, FOXA2, HNF4α and RXR, which have binding sites in the promoter of *bsep/abcb11* gene (https://www.genecards.org/cgi-bin/carddisp.pl?gene=ABCB11). In liver tissue, qPCR assay showd significantly elevated FOXA2 mRNA expression in ACLF patients compared to controls (**Figure 11C**). IHC staining showed that among these transcription factors, only FOXA2 was robustly expressed in nuclei of hepatocytes in 10 irreversible ACLF patients who maintained BSEP expression in hepatocytes (**Figure 11A-B**, IHC data not shown for additional transcription factors). In 3 ACLF patients without detectable BSEP, FOXA2 was also undectactable (**Figure 11A-B**). Notably, in 5 HBV patients with intact FXR expression, FOXA2 expression was also undectable (**Figure 11A-B**). These results suggested that FOXA2 might be required for BSEP expression on hepatocytes when FXR is silence.

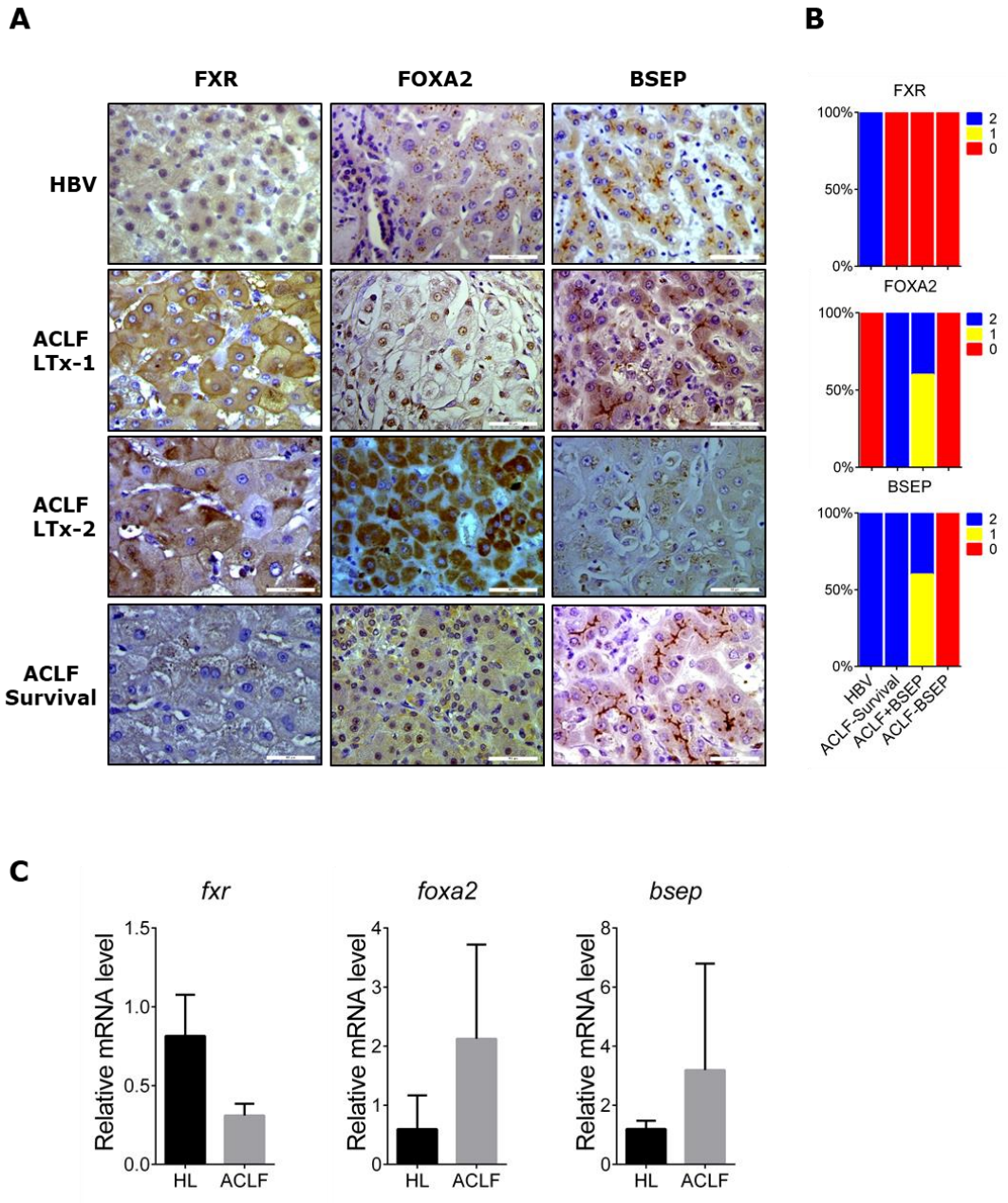

Figure 11. Immunohistochemistry staining depicts expression of FXR, FOXA2 and BSEP in HBV infection and acute-on-chronic liver failure (ACLF). (**A**) Representative staining depicted FXR, FOXA2 and BSEP expression in hepatocytes of 1 HBV and 3 ACLF patients respectively. (**B**) Immunostatining detection of FXR, FOXA2 and BSEP in the livers of 5 patients with chronic HBV infection and 18 patients with ACLF. (**C**) qPCR was performed in measuring mRNA expression of FXR, FOXA2 and BSEP in the liver tissues collected from three controls and 5 irreversible ACLF patients.

3.5 FOXA2 is required for BSEP expression in hepatocytes.

3.5.1 FOXA2 overexpression promotes BSEP expression in hepatocytes.

Next, we evaluated the role of FOXA2 in BSEP expression on bile canaliculi of hepatocytes. In cultured AMl12 and mouse/human primary hepatocytes, overexpressed FOXA2 significantly increased mRNA and protein expression of BSEP (**Figure 12A-F**). FOXA2 overexpression did not alter the morphological profile of bile canaliculi in hepatocytes (**Figure 12G**).

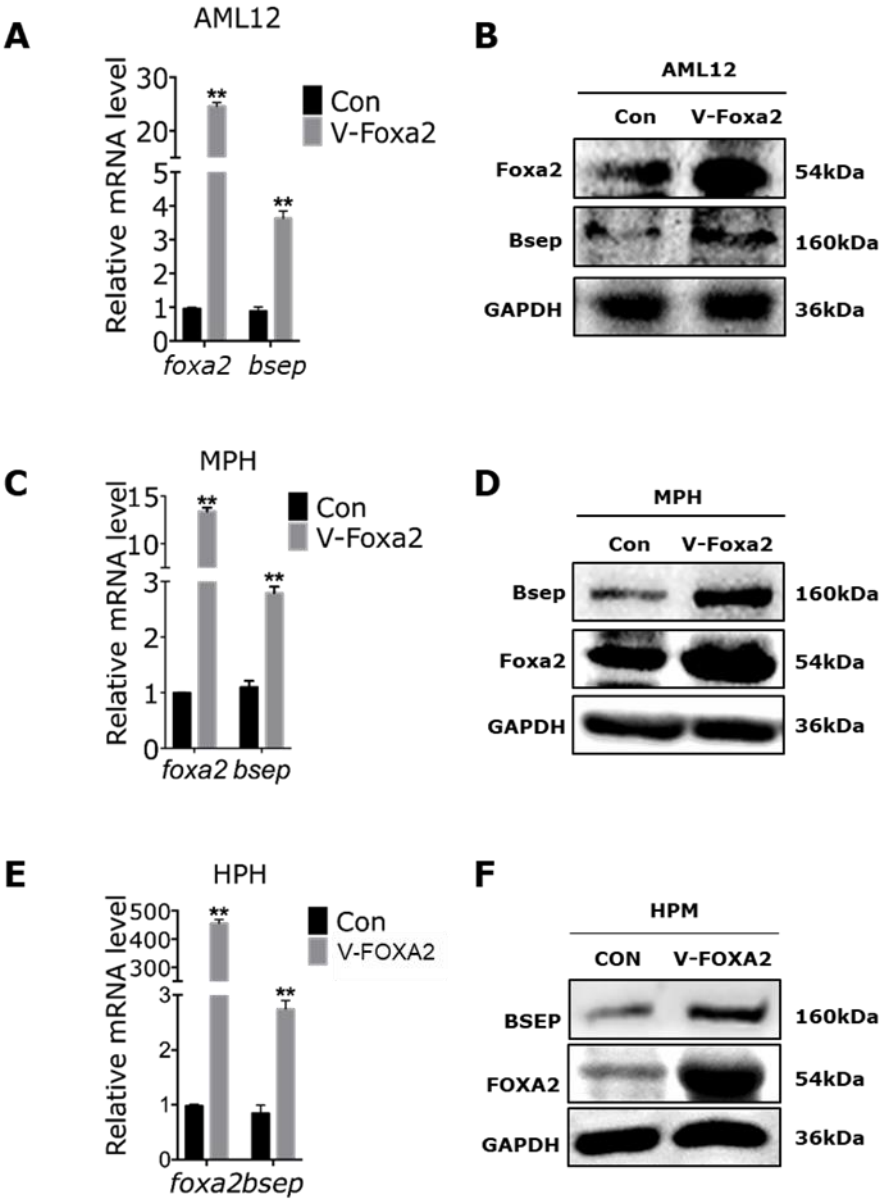

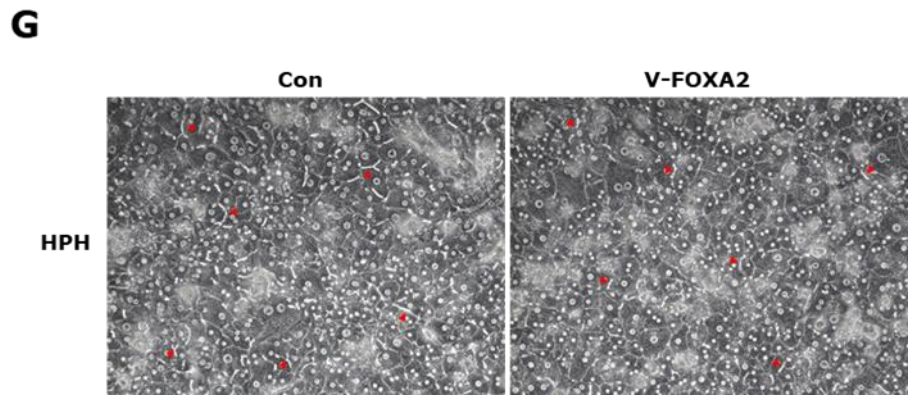

Figure 12. Overexpression of FOXA2 promotes BSEP expression in hepatocytes. (**A-D**) qPCR and Western blotting were performed to analyze mRNA and protein expression of Foxa2 and Bsep in AML-12 cells and MPHs with or without Foxa2 overexpression. (**E-F**) qPCR and Western blotting were performed to analyze mRNA and protein expression of FOXA2 and BSEP in HPHs with or without FOXA2 overexpression. (**G**) Polarized microscopy showed the morphological profile of bile canaliculi in HPHs with or without treatment by FOXA2 construct.

3.5.2 FOXA2 knockdown reduces BSEP expression in hepatocytes.

Consistent with the overexpression experiment, FOXA2 silence remarkably reduced mRNA and protein expression of BSEP in AML12 (**Figure 13A-B**), mouse primary hepatocytes (**Figure 13C-D**) and human primary hepatocytes (**Figure 13E-F**). In sandwich-collagen cultured primary hepatocytes, knockdown of Foxa2 did not alter the bile canaliculi morphological profile (Data not shown). However, knockdown of Foxa2 reduced mRNA and protein level of Bsep. Immunofluorescence staining further showed the reduction of Bsep on bile canaliculi of mouse primary hepatocytes when Foxa2 was knocked down (**Figure 13G**). These results suggested that FOXA2 is required for BSEP expression in hepatocytes.

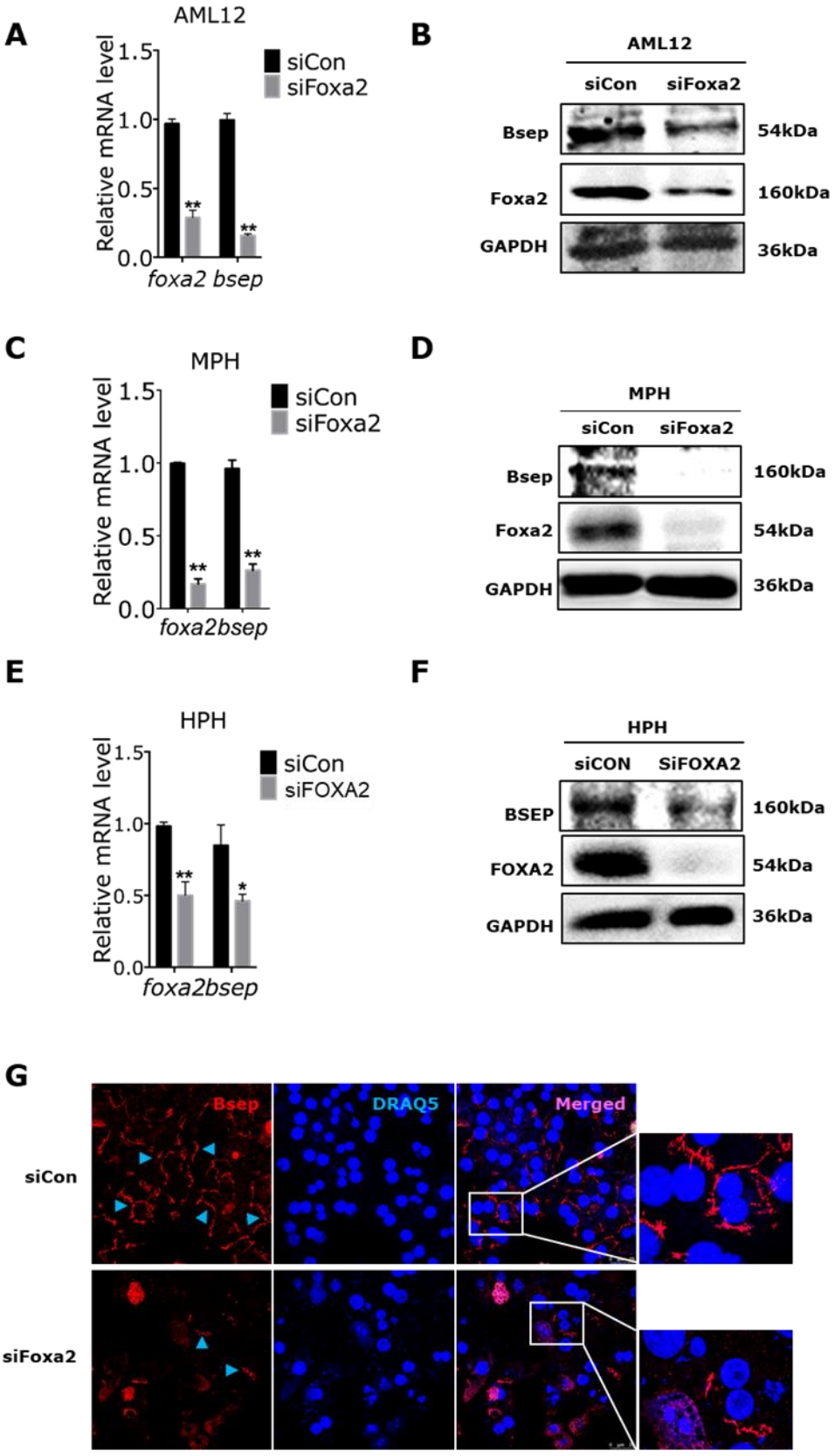

Figure 13. Knockdown of FOXA2 impacts BSEP expression in hepatocytes. qPCR and Western blotting were performed to analyze mRNA and protein expression of Foxa2 and Bsep in AML-12 cells (**A-B**), MPHs (**C-D**) and HPHs (**E-F**) with or without FOXA2 knockdown. Immunofluorescence staining shows Bsep in MPHs with or without Foxa2 knockdown (**G**). DRAQ5 was used to highlight nuclei of MPHs. For Western blotting, GAPDH was used as loading control.

3.6 Ectopic Foxa2 expression rescues Bsep expression on bile canaliculi when Fxr is disrupted *in vitro*

Subsequently, we investigated the relationship between Fxr and Foxa2 in the regulation of Bsep expression. In MPHs, knockdown of Fxr by shRNA and/or overexpression of Foxa2 did not alter the morphological profile of bile canalicular (**Figure 14A**). Overexpression of Foxa2 induced, but knockdown of Fxr reduced mRNA and protein expression of Bsep (**Figure 14B-E**). Impressively, ectopic Foxa2 expression restored shFxr-inhibited mRNA and protein expression of Bsep (**Figure 14D-E**). Morphological observation based on IF staining confirmed that shFxr-dependent Bsep reduction was restored by ectopic Foxa2 expression (**Figure 14F**). In addition, a similar phenomenon was observed in AML-12 cells (**Figure 15A-D**). These results suggested that Foxa2 was capable of rescuing Bsep expression on bile canaliculi when hepatocytes lost Fxr expression.

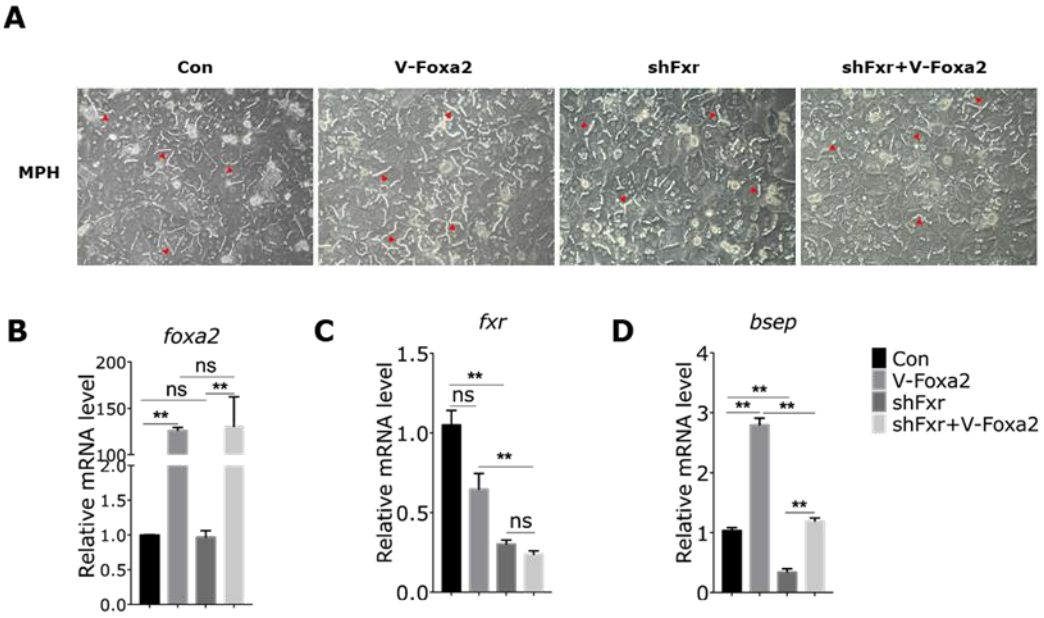

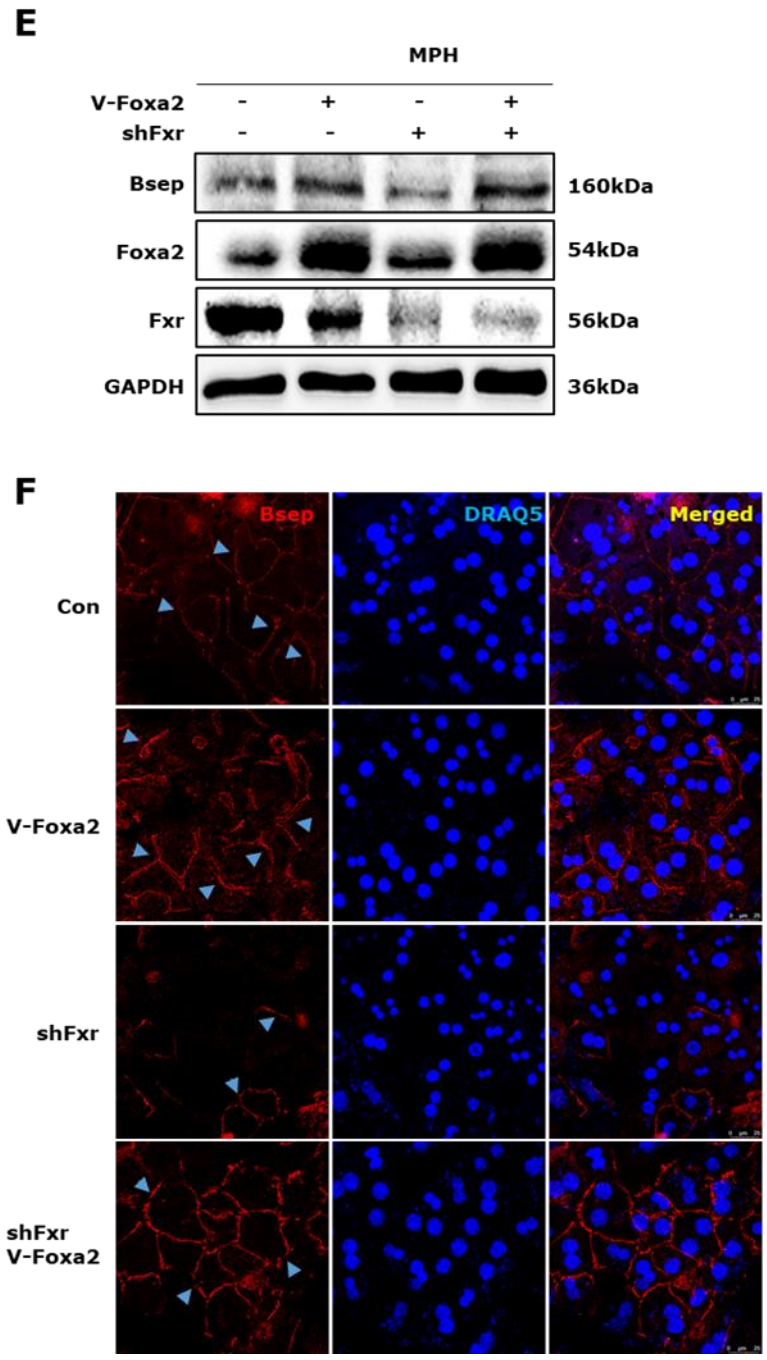

Figure 14. Ectopic Foxa2 expression restores Bsep expression in hepatocytes with Fxr knockdown. (**A**) Polarized microscopy showed bile canaliculi in MPHs, which were treated by shFxr and Foxa2 construct as indicated. (**B-E**) qPCR and Western blotting were performed to measure mRNA and protein expression of Foxa2, Fxr and Bsep in MPHs treated as indicated. For Western blotting, GAPDH was used as loading control. (**F**) Immunofluorescence staining was performed to measure Bsep expression in MPHs. DRAQ5 was used to highlight nuclei of MPHs.

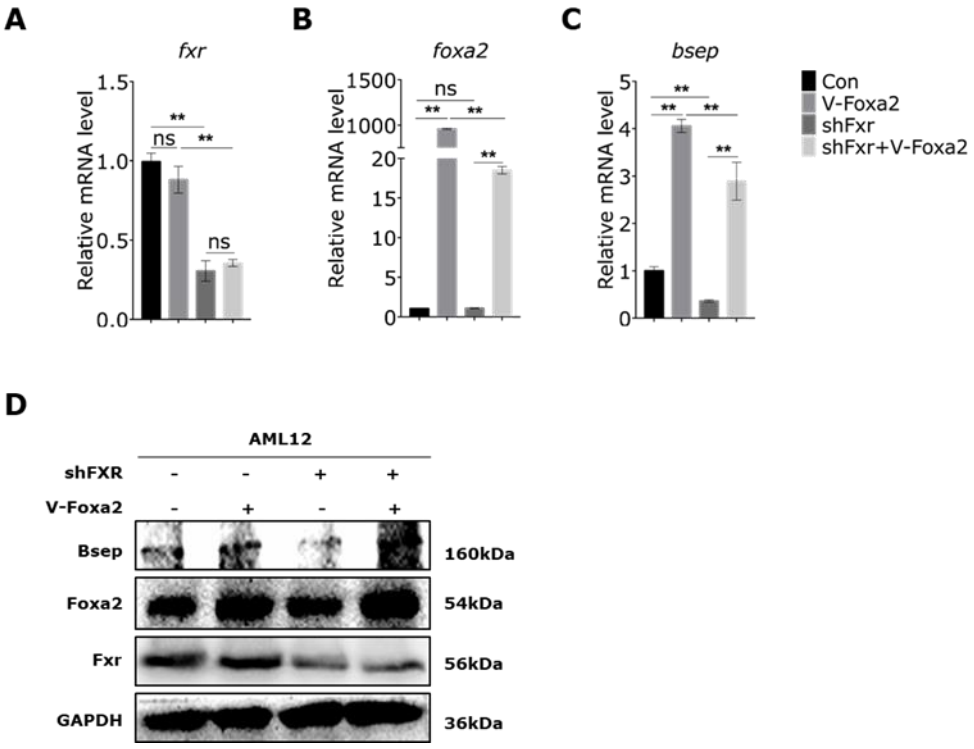

Figure 15. Ectopic Foxa2 expression restores Bsep expression in AML12 cells with Fxr knockdown. qPCR (**A-C**) and Western blotting (**D**) were performed to measure mRNA and protein expression of Foxa2, Fxr and Bsep in AML-12 cells as indicated treatment. For Western blotting, GAPDH was used as loading control.

3.7 Ectopic Foxa2 expression restores Bsep expression in *fxr* knockout mice

3.7.1 Bsep expression is remarkably decreased in *fxr* knockout mice

Next, we investigated Bsep expression in *fxr* knockout mice. In the livers of *fxr* knockout mice, mRNA and protein expression of Bsep were remarkably decreased (**Figure 16A-B**). IF staining further showed that Bsep expression was significantly reduced at bile canaliculi (**Figure 16C**).

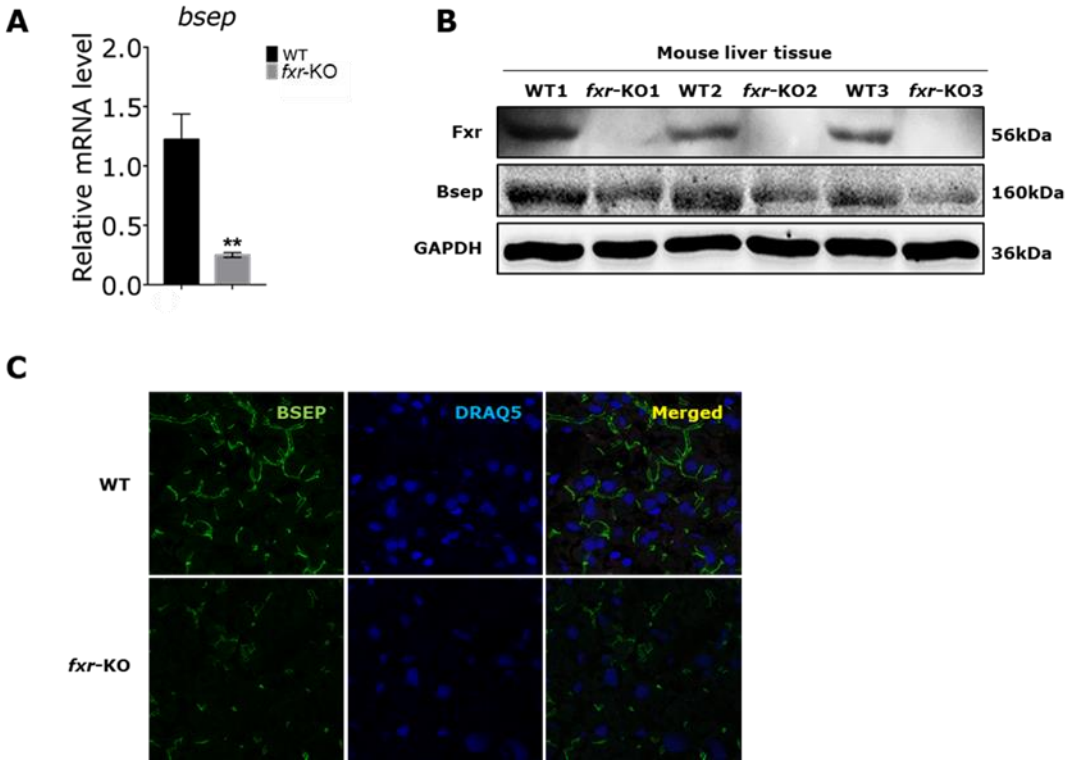

Figure 16. Bsep expression is significantly decreased in *fxr-/-* mice. (**A-B**) qPCR and Western blotting were performed to measure mRNA and protein expression of Bsep and Fxr in liver tissues of wild type and *fxr*$^{-/-}$ mice. For Western blotting, GAPDH was used as loading control. (**C**) Immunofluorescence staining was performed to measure Bsep expression in liver tissues of wild type and *fxr*$^{-/-}$ mice. DRAQ5 was used to highlight nuclei of hepatocytes.

3.7.2 Ectopic Foxa2 expression restores Bsep expresson in primay hepatocytes of *fxr* knockout mice.

Subsequently, we isolated hepatocytes from wild type and *fxr* knockout mice and transfected the cells by Foxa2 construct (V-Foxa2). Ectopic Foxa2 expression did not impact Fxr expression in hepatocytes, but restored Bsep expression on bile canaliculi of hepatocytes isolated from *fxr* knockout mice (**Figure 17A-C**). In addition, Ectopic Foxa2 expression also restored mRNA and protein expression of Bsep in the hepatocytes from *fxr* knockout mice (**Figure 17A-C**).

These results demonstrated that the lack of apical expression of Bsep due to Fxr gene knockout can be restored by ectopic Foxa2 expression at least *in vitro*.

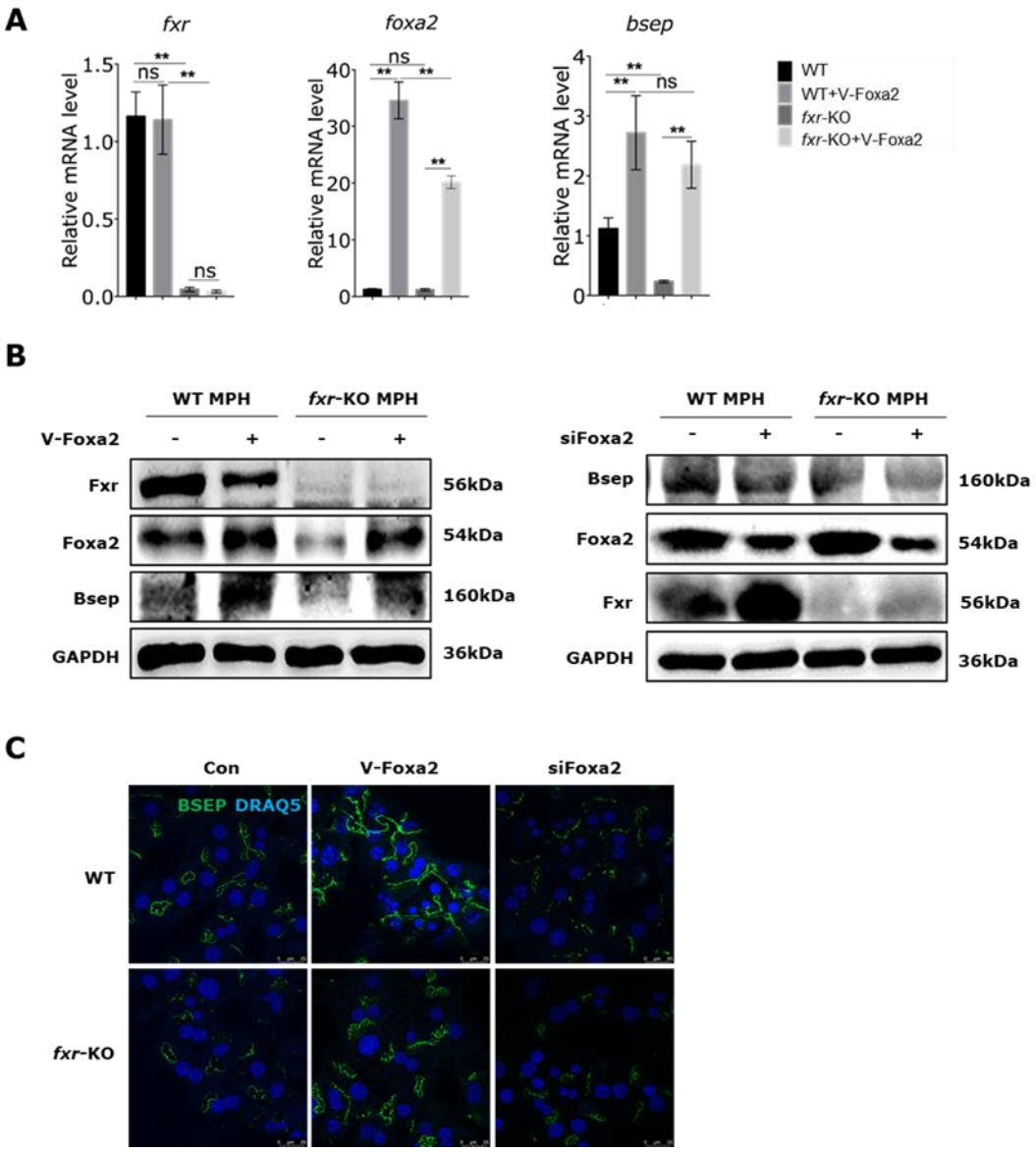

Figure 17. Ectopic Foxa2 expression restores apical Bsep expression in hepatocytes isolated from *fxr* knockout mice. (**A-B**) qPCR and Western blotting were performed to measure mRNA and protein expression of Foxa2, Fxr and Bsep in hepatocytes isolated from wild type or *fxr*$^{-/-}$ mice. The MPHs were transfected with control vector or Foxa2 construct. For Western blotting, GAPDH was used as loading control. (**C**) Immunofluorescence staining was performed to measure Bsep expression in hepatocytes isolated from wild type or *fxr*$^{-/-}$ mice. The MPHs were transfected with control vector or Foxa2 construct (V-Foxa2). DRAQ5 was used to highlight nuclei of MPHs.

3.7.3 Ectopic Foxa2 expression restores apical Bsep expression in hepatocytes of *fxr* knockout mice.

Next, we investigated Bsep expression on fxr knockout mice. In *fxr* knockout mice, mRNA and protein expression of Bsep in the liver tissues were remarkably decreased (**Figure 18 A-B**). IF staining further showed that Bsep expression was significantly reduced on bile canaliculai (**Figure 18C**). To clarify the role of Foxa2 in the regulation of Bsep expression, we injected adenovirus Foxa2 into wild type and *fxr* knockout mice. As shown in Figure 18A-B, administration of adenovirus of Foxa2 did not impact mRNA and protein expression of Fxr in the livers. However, the viral partially restored mRNA and protein expression of Bsep in the *fxr* knockout mice. IF staining displayed increased apical Bsep expression in hepatocytes of the *fxr* knockout mice (**Figure 18C**).

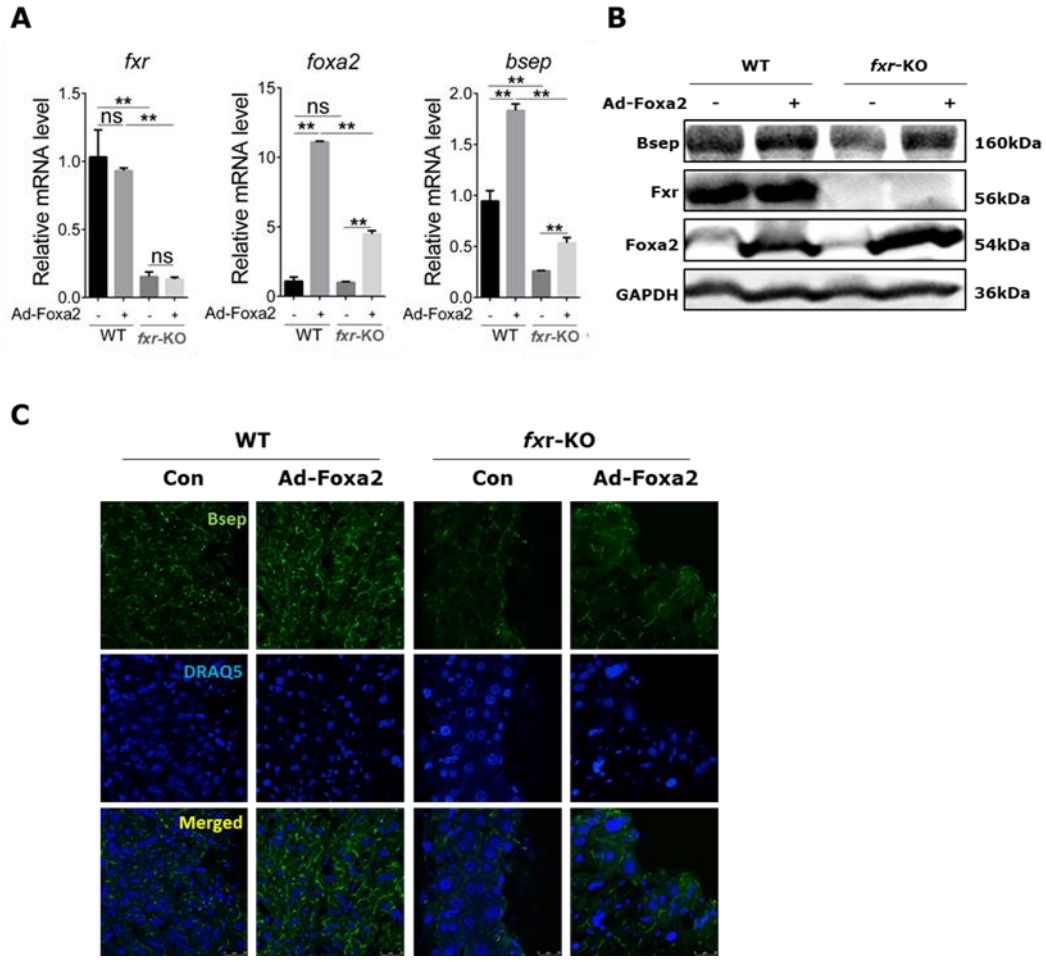

Figure 18. Ectopic Foxa2 expression restores apical Bsep expression in *fxr* knockout mice. (A-B) qPCR and Western blotting were performed to measure mRNA and protein expression of Bsep and Fxr in liver tissues of wild type and *fxr* knockout mice. (C) Immunofluorescence staining was performed to measure Bsep expression in liver tissues of wild type and *fxr* knockout mice.

3.8 Foxa2 up-regulates Bsep through binding to its promoter

Subsequently, ChIP assay confirmed that Foxa2 bound to the promoter of *bsep* at 1170 – 1625 bp upstream from the transcription start site in both AML-12 and MPHs (**Figure 19A**). Knockdown of Foxa2 by RNAi or ectopic expression of Foxa2 significantly reduced or increased the binding, respectively. Consistant with mouse hepatocytes, ectopic expression of Foxa2 also bound to the *bsep* promoter in HPHs (**Figure 19B**). Interestingly, compared to MPHs obtained from wild type mice, ectopic Foxa2 displayed much higher binding activity to *bsep* promoter in MPHs isolated from *fxr* knockout mice (**Figure 19C**). It appears that the presence of Fxr might inhibit Foxa2 binding to the *bsep* gene promoter. To clarify the issue, we examined Fxr binding sites in *bsep* promoter. ChIP assay showed that FXR also bound to the promoter of bsep at 1170-1625 bp uostream from the transcription atart site in MPHs (**Figure 19D**). Subsequently, we observed whether Fxr agonist GW4064 impacted on Foxa2 binding to the *bsep* gene promoter. ChIP analysis showed that GW4064 inhibited Foxa2 binding to the promoter of *bsep* gene in MPHs (**Figure 19E**). These results suggested that FXR and FOXA2 competed binding sites in the promoter of bsep gene.

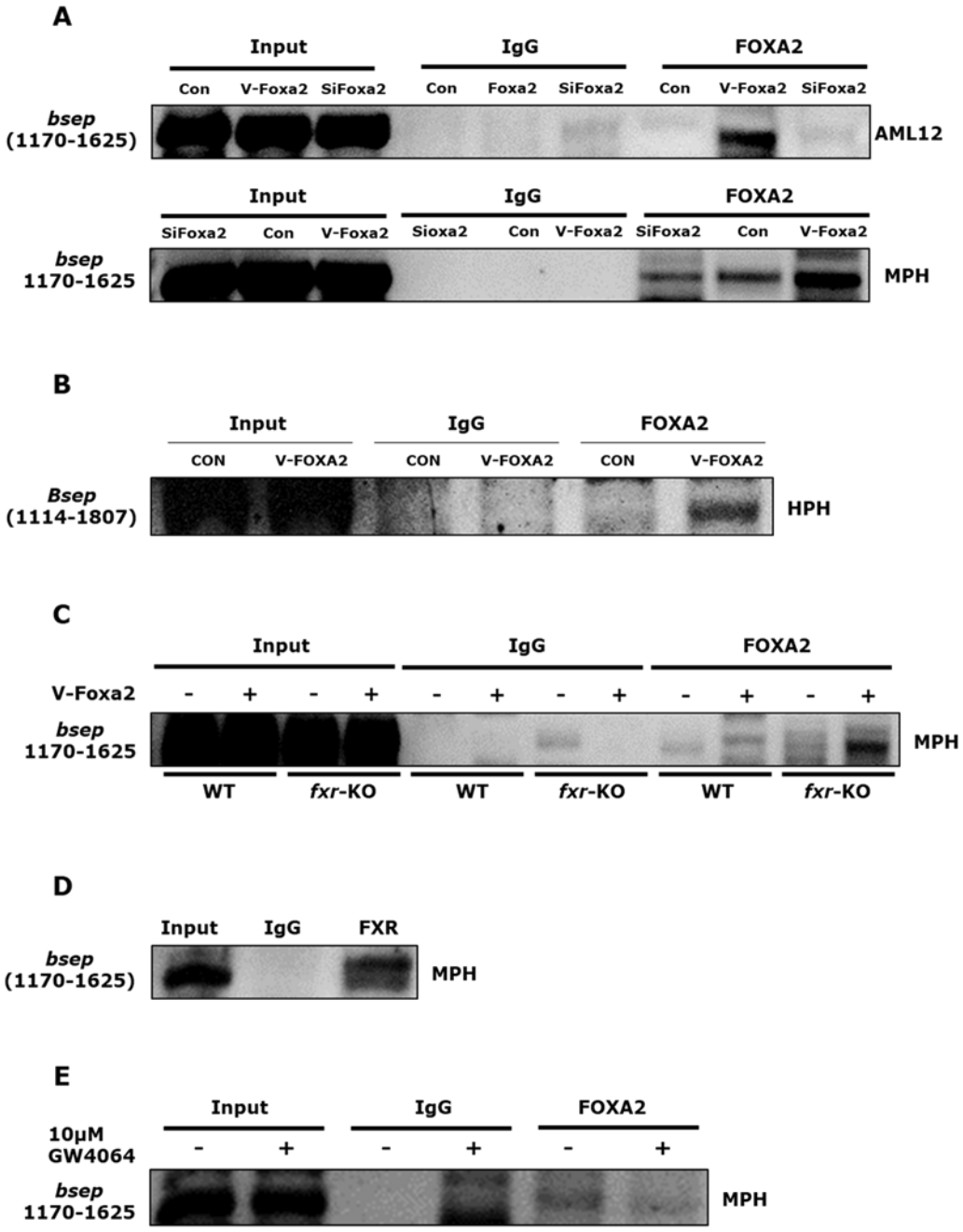

Figure 19. Foxa2 binds to the *bsep* gene promoter, which is impacted by Fxr. (**A**) ChIP assay was used to measure the binging of protein Foxa2 on 1170 – 1625 bp upstream from transcription starting site of *bsep* gene in AML-12 cells and mouse primary hepatocytes (MPHs) with or without Foxa2 siRNA or Foxa2 construct (V-Foxa2) as indicated. (**B**) ChIP assay was used to measure the binding of protein FOXA2 on 1114-1807 bp upstream from transcription starting site of bsep gene in HPHs with FOXA2 construct (V-FOXA2). (**C**) ChIP assay was used to measure the binging of protein Foxa2 on 1170 – 1625 bp upstream from transcription starting site of *bsep* gene in WT and FXR-KO primary hepatocytes with or without Foxa2 construct. (**D**) ChIP assay was used to measure the binging of protein Fxr on 1170 – 1625 bp upstream from transcription starting site of *bsep* gene in MPHs. (**E**) ChIP assay showed the impact of Fxr agonist GW4064 in Foxa2 binding to the promoter of *bsep* gene in MPHs.

3.9 Balance between insulin and glucagon influences Foxa2-dependent Bsep expression

3.9.1 Glucagon induces Bsep expression through upregulating Foxa2.

Previous studies found the regulatory effects of glucagon and insulin on Foxa2 expression and localization in hepatocytes (von Meyenn et al., 2013; Wolfrum et al., 2004). Thus, we examined the effect of glucagon and insulin on Foxa2 expression in hepatocytes. Administration of glucagon significantly induced mRNA and protein expression of Foxa2 and Bsep in MPHs, HPHs and AML-12 cells (**Figure 20A, B, D, E** and **Figure 21A-B**). Knockdown of Foxa2 compromised the stimulatory effects of glucagon on Bsep expression (**Figure 20A-B** and **Figure 21A-B**). ChIP assay showed that glucagon administration increased Foxa2 binding to bsep gene promoter in MPHs (**Figure 20C**).

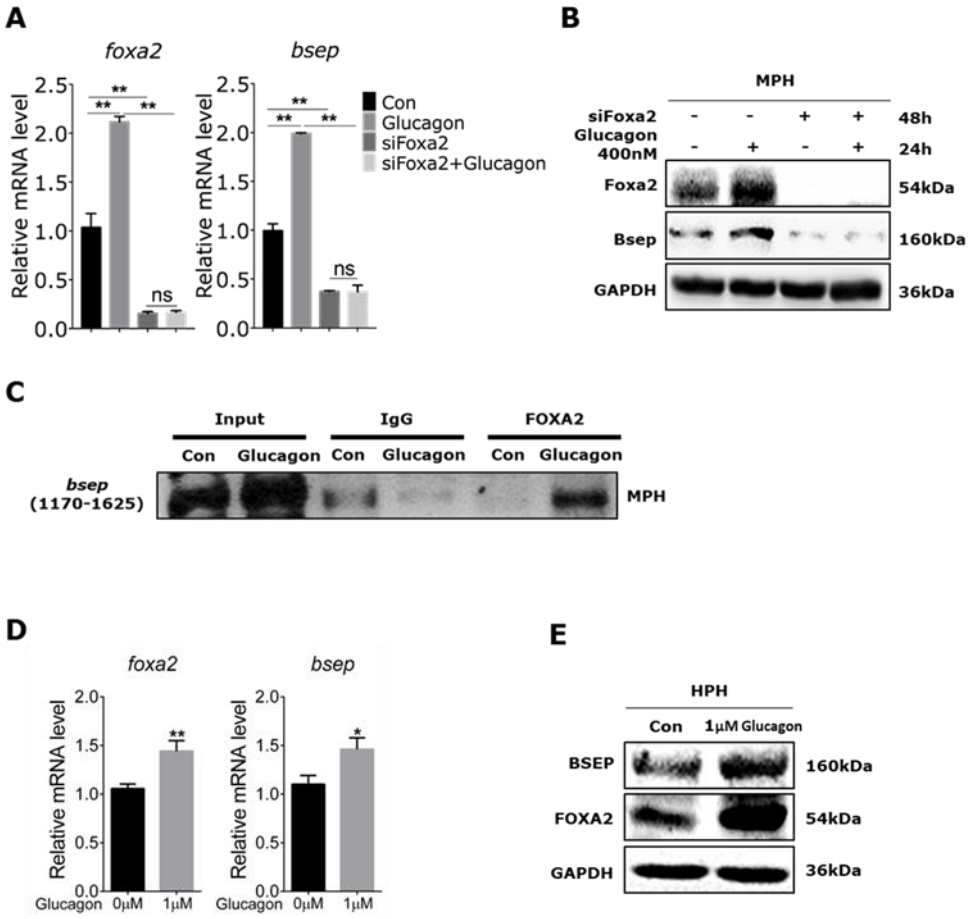

Figure 20. Glucagon induces Bsep expression through upregulating Foxa2. (**A-B**) qPCR and Western blotting were performed to measure mRNA and protein expression of Bsep and Foxa2 in MPHs with treatment as indicated. (**C**) ChIP assay showed the impact of glucagon in Foxa2 binding to the

promoter of *bsep* gene in MPHs. (**D-E**) qPCR and Western blotting were performed to measure mRNA and protein expression of Bsep and Foxa2 in HPHs with treatment as indicated.

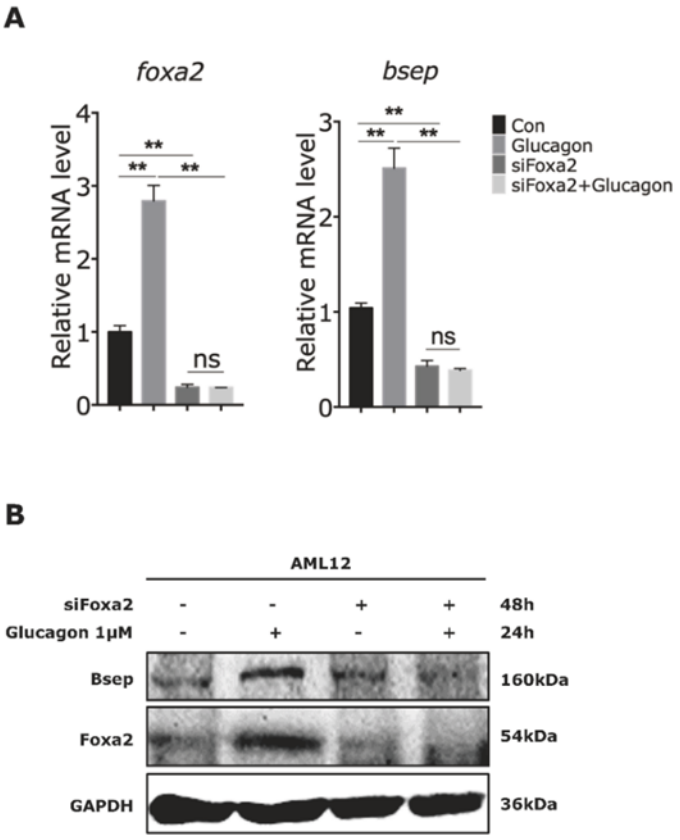

Figure 21. Glucagon induces Bsep expression through upresulating Foxa2 in AML-12 cells. qPCR (**A**) and Western blotting (**B**) analyses were performed to measure mRNA and protein expression of Bsep and Foxa2 in AML-12 cells with treatment as indicated. For Western blotting, GAPDH was used as loading control.

3.9.2 Insulin inhibits Foxa2 activation via insulin-Akt signaling-mediated phosphorylation at Thr156 and nuclear exclusion.

In contrast to glucagon, administration of 400nM insulin for 2h inhibited Foxa2 activation via phosphor-Akt-mediated phosphorylation at Thr156 of Foxa2 (**Figure 22A**). Besides, the subcellular fraction and western blotting indicated 400nM insulin treatment for 2h induced Foxa2 nuclear exclusion in MPHs (**Figure 22B**). The immunofluorescence of Foxa2 and ZO-1 (which is the maker of the tight junction, to show the MPHs are in normal condition.) also showed insulin induced Foxa2 nuclear exclusion in MPHs (**Figure 22C**).

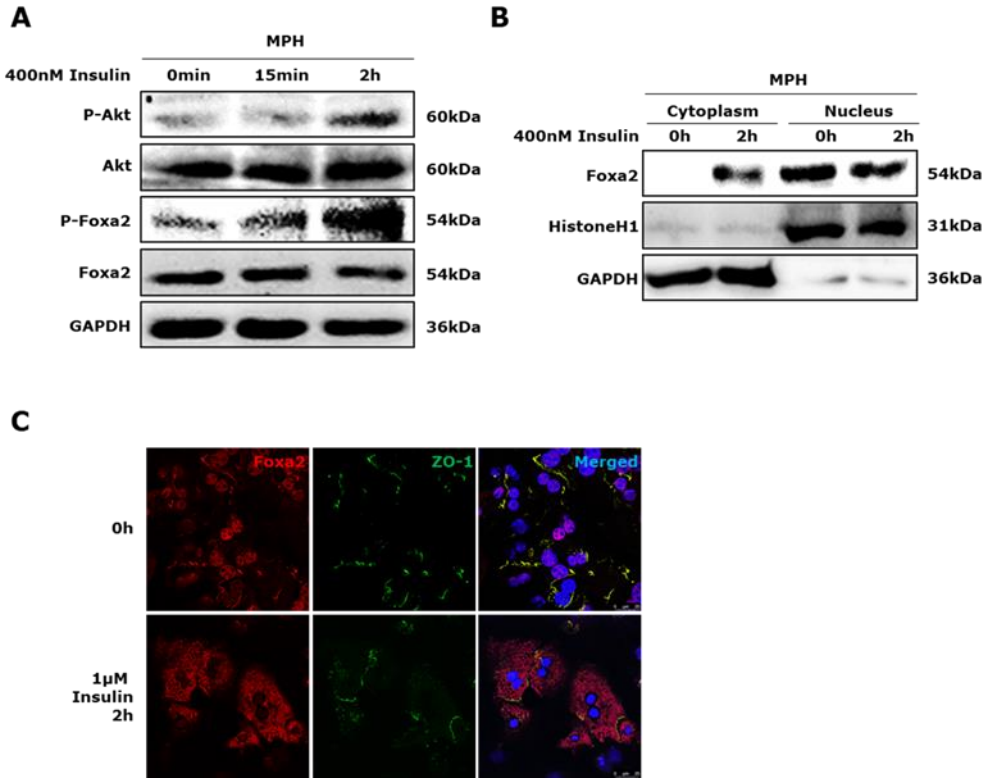

Figure 22. Insulin inhibits Foxa2 activation. (**A**) Western blotting measured phosphor-Akt (Ser473) and phosphor-Foxa2 (Thr156) in MPHs with 400nM insulin for 0min, 15min and 2h. (**B**) Western blotting measured cytoplasm and nucleus expression of Foxa2 in MPHs with or without insulin treatment. (**C**) Immunofluorescence staining was performed to measure Foxa2 and ZO-1 expression in MPHs with or without insulin treatment. DRAQ5 was used to highlight nuclei of MPHs.

3.9.3 Glucagon restores insulin-mediated inhibition to Foxa2 and Bsep.

Considering there are both high level of insulin and glucagon in ACLF condition, next we treated the MPHs with insulin and glucagon in the same time for 24h, to identify how it will affect Foxa2 activation and Bsep expression. We found that insulin treatment for 24h inhibited Foxa2 and Bsep expression, but high levels of glucagon administration restored insulin-inhibited effect (**Figure 23A-B**).

These results suggested that the balance of glucagon and insulin determined Foxa2-dependent Bsep expression in hepatocytes.

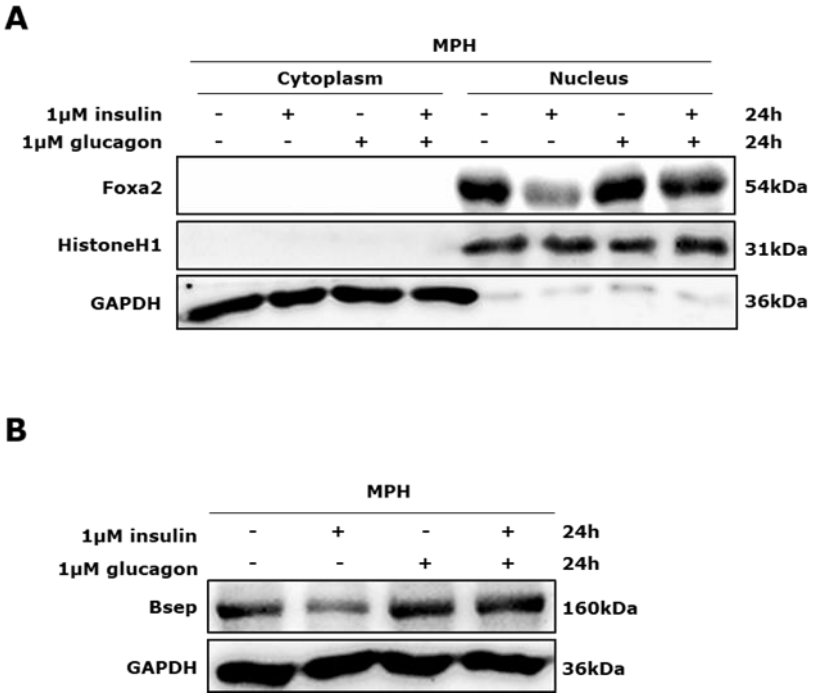

Figure 23. Glucagon restored insulin-mediated inhibition to Foxa2 and Bsep. (**A**) Western blotting measured cytoplasm and nucleus expression of Foxa2 in MPHs with or without insulin and/or glucagon treatment. For Western blotting, GAPDH was used as loading control. HistoneH1 was used as load control for nucleus protein. (**B**) Western blotting measured protein expression of Bsep in MPHs with treatment as indicated.

3.10 Inflammation inhibits Fxr but induces Foxa2 in hepatocytes

3.10.1 TNFα and LPS induce Foxa2-dependent Bsep expression.

ACLF patients undergo SIRS, which is characterized by a pro-inflammatory cytokine storm in response to acute infection by e.g. simultaneous peritoneal relevant to gram-negative infection (Jalan et al., 2012). In such a condition, bacterial components, e.g. LPS and pro-inflammatory cytokines such as TNFα might remarkably influence hepatocyte behavior, including FXR, FOXA2 and BSEP expression and insulin resistance. *In vitro*, we observed expression of Bsep, Fxr, and Foxa2 in MPHs and HPHs upon LPS or TNFα treatment for 24h. As shown in **Figure 24A-B**, both LPS and TNFα incubation for 24 h inhibited protein expression of Fxr and induced Foxa2 and Bsep. In addition, ChIP assay indicates that the inflammation promotes Foxa2 binding to *bsep* gene promoter in MPHs (**Figure 24C-D**). To further identify if Bsep induction by TNFα/LPS was dependent on Foxa2, we knocked down Foxa2 with siRNA and administrated the MPH with LPS or TNFα. Knockdown of Foxa2 compromised the stimulatory effects of inflamation on Bsep expression (**Figure 24E-F**).

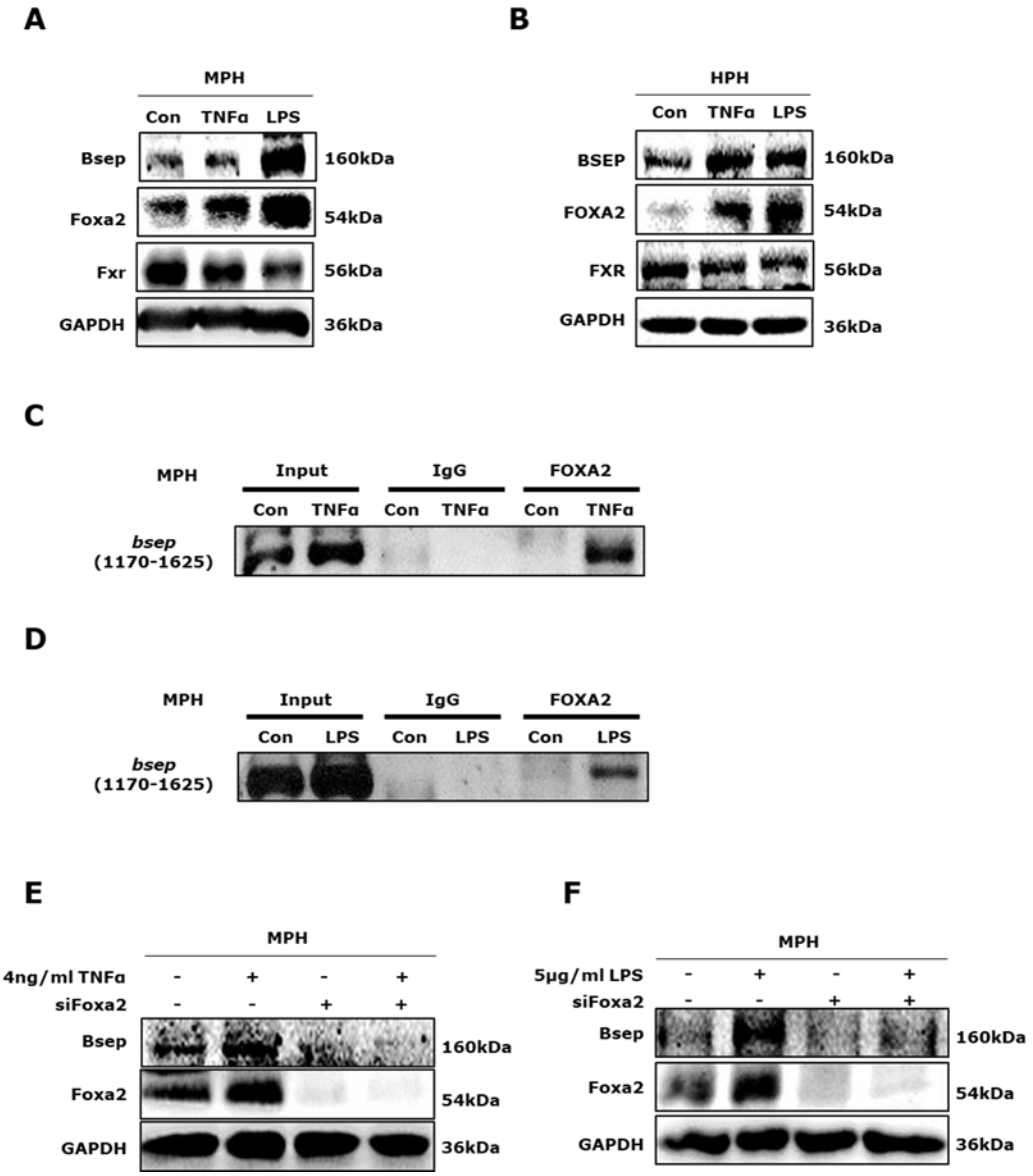

Figure 24. TNFα and LPS induce Foxa2-dependent Bsep expression. (**A-B**) Western blotting measures protein expression of Fxr, Bsep, and Foxa2 in MPHs and HPHs with LPS and/or TNFα treatment. (**C-D**) ChIP assay shows the impact of TNFα and LPS in Foxa2 binding to the promoter of *bsep* gene. (**E-F**) Western blotting was performed to measure protein expression of Bsep and Foxa2 in MPHs as indicated. GAPDH was used as loading control.

3.10.2 TNFα administration induces insulin resistance in hepatocytes.

Administration of TNFα significantly inhibited insulin-induced Akt phosphorylation in mouse and human hepatocytes, indicating the occurrence of insulin resistance (**Figure 25A, C**). In insulin resistance situation, total Foxa2 protein expression was induced while the Thr156 phosphorylation in Foxa2 wass inhibited, which means administration of TNFα inhibited insulin-induced p-Foxa2 expression (**Figure 25B, D**). The results suggested that TNFα induced Foxa2-dependent Bsep expression at least through inhibiting Fxr and inducing insulin resistance in hepatocytes.

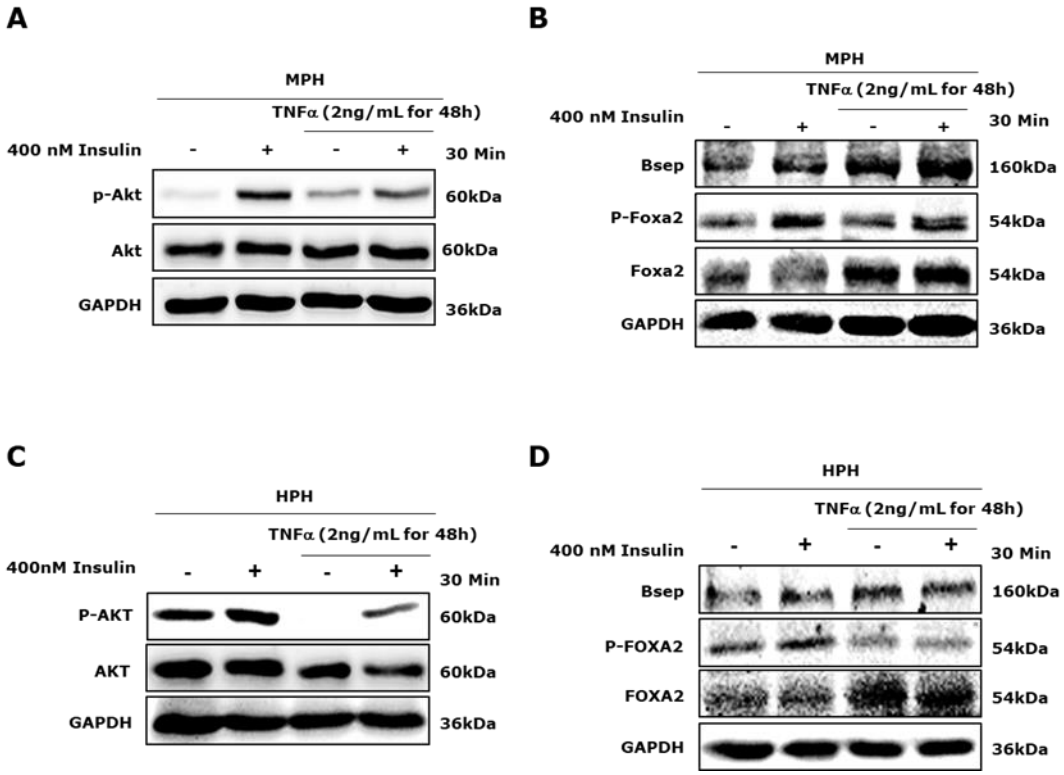

Figure 25. TNFα induces insulin resistance in MPHs and HPHs. (**A**) Western blotting measured protein expression of phosphorylated Akt (p-Akt) and total Akt in MPHs as indicated treatment. (**B**) Western blotting measured protein expression of Bsep, phosphorylated Foxa2 (p-Foxa2) and total Foxa2 in MPHs with treatment as indicated administration. (**C**) Western blotting measured protein expression of phosphorylated AKT (p-AKT) and total AKT in HPHs as indicated treatment. (**D**) Western blotting measured protein expression of Bsep, phosphorylated FOXA2 (p-FOXA2) and total FOXA2 in HPHs as indicated. GAPDH was used as loading control.

3.10.3 LPS induces Foxa2-dependent Bsep expression through NFκB signaling

Like TNFα, 2-5ug/ml LPS induced Foxa2 and Bsep expression in MPHs after 24h incubation (**Figure 26A**). LPS often exploits NFκB signaling to initiate target gene transcription (Oeckinghaus A 2011 Nature immunology). Therefore, we examined whether p65, a NFκB signaling protein possessing binding sites in the *foxa2* gene promoter, was the transcription factore initiating Foxa2 expression in hepatocytes. ChIP analysis confirmed the binding of p65 in the *foxa2* gene promotor in MPHs (**Figure 26B**).When MPHs were treated by p65 nuclear translocation inhibitor JSH23 (**Figure 26C-D**), p65 binding to the *foxa2* gene promoter was blocked (**Figure 26B**). Expression of Foxa2 and Bsep were subsequently inhibited (**Figure 26E**).

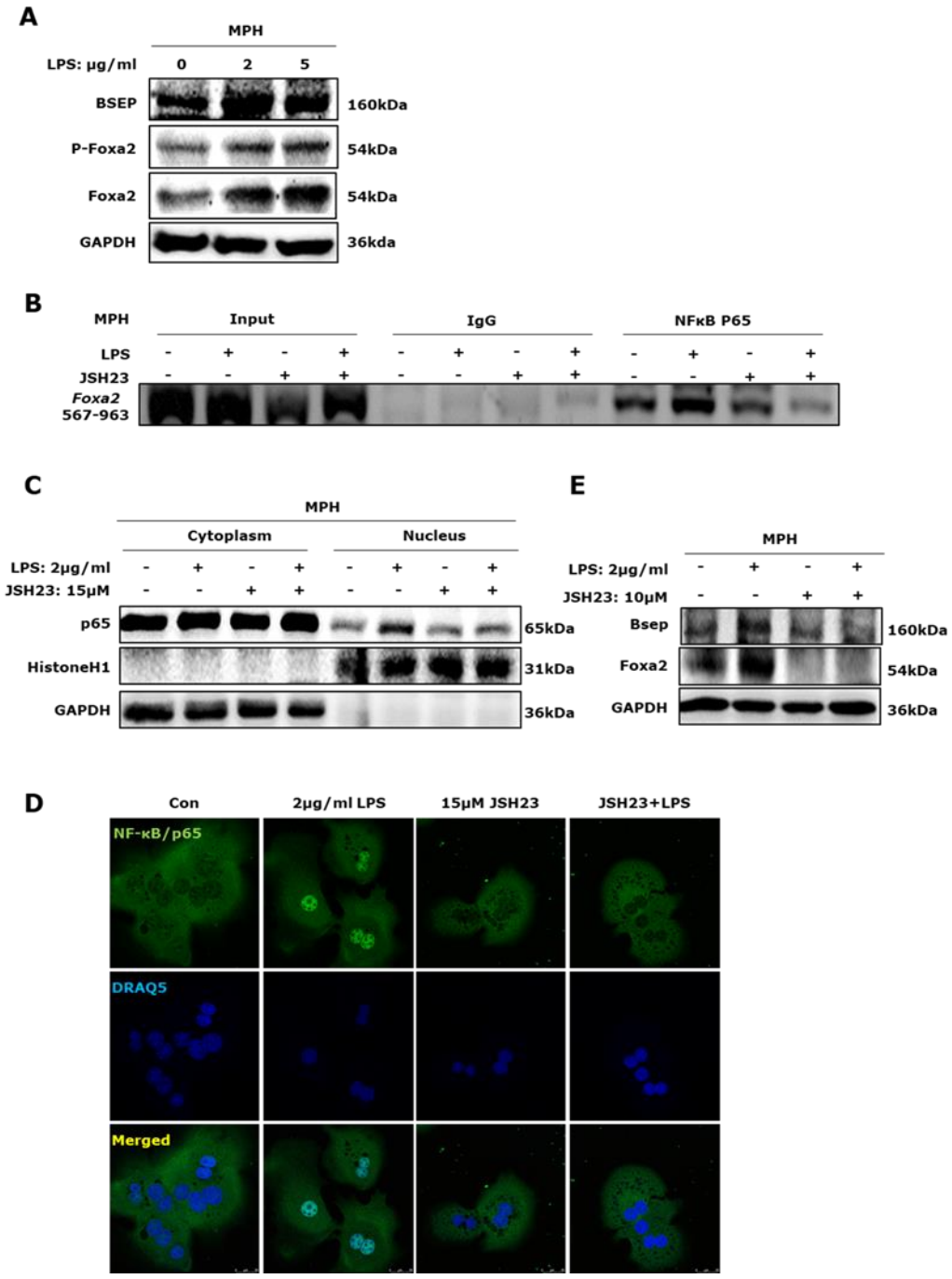

Figure 26. LPS induces Foxa2-dependent Bsep expression through NFκB signaling. (**A**) Western blotting measured protein expression of Bsep, p-Foxa2 and Foxa2 in MPHs with or without LPS treatment. (**B**) ChIP assay showed p65 binding to the foxa2 gene promoter in MPHs. (**C-D**) Subcellular fraction and IF were used to measure the effect of JSH23 in inhibiting LPS-induced p65 nuclear translocation. (**E**) Western blotting was used to measure LPS-induced Bsep and Foxa2 expression in MPHs with or without JSH23 treatment.

3.10.4 High concentration of LPS induces Foxa2 nuclear exclusion.

In some ACLF-LTx patients, BSEP could not be located on bile canaliculi without FOXA2 positive staining in hepatocytes nucleis (**Figure 11A**). We speculate whether severe infection or inflammation might play a role in these patients. In vitro, when the MPHs were treated with 20μg/ml LPS for 24h, we observed that high concentration of LPS inhibited Foxa2 nuclear translocation (**Figure 27A,B**) and induced high level of p-Foxa2 (**Figure 27C,D**). Western blot further showed that 20μg/ml LPS inhibited p65 and Bsep expression (**Figure 27C**). As a result, with the LPS treatment, the balance between total Foxa2 and p-Foxa2 regulated the expression of Bsep in MPHs. And this result may explain that in some ACLF patients, the very severe inflammation caused phosphorylation at Thr156 at FOXA2, resulting in FOXA2 nuclear exclusion and lost of BSEP on bile canaliculi (**Figure 11A ACLF-2**).

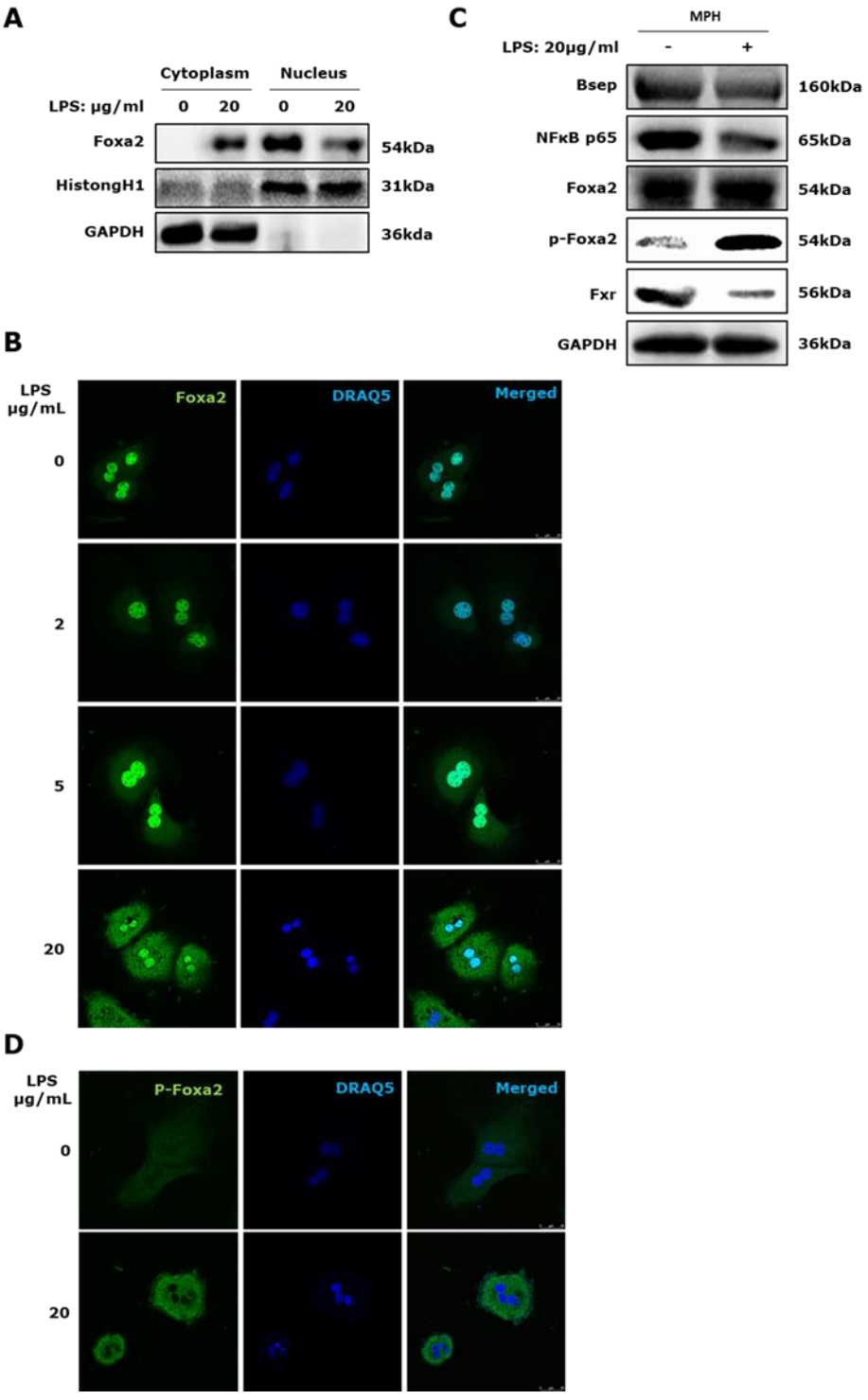

Figure 27. High concentration of LPS induces Foxa2 nuclear exclusion in MPHs. (**A-B**) Subcellular fraction and IF measured the effects of 20μg/ml LPS on Foxa2 expression in nuclei and cytoplasm of MPHs. (**C**) Western blotting measured protein expression of Bsep, p65, p-Foxa2, total Foxa2 and Fxr in MPHs with 20μg/ml LPS treatment. (D) IF showed p-Foxa2 localization in MPHs with or withour 20μg/ml LPS treatment. DRAQ5 was used as a marker of nuclei. GAPDH was used as loading control. HistoneH1 was used as loading control for nucleus protein.

4. DISCUSSION

As a key transporter in charge of bile acid, BSEP functional impairment or mutations results in severe cholestasis (Soroka CJ, Boyer JL 2014 molecular aspects of medicine). Under physiological circumstance, FXR is the key transcription factor controlling BSEP expression in hepatocytes (Wagner M 2003 Gastroenterology; Gomez-Ospina 2016 nature communication). The current study demonstrates a critical role of FOXA2 in the maintenance of apical BSEP in an end-stage liver disease ACLF. We found that:

(1) robust FOXA2 exists in hepatocytes of some ACLF patients who lost nuclear FXR expression;

(2) FOXA2 controls *bsep* gene transcription through binding to the gene promoter in hepatocytes;

(3) Foxa2 is capable of restoring Bsep expression when Fxr is silenced;

(4) Foxa2 expression, subcellular location and affinity to *bsep* gene promoter in hepatocytes is regulated by inflammatory relevant factor, e.g. LPS, TNFα and level of insulin and glucagon;

(5) LPS drives p65 nuclear translocation and thus binds to the promotor of foxa2 gene. This FOXA2-dependent regulatory mechanism plays a critical role in the maintenance of apical BSEP expression when FXR function is compromised.

4.1 Significance of BSEP maintanence in hepatocytes of ACLF patients

BSEP, bile salt export pump, is responsible for bile salt dependent bile flow, which transport of bile salts is dependent on ATP hydrolysis (Nishida et al., 1991). Several studies has found that FXR regulates BSEP expression (Ananthanarayanan et al., 2001), which is also identified in this study. In critical illness, including ACLF and sepsis, infection and inflammation completely inhibits FXR expression (Jenniskens et al., 2016). However, we found that some irreversible ACLF patients still maintain BSEP expression, which is related with the prognosis. ACLF patients without BSEP expression on bile canaliculi have more severe cholestasis with higher serum total bilirubin, INR and MELD, and much shorter clinical duration. These results suggest that in ACLF condition, BSEP expression and localization on bile canaliculi are very

important for survival and recovery. Further more, we found that Foxa2 takes over FXR's function in regulating BSEP expression in ACLF.

4.2 FXR and FOXA2 in physiological condition or chronic liver disease

In physiological condition or liver diseases without severe inflammation, FXR is the major transcription factor maintaining BSEP expression in hepatocytes (Soroka and Boyer, 2014; Wagner et al., 2003). Given that the half-life of BSEP is six days, normal diet-stimulated FXR expression is sufficient to maintain BSEP expression in hepatocytes (Soroka and Boyer, 2014). Besides governing BSEP expression, FXR contributes to a key regulatory loop controlling homeostasis of bile acid metabolism by forming an FXR-SHP-CYP7A1 axis with additional nuclear receptors (Boyer, 2013; Wagner et al., 2011). In addition, FXR has an important role in glucose homeostasis, which activation can decrease serum glucose and insulin tolerance. Hypoglycemic effects of FXR activation rely on repression of gluconeogenesis and induction of glycogen synthesis.

In contrast to FXR, FOXA2 is usually undetectable in normal hepatocytes. We examined FOXA2 expression in surrounding non-tumor liver tissue of 90 liver cancer patients by IHC. Only around 10% patients showed FOXA2 immune positivity in the nuclei of hepatocytes (data not shown). In normal hepatocytes, we found that FOXA2 subcellular location and function are controlled at least by two regulatory inputs. Firstly, FOXA2 nuclear translocation in hepatocytes is impeded by insulin administration as previously described (Wolfrum et al., 2004). Secondly, the capacity of FOXA2 binding to the *bsep* gene promoter is inhibited by FXR. In previous studies, in physiological condition, FOXA2 is necessary for the development of the foregut endoderm and is a transcriptional activator for liver-specific genes such as albumin and transthyretin. In addition, Foxa2 plays a significant role in maintaining normal glucose homeostasis by regulating gene expression of rate-limiting enzymes of gluconeogenesis and glycogenolysis, which function can be activated by glucgaon or inhibited by insulin respectively. These results illustrate why FOXA2 is not a major regulator of apical BSEP expression in physiological circumstance.

4.3 FXR and FOXA2 in ACLF

The expression of FXR is negatively impacted by inflammation, particularly in serious infection and inflammatory response, e.g. sepsis and ACLF (Jenniskens et al., 2016). In these circumstances, downregulation of FXR has beneficial effects for patients undergoing SIRS (Jenniskens et al., 2016). Besides regulating bile acid metabolism, FXR participates in the regulation of blood glucose through increasing insulin secretion, enhancing host sensitivity to insulin and reducing glucagon-like peptide-1 (GLP-1) (Wagner et al., 2011). In general, FXR is a nuclear receptor which inhibits gluconeogenesis (Wagner et al., 2011). In harsh diseases such as ACLF, patients usually suffer from anorexia, however, high levels of blood glucose are urgently required for protecting priority organs, e.g. the brain (Van Wyngene et al., 2018). Therefore, the inhibition of FXR benefits gluconeogenesis-dependent energy supply. To sustain blood glucose levels, a large amount of glucagon is produced and released from pancreatic α cells (Rui, 2014). Patients with sepsis and ACLF usually maintain high levels of circulation glucagon (Van Wyngene et al., 2018). On the other hand, hyperglycemia induces hyperinsulinemia (Van Wyngene et al., 2018). To inhibit insulin-dependent glycogen deposition, insulin resistance occurs in major metabolic organs, including skeletal muscle, adipose tissue and hepatocytes (Jenniskens et al., 2016). In parallel with FXR inhibition, these pathophysiological alterations result in at least three positive regulatory signals for FOXA2 expression and functions: (1) Glucagon induces high levels of FOXA2 expression; (2) Insulin resistance eliminates a negative regulatory signal impeding FOXA2 nuclear translocation; (3) FOXA2 binding to the *bsep* gene promoter is not competitively inhibited by the presence of nuclear FXR anymore. These alterations result in FOXA2 as a qualified FXR replacer to maintain apical BSEP expression in ACLF.

In this study, we found that FXR and FOXA2 govern two complementary regulatory mechanisms to guarantee apical BSEP expression in hepatocytes. But it is still not clear the relationship between FXR and FOXA2 in regulating bsep gene. Maheul Ploton et al. found that glucagon-regulated transcription factor FOXA2 negatively regulates FXR-mediated *Nr0b2/shp* gene transcription through competitively occupying the binding sites of the (Ploton et al., 2018). On the other handm FXR-induced SHP inhibits FOXA2 expression (Choi et al., 2004). GST pulldown and co-

immunoprecipitation assays confirmed that FXR specifically interacts with FOXA2 in HepG2 cells and in mouse liver (Ploton et al., 2018). The effects of FXR and FOXA2 in the regulation of BSEP expression and bile acid homeostasis have also been investigated previously (Bochkis et al., 2008; Gomez-Ospina et al., 2016). Mutation of NR1H4, which encodes the FXR, leads to undetectable BSEP expression and severe cholestasis (Gomez-Ospina et al., 2016), whereas deletion of Foxa2 in mouse hepatocytes using Cre-lox system does not affect BSEP expression (Bochkis et al., 2008). These results suggest that FXR, but not FOXA2, is a key regulator in charge of BSEP expression in normal hepatocytes. The current study is not completely consistant with the previous findings. In the hepatocytes of fxr knockout mice, apical BSEP expression in hepatocytes is still detectable although the levels are reduced remarkably compared to hepatocytes in the wild type mice (**Figure16**). Only when we knocked down FOXA2 in the fxr knockout mice-derived hepatocytes, BSEP is almost undetectable. ChIP assay shows that FXR and FOXA2 possess overlapped binding sites in the *bsep* gene promoter (1170-1625 bp upstream from the transcription start site). Administration of FXR agonist inhibits FOXA2 binding to the *bsep* gene promoter (**Figure 19E**), indicating a competitive relationship between FXR and FOXA2 in the regulation of the bsep *gene* transcript. These data suggest that loss of BSEP expression requires inhibition of both transcription factors. The notion is supports by the current clinical observation (**Figure 11**).

The role of FOXA2 in the regulation of BSEP is indispensable in the scenario with severe infection and inflammation. Besides aforementioned situation from high glucagon, we observed that TNFα and LPS as well upregulate FOXA2 and thus benefit BSEP expression. As mentioned above, TNFα induces insulin resistance and inhibits FXR, which abolishes two factors impeding FOXA2 binding to the *bsep* gene promoter. Both TNFα and LPS activates its canconical NFκB signaling and initiates the *foxa2* gene transcription through p65 binding to the promoter. Notably, different LPS dosages demonstrate different effects on FOXA2 activity and expression. In contrast to relatively low dosage such as 5mg/ml, high concentration of LPS, e.g. 20 mg/ml, induces p-FOXA2 and thus results in FOXA2 nuclear exclusion and reduced BSEP expression in hepatocytes. These in vitro observations might be useful to explain why a portion of irreversible patients lost BSEP. In the current observed 13 irreversible ACLF patients, 10 patients maintaining apical BSEP expression display robust nuclear

FOXA2 expression in hepatocytes, whereas 3 patients who lost apical BSEP expression show cytoplasmic, but not nuclear FOXA2 expression. Unfortunately, as a retrospective clinical study, we are not capable of investigating whether these patients suffured from LPS endotoxemia and had high levels of TNFα.

4.4 Clinical significance

Apical BSEP expression is closely associated with disease consequence. The current clinical observation provides clear clues in this regarding. The important observation include: (1) all recovered ACLF patients possess intact BSEP expression in hepatocytes; (2) even in the irreversible patients, those who still maintain BSEP demonstrate better key clinical parameters, including longer clinical duration, low serum bilirubin levels, low INR and MELD scores, rather than the patients who lost BSEP expression. These evidences suggest a crucial role of BSEP in the progress of the recovery of ACLF.

In summary, the current study has multiple limitations. As a comlex clinical syndrome, there is no ideal animal model to mimic ACLF to confirm the observed clinical and in vivo mechanisms. Assessment of BSEP, FXR and FOXA2 expression in hepatocytes requires liver biopsy. In the severe disease such as ACLF, liver biopsy in clinical practice is not popular due to the invasive risk. It is interesting to further explore in the future whether the FOXA2 rescue strategy is also relevant to a range of cholestatic or other liver diseases, in particular human PFIC5, which presents with severe cholestasis and absent BSEP due to genetic loss of FXR (Soroka and Boyer, 2014).

5. SUMMARY

The findings of this study are summarized in a schematic diagram (**Figure 28**) illustrating the two regulatory mechanisms relevant for the maintenance of BSEP on bile canaliculi in physiological and pathological condition.

(1) In physiological condition, FXR regulates BSEP expression.

(2) In inflammatory circumstance, FXR is significantly inhibited. Inflammation-dependent insulin resistance, high level of glucagon and NFκB p65 signaling induce FOXA2 expression and activity to maintain BSEP expression, which is important for ACLF patients' survival and recovery.

(3) In sepsis condition, severe infection and inflammation, e.g. high levels of LPS, inhibit FOXA2 activation and thus lead to the loss of BSEP expression on bile canaliculi, which are associated with poor prognosis of ACLF patients.

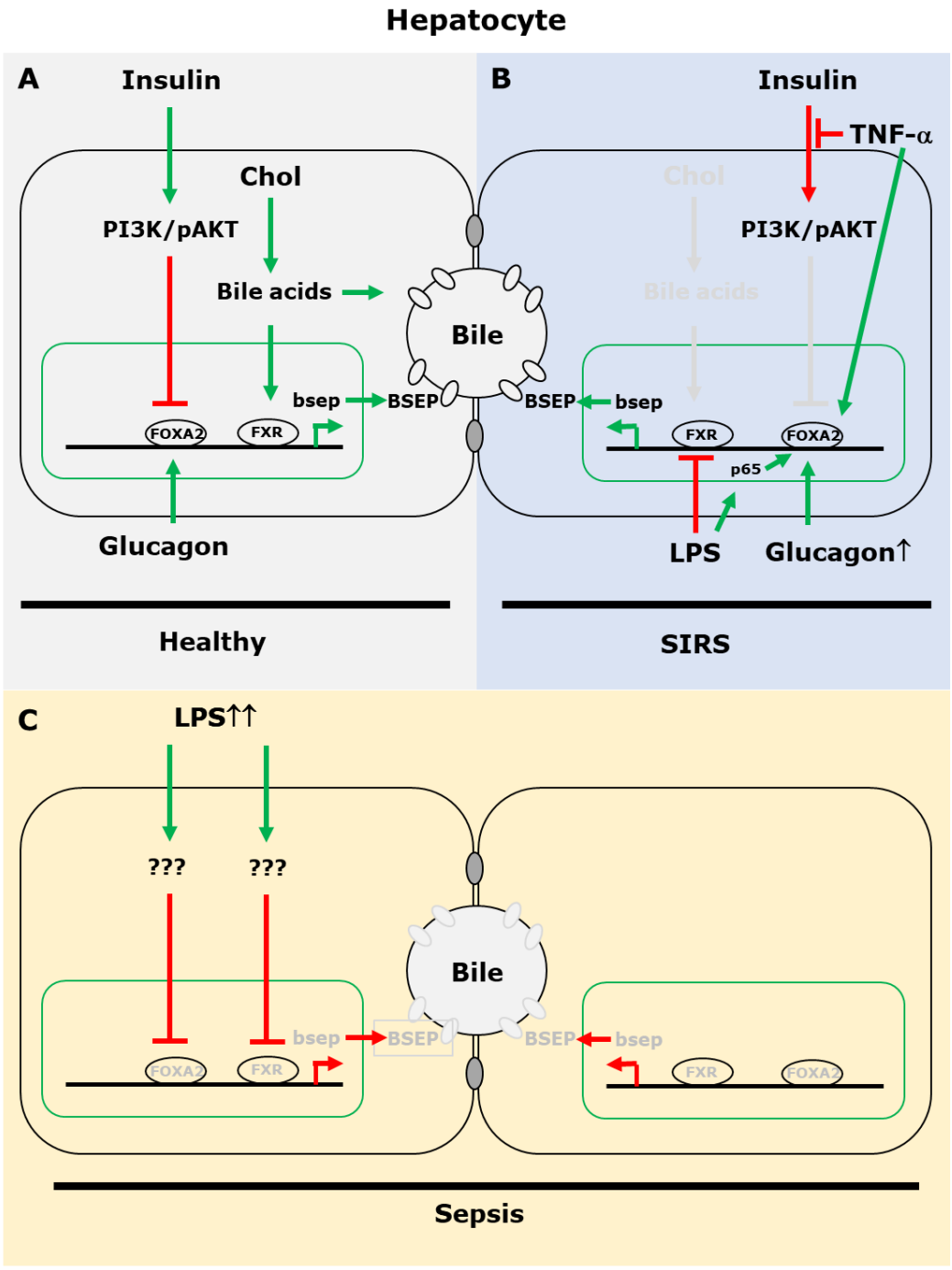

Chol, Cholesterol
FXR, Farnesoid X receptor
ACLF, acute-on-chronic liver failure
SIRS, systemic inflammatory response

Figure 28. The scheme depicts two regulatory mechanisms maintaining Bsep expression on bile canaliculi in healthy and ACLF conditions.

6. REFERENCES

Adachi, Y., Kobayashi, H., Kurumi, Y., Shouji, M., Kitano, M., and Yamamoto, T. (1991). ATP-dependent taurocholate transport by rat liver canalicular membrane vesicles. Hepatology *14*, 655-659.

Ananthanarayanan, M., Balasubramanian, N., Makishima, M., Mangelsdorf, D.J., and Suchy, F.J. (2001). Human bile salt export pump promoter is transactivated by the farnesoid X receptor/bile acid receptor. The Journal of biological chemistry *276*, 28857-28865.

Anderson, J.M. (1996). Leaky junctions and cholestasis: a tight correlation. Gastroenterology *110*, 1662-1665.

Arroyo, V., and Moreau, R. (2017). Diagnosis and prognosis of acute on chronic liver failure (ACLF) in cirrhosis. Journal of hepatology *66*, 451-453.

Arroyo, V., Moreau, R., Kamath, P.S., Jalan, R., Gines, P., Nevens, F., Fernandez, J., To, U., Garcia-Tsao, G., and Schnabl, B. (2016). Acute-on-chronic liver failure in cirrhosis. Nature reviews Disease primers *2*, 16041.

Attili, A.F., Angelico, M., Cantafora, A., Alvaro, D., and Capocaccia, L. (1986). Bile acid-induced liver toxicity: relation to the hydrophobic-hydrophilic balance of bile acids. Medical hypotheses *19*, 57-69.

Bensinger, S.J., and Tontonoz, P. (2008). Integration of metabolism and inflammation by lipid-activated nuclear receptors. Nature *454*, 470-477.

Bernsmeier, C., Pop, O.T., Singanayagam, A., Triantafyllou, E., Patel, V.C., Weston, C.J., Curbishley, S., Sadiq, F., Vergis, N., Khamri, W*., et al.* (2015). Patients with acute-on-chronic liver failure have increased numbers of regulatory immune cells expressing the receptor tyrosine kinase MERTK. Gastroenterology *148*, 603-615 e614.

Bishop-Bailey, D., Walsh, D.T., and Warner, T.D. (2004). Expression and activation of the farnesoid X receptor in the vasculature. Proceedings of the National Academy of Sciences of the United States of America *101*, 3668-3673.

Bochkis, I.M., Rubins, N.E., White, P., Furth, E.E., Friedman, J.R., and Kaestner, K.H. (2008). Hepatocyte-specific ablation of Foxa2 alters bile acid homeostasis and results in endoplasmic reticulum stress. Nature medicine *14*, 828-836.

Boyer, J.L. (2013). Bile formation and secretion. Comprehensive Physiology *3*, 1035-1078.

Boyer, J.L., Trauner, M., Mennone, A., Soroka, C.J., Cai, S.Y., Moustafa, T., Zollner, G., Lee, J.Y., and Ballatori, N. (2006). Upregulation of a basolateral FXR-dependent bile acid efflux transporter OSTalpha-OSTbeta in cholestasis in humans and rodents. American journal of physiology Gastrointestinal and liver physiology *290*, G1124-1130.

Brennan, R.G. (1993). The winged-helix DNA-binding motif: another helix-turn-helix takeoff. Cell *74*, 773-776.

Byrne, J.A., Strautnieks, S.S., Mieli-Vergani, G., Higgins, C.F., Linton, K.J., and Thompson, R.J. (2002). The human bile salt export pump: characterization of substrate specificity and identification of inhibitors. Gastroenterology *123*, 1649-1658.

Cai, S.Y., and Boyer, J.L. (2006). FXR: a target for cholestatic syndromes? Expert Opin Ther Targets *10*, 409-421.

Cai, S.Y., Lionarons, D.A., Hagey, L., Soroka, C.J., Mennone, A., and Boyer, J.L. (2013). Adult sea lamprey tolerates biliary atresia by altering bile salt composition and renal excretion. Hepatology *57*, 2418-2426.

Cai, S.Y., Wang, L., Ballatori, N., and Boyer, J.L. (2001). Bile salt export pump is highly conserved during vertebrate evolution and its expression is inhibited by PFIC type II mutations. American journal of physiology Gastrointestinal and liver physiology *281*, G316-322.

Carlsson, P., and Mahlapuu, M. (2002). Forkhead transcription factors: key players in development and metabolism. Developmental biology *250*, 1-23.

Caron, S., Huaman Samanez, C., Dehondt, H., Ploton, M., Briand, O., Lien, F., Dorchies, E., Dumont, J., Postic, C., Cariou, B.*, et al.* (2013). Farnesoid X receptor inhibits the transcriptional activity of carbohydrate response element binding protein in human hepatocytes. Molecular and cellular biology *33*, 2202-2211.

Cave, M.C., Clair, H.B., Hardesty, J.E., Falkner, K.C., Feng, W., Clark, B.J., Sidey, J., Shi, H., Aqel, B.A., McClain, C.J.*, et al.* (2016). Nuclear receptors and nonalcoholic fatty liver disease. Biochimica et biophysica acta *1859*, 1083-1099.

Chiang, J.Y. (1998). Regulation of bile acid synthesis. Frontiers in bioscience : a journal and virtual library *3*, d176-193.

Chiang, J.Y. (2002). Bile acid regulation of gene expression: roles of nuclear hormone receptors. Endocrine reviews *23*, 443-463.

Chiang, J.Y. (2009). Bile acids: regulation of synthesis. Journal of lipid research *50*, 1955-1966.

Childs, S., Yeh, R.L., Georges, E., and Ling, V. (1995). Identification of a sister gene to P-glycoprotein. Cancer research *55*, 2029-2034.

Choi, Y.H., Park, M.J., Kim, K.W., Lee, H.C., and Cheong, J. (2004). The orphan nuclear receptor SHP is involved in monocytic differentiation, and its expression is increased by c-Jun. Journal of leukocyte biology *76*, 1082-1088.

Claria, J., Stauber, R.E., Coenraad, M.J., Moreau, R., Jalan, R., Pavesi, M., Amoros, A., Titos, E., Alcaraz-Quiles, J., Oettl, K.*, et al.* (2016). Systemic inflammation in decompensated cirrhosis: Characterization and role in acute-on-chronic liver failure. Hepatology *64*, 1249-1264.

Clark, K.L., Halay, E.D., Lai, E., and Burley, S.K. (1993). Co-crystal structure of the HNF-3/fork head DNA-recognition motif resembles histone H5. Nature *364*, 412-420.

Craddock, A.L., Love, M.W., Daniel, R.W., Kirby, L.C., Walters, H.C., Wong, M.H., and Dawson, P.A. (1998). Expression and transport properties of the human ileal and renal sodium-dependent bile acid transporter. The American journal of physiology *274*, G157-169.

Dawson, P.A., Hubbert, M., Haywood, J., Craddock, A.L., Zerangue, N., Christian, W.V., and Ballatori, N. (2005). The heteromeric organic solute transporter alpha-beta, Ostalpha-Ostbeta, is an ileal basolateral bile acid transporter. The Journal of biological chemistry *280*, 6960-6968.

Demas, G.E., Chefer, V., Talan, M.I., and Nelson, R.J. (1997). Metabolic costs of mounting an antigen-stimulated immune response in adult and aged C57BL/6J mice. The American journal of physiology *273*, R1631-1637.

Denson, L.A., Sturm, E., Echevarria, W., Zimmerman, T.L., Makishima, M., Mangelsdorf, D.J., and Karpen, S.J. (2001). The orphan nuclear receptor, shp, mediates bile acid-induced inhibition of the rat bile acid transporter, ntcp. Gastroenterology *121*, 140-147.

Downes, M., Verdecia, M.A., Roecker, A.J., Hughes, R., Hogenesch, J.B., Kast-Woelbern, H.R., Bowman, M.E., Ferrer, J.L., Anisfeld, A.M., Edwards, P.A.*, et al.* (2003). A chemical, genetic, and structural analysis of the nuclear bile acid receptor FXR. Molecular cell *11*, 1079-1092.

Duran-Sandoval, D., Cariou, B., Percevault, F., Hennuyer, N., Grefhorst, A., van Dijk, T.H., Gonzalez, F.J., Fruchart, J.C., Kuipers, F., and Staels, B. (2005). The farnesoid X receptor modulates hepatic carbohydrate metabolism during the fasting-refeeding transition. The Journal of biological chemistry *280*, 29971-29979.

Forman, B.M., Goode, E., Chen, J., Oro, A.E., Bradley, D.J., Perlmann, T., Noonan, D.J., Burka, L.T., McMorris, T., Lamph, W.W.*, et al.* (1995). Identification of a nuclear receptor that is activated by farnesol metabolites. Cell *81*, 687-693.

Galle, P.R., Theilmann, L., Raedsch, R., Otto, G., and Stiehl, A. (1990). Ursodeoxycholate reduces hepatotoxicity of bile salts in primary human hepatocytes. Hepatology *12*, 486-491.

Galman, C., Angelin, B., and Rudling, M. (2005). Bile acid synthesis in humans has a rapid diurnal variation that is asynchronous with cholesterol synthesis. Gastroenterology *129*, 1445-1453.

Gartung, C., Ananthanarayanan, M., Rahman, M.A., Schuele, S., Nundy, S., Soroka, C.J., Stolz, A., Suchy, F.J., and Boyer, J.L. (1996). Down-regulation of expression and function of the rat liver Na+/bile acid cotransporter in extrahepatic cholestasis. Gastroenterology *110*, 199-209.

Geier, A., Fickert, P., and Trauner, M. (2006). Mechanisms of disease: mechanisms and clinical implications of cholestasis in sepsis. Nature clinical practice Gastroenterology & hepatology *3*, 574-585.

Gerloff, T., Geier, A., Roots, I., Meier, P.J., and Gartung, C. (2002). Functional analysis of the rat bile salt export pump gene promoter. European journal of biochemistry *269*, 3495-3503.

Gerloff, T., Stieger, B., Hagenbuch, B., Madon, J., Landmann, L., Roth, J., Hofmann, A.F., and Meier, P.J. (1998). The sister of P-glycoprotein represents the canalicular bile salt export pump of mammalian liver. The Journal of biological chemistry *273*, 10046-10050.

Gerrish, K., Gannon, M., Shih, D., Henderson, E., Stoffel, M., Wright, C.V., and Stein, R. (2000). Pancreatic beta cell-specific transcription of the pdx-1 gene. The role of conserved upstream control regions and their hepatic nuclear factor 3beta sites. The Journal of biological chemistry *275*, 3485-3492.

Godoy, P., Hengstler, J.G., Ilkavets, I., Meyer, C., Bachmann, A., Muller, A., Tuschl, G., Mueller, S.O., and Dooley, S. (2009). Extracellular matrix modulates sensitivity of hepatocytes to fibroblastoid dedifferentiation and transforming growth factor beta-induced apoptosis. Hepatology *49*, 2031-2043.

Gomez-Ospina, N., Potter, C.J., Xiao, R., Manickam, K., Kim, M.S., Kim, K.H., Shneider, B.L., Picarsic, J.L., Jacobson, T.A., Zhang, J.*, et al.* (2016). Mutations in the

nuclear bile acid receptor FXR cause progressive familial intrahepatic cholestasis. Nature communications *7*, 10713.

Gong, Y.Z., Everett, E.T., Schwartz, D.A., Norris, J.S., and Wilson, F.A. (1994). Molecular cloning, tissue distribution, and expression of a 14-kDa bile acid-binding protein from rat ileal cytosol. Proceedings of the National Academy of Sciences of the United States of America *91*, 4741-4745.

Goodwin, B., Jones, S.A., Price, R.R., Watson, M.A., McKee, D.D., Moore, L.B., Galardi, C., Wilson, J.G., Lewis, M.C., Roth, M.E.*, et al.* (2000). A regulatory cascade of the nuclear receptors FXR, SHP-1, and LRH-1 represses bile acid biosynthesis. Molecular cell *6*, 517-526.

Green, R.M., Beier, D., and Gollan, J.L. (1996). Regulation of hepatocyte bile salt transporters by endotoxin and inflammatory cytokines in rodents. Gastroenterology *111*, 193-198.

Green, R.M., Hoda, F., and Ward, K.L. (2000). Molecular cloning and characterization of the murine bile salt export pump. Gene *241*, 117-123.

Grober, J., Zaghini, I., Fujii, H., Jones, S.A., Kliewer, S.A., Willson, T.M., Ono, T., and Besnard, P. (1999). Identification of a bile acid-responsive element in the human ileal bile acid-binding protein gene. Involvement of the farnesoid X receptor/9-cis-retinoic acid receptor heterodimer. The Journal of biological chemistry *274*, 29749-29754.

Guo, G.L., Lambert, G., Negishi, M., Ward, J.M., Brewer, H.B., Jr., Kliewer, S.A., Gonzalez, F.J., and Sinal, C.J. (2003). Complementary roles of farnesoid X receptor, pregnane X receptor, and constitutive androstane receptor in protection against bile acid toxicity. The Journal of biological chemistry *278*, 45062-45071.

Gupta, S., Stravitz, R.T., Dent, P., and Hylemon, P.B. (2001). Down-regulation of cholesterol 7alpha-hydroxylase (CYP7A1) gene expression by bile acids in primary rat hepatocytes is mediated by the c-Jun N-terminal kinase pathway. The Journal of biological chemistry *276*, 15816-15822.

Gustot, T., Durand, F., Lebrec, D., Vincent, J.L., and Moreau, R. (2009). Severe sepsis in cirrhosis. Hepatology *50*, 2022-2033.

Habegger, K.M., Heppner, K.M., Geary, N., Bartness, T.J., DiMarchi, R., and Tschop, M.H. (2010). The metabolic actions of glucagon revisited. Nature reviews Endocrinology *6*, 689-697.

Hagenbuch, B., and Meier, P.J. (1994). Molecular cloning, chromosomal localization, and functional characterization of a human liver Na+/bile acid cotransporter. The Journal of clinical investigation *93*, 1326-1331.

Hagenbuch, B., and Meier, P.J. (2003). The superfamily of organic anion transporting polypeptides. Biochimica et biophysica acta *1609*, 1-18.

Hayashi, H., and Sugiyama, Y. (2009). Short-chain ubiquitination is associated with the degradation rate of a cell-surface-resident bile salt export pump (BSEP/ABCB11). Molecular pharmacology *75*, 143-150.

Herbst, R.S., Nielsch, U., Sladek, F., Lai, E., Babiss, L.E., and Darnell, J.E., Jr. (1991). Differential regulation of hepatocyte-enriched transcription factors explains changes in albumin and transthyretin gene expression among hepatoma cells. The New biologist *3*, 289-296.

Hernaez, R., Sola, E., Moreau, R., and Gines, P. (2017). Acute-on-chronic liver failure: an update. Gut *66*, 541-553.

Hofmann, A.F., and Hagey, L.R. (2008). Bile acids: chemistry, pathochemistry, biology, pathobiology, and therapeutics. Cellular and molecular life sciences : CMLS *65*, 2461-2483.

Hotamisligil, G.S. (2006). Inflammation and metabolic disorders. Nature *444*, 860-867.

Huang, L., Zhao, A., Lew, J.L., Zhang, T., Hrywna, Y., Thompson, J.R., de Pedro, N., Royo, I., Blevins, R.A., Pelaez, F.*, et al.* (2003). Farnesoid X receptor activates transcription of the phospholipid pump MDR3. The Journal of biological chemistry *278*, 51085-51090.

Huber, R.M., Murphy, K., Miao, B., Link, J.R., Cunningham, M.R., Rupar, M.J., Gunyuzlu, P.L., Haws, T.F., Kassam, A., Powell, F.*, et al.* (2002). Generation of multiple farnesoid-X-receptor isoforms through the use of alternative promoters. Gene *290*, 35-43.

Inagaki, T., Choi, M., Moschetta, A., Peng, L., Cummins, C.L., McDonald, J.G., Luo, G., Jones, S.A., Goodwin, B., Richardson, J.A.*, et al.* (2005). Fibroblast growth factor 15 functions as an enterohepatic signal to regulate bile acid homeostasis. Cell metabolism *2*, 217-225.

Iwasaki, A., and Medzhitov, R. (2015). Control of adaptive immunity by the innate immune system. Nature immunology *16*, 343-353.

Jacquemin, E., De Vree, J.M., Cresteil, D., Sokal, E.M., Sturm, E., Dumont, M., Scheffer, G.L., Paul, M., Burdelski, M., Bosma, P.J.*, et al.* (2001). The wide spectrum

of multidrug resistance 3 deficiency: from neonatal cholestasis to cirrhosis of adulthood. Gastroenterology *120*, 1448-1458.

Jalan, R., Gines, P., Olson, J.C., Mookerjee, R.P., Moreau, R., Garcia-Tsao, G., Arroyo, V., and Kamath, P.S. (2012). Acute-on chronic liver failure. Journal of hepatology *57*, 1336-1348.

Jenniskens, M., Langouche, L., Vanwijngaerden, Y.M., Mesotten, D., and Van den Berghe, G. (2016). Cholestatic liver (dys)function during sepsis and other critical illnesses. Intensive care medicine *42*, 16-27.

Kaestner, K.H., Hiemisch, H., Luckow, B., and Schutz, G. (1994). The HNF-3 gene family of transcription factors in mice: gene structure, cDNA sequence, and mRNA distribution. Genomics *20*, 377-385.

Kaestner, K.H., Lee, K.H., Schlondorff, J., Hiemisch, H., Monaghan, A.P., and Schutz, G. (1993). Six members of the mouse forkhead gene family are developmentally regulated. Proceedings of the National Academy of Sciences of the United States of America *90*, 7628-7631.

Kakyo, M., Unno, M., Tokui, T., Nakagomi, R., Nishio, T., Iwasashi, H., Nakai, D., Seki, M., Suzuki, M., Naitoh, T.*, et al.* (1999). Molecular characterization and functional regulation of a novel rat liver-specific organic anion transporter rlst-1. Gastroenterology *117*, 770-775.

Kast, H.R., Goodwin, B., Tarr, P.T., Jones, S.A., Anisfeld, A.M., Stoltz, C.M., Tontonoz, P., Kliewer, S., Willson, T.M., and Edwards, P.A. (2002). Regulation of multidrug resistance-associated protein 2 (ABCC2) by the nuclear receptors pregnane X receptor, farnesoid X-activated receptor, and constitutive androstane receptor. The Journal of biological chemistry *277*, 2908-2915.

Keppler, D., and Konig, J. (1997). Hepatic canalicular membrane 5: Expression and localization of the conjugate export pump encoded by the MRP2 (cMRP/cMOAT) gene in liver. FASEB journal : official publication of the Federation of American Societies for Experimental Biology *11*, 509-516.

Kerr, T.A., Saeki, S., Schneider, M., Schaefer, K., Berdy, S., Redder, T., Shan, B., Russell, D.W., and Schwarz, M. (2002). Loss of nuclear receptor SHP impairs but does not eliminate negative feedback regulation of bile acid synthesis. Developmental cell *2*, 713-720.

Kim, I., Morimura, K., Shah, Y., Yang, Q., Ward, J.M., and Gonzalez, F.J. (2007). Spontaneous hepatocarcinogenesis in farnesoid X receptor-null mice. Carcinogenesis *28*, 940-946.

Kim, M.S., Shigenaga, J., Moser, A., Feingold, K., and Grunfeld, C. (2003). Repression of farnesoid X receptor during the acute phase response. The Journal of biological chemistry *278*, 8988-8995.

Kipp, H., and Arias, I.M. (2000). Newly synthesized canalicular ABC transporters are directly targeted from the Golgi to the hepatocyte apical domain in rat liver. The Journal of biological chemistry *275*, 15917-15925.

Kir, S., Beddow, S.A., Samuel, V.T., Miller, P., Previs, S.F., Suino-Powell, K., Xu, H.E., Shulman, G.I., Kliewer, S.A., and Mangelsdorf, D.J. (2011). FGF19 as a postprandial, insulin-independent activator of hepatic protein and glycogen synthesis. Science *331*, 1621-1624.

Knisely, A.S., Strautnieks, S.S., Meier, Y., Stieger, B., Byrne, J.A., Portmann, B.C., Bull, L.N., Pawlikowska, L., Bilezikci, B., Ozcay, F.*, et al.* (2006). Hepatocellular carcinoma in ten children under five years of age with bile salt export pump deficiency. Hepatology *44*, 478-486.

Kubitz, R., Droge, C., Stindt, J., Weissenberger, K., and Haussinger, D. (2012). The bile salt export pump (BSEP) in health and disease. Clinics and research in hepatology and gastroenterology *36*, 536-553.

Kubitz, R., Sutfels, G., Kuhlkamp, T., Kolling, R., and Haussinger, D. (2004). Trafficking of the bile salt export pump from the Golgi to the canalicular membrane is regulated by the p38 MAP kinase. Gastroenterology *126*, 541-553.

Kullak-Ublick, G.A., Stieger, B., and Meier, P.J. (2004). Enterohepatic bile salt transporters in normal physiology and liver disease. Gastroenterology *126*, 322-342.

Lai, E., Prezioso, V.R., Smith, E., Litvin, O., Costa, R.H., and Darnell, J.E., Jr. (1990). HNF-3A, a hepatocyte-enriched transcription factor of novel structure is regulated transcriptionally. Genes & development *4*, 1427-1436.

Lam, C.W., Cheung, K.M., Tsui, M.S., Yan, M.S., Lee, C.Y., and Tong, S.F. (2006). A patient with novel ABCB11 gene mutations with phenotypic transition between BRIC2 and PFIC2. Journal of hepatology *44*, 240-242.

Lam, P., Pearson, C.L., Soroka, C.J., Xu, S., Mennone, A., and Boyer, J.L. (2007). Levels of plasma membrane expression in progressive and benign mutations of the

bile salt export pump (Bsep/Abcb11) correlate with severity of cholestatic diseases. American journal of physiology Cell physiology *293*, C1709-1716.

Landrier, J.F., Eloranta, J.J., Vavricka, S.R., and Kullak-Ublick, G.A. (2006). The nuclear receptor for bile acids, FXR, transactivates human organic solute transporter-alpha and -beta genes. American journal of physiology Gastrointestinal and liver physiology *290*, G476-485.

Langheim, S., Yu, L., von Bergmann, K., Lutjohann, D., Xu, F., Hobbs, H.H., and Cohen, J.C. (2005). ABCG5 and ABCG8 require MDR2 for secretion of cholesterol into bile. Journal of lipid research *46*, 1732-1738.

Lazaridis, K.N., Pham, L., Tietz, P., Marinelli, R.A., deGroen, P.C., Levine, S., Dawson, P.A., and LaRusso, N.F. (1997). Rat cholangiocytes absorb bile acids at their apical domain via the ileal sodium-dependent bile acid transporter. The Journal of clinical investigation *100*, 2714-2721.

Lecureur, V., Sun, D., Hargrove, P., Schuetz, E.G., Kim, R.B., Lan, L.B., and Schuetz, J.D. (2000). Cloning and expression of murine sister of P-glycoprotein reveals a more discriminating transporter than MDR1/P-glycoprotein. Molecular pharmacology *57*, 24-35.

Lee, C.S., Friedman, J.R., Fulmer, J.T., and Kaestner, K.H. (2005). The initiation of liver development is dependent on Foxa transcription factors. Nature *435*, 944-947.

Lee, S.M., Schelcher, C., Demmel, M., Hauner, M., and Thasler, W.E. (2013). Isolation of human hepatocytes by a two-step collagenase perfusion procedure. Journal of visualized experiments : JoVE.

Lew, J.L., Zhao, A., Yu, J., Huang, L., De Pedro, N., Pelaez, F., Wright, S.D., and Cui, J. (2004). The farnesoid X receptor controls gene expression in a ligand- and promoter-selective fashion. The Journal of biological chemistry *279*, 8856-8861.

Li, H., Xia, Q., Zeng, B., Li, S.T., Liu, H., Li, Q., Li, J., Yang, S.Y., Dong, X.J., Gao, T., *et al.* (2015). Submassive hepatic necrosis distinguishes HBV-associated acute on chronic liver failure from cirrhotic patients with acute decompensation. Journal of hepatology *63*, 50-59.

Li, M., Cai, S.Y., and Boyer, J.L. (2017). Mechanisms of bile acid mediated inflammation in the liver. Molecular aspects of medicine *56*, 45-53.

Li, T., Kong, X., Owsley, E., Ellis, E., Strom, S., and Chiang, J.Y. (2006). Insulin regulation of cholesterol 7alpha-hydroxylase expression in human hepatocytes: roles

of forkhead box O1 and sterol regulatory element-binding protein 1c. The Journal of biological chemistry *281*, 28745-28754.

Liu, N., Meng, Z., Lou, G., Zhou, W., Wang, X., Zhang, Y., Zhang, L., Liu, X., Yen, Y., Lai, L.*, et al.* (2012). Hepatocarcinogenesis in FXR-/- mice mimics human HCC progression that operates through HNF1alpha regulation of FXR expression. Mol Endocrinol *26*, 775-785.

Ma, K., Saha, P.K., Chan, L., and Moore, D.D. (2006). Farnesoid X receptor is essential for normal glucose homeostasis. The Journal of clinical investigation *116*, 1102-1109.

Makishima, M., Okamoto, A.Y., Repa, J.J., Tu, H., Learned, R.M., Luk, A., Hull, M.V., Lustig, K.D., Mangelsdorf, D.J., and Shan, B. (1999). Identification of a nuclear receptor for bile acids. Science *284*, 1362-1365.

Mangelsdorf, D.J., and Evans, R.M. (1995). The RXR heterodimers and orphan receptors. Cell *83*, 841-850.

Marschall, H.U., Wagner, M., Bodin, K., Zollner, G., Fickert, P., Gumhold, J., Silbert, D., Fuchsbichler, A., Sjovall, J., and Trauner, M. (2006). Fxr(-/-) mice adapt to biliary obstruction by enhanced phase I detoxification and renal elimination of bile acids. Journal of lipid research *47*, 582-592.

Marti, A., Marcos, A., and Martinez, J.A. (2001). Obesity and immune function relationships. Obesity reviews : an official journal of the International Association for the Study of Obesity *2*, 131-140.

Medzhitov, R. (2008). Origin and physiological roles of inflammation. Nature *454*, 428-435.

Medzhitov, R. (2010). Inflammation 2010: new adventures of an old flame. Cell *140*, 771-776.

Meier, P.J. (1995). Molecular mechanisms of hepatic bile salt transport from sinusoidal blood into bile. The American journal of physiology *269*, G801-812.

Mochizuki, K., Kagawa, T., Numari, A., Harris, M.J., Itoh, J., Watanabe, N., Mine, T., and Arias, I.M. (2007). Two N-linked glycans are required to maintain the transport activity of the bile salt export pump (ABCB11) in MDCK II cells. Am J Physiol Gastrointest Liver Physiol *292*, G818-828.

Monaghan, A.P., Kaestner, K.H., Grau, E., and Schutz, G. (1993). Postimplantation expression patterns indicate a role for the mouse forkhead/HNF-3 alpha, beta and gamma genes in determination of the definitive endoderm, chordamesoderm and neuroectoderm. Development *119*, 567-578.

Moreau, R. (2016). The Pathogenesis of ACLF: The Inflammatory Response and Immune Function. Seminars in liver disease *36*, 133-140.

Moreau, R., Jalan, R., Gines, P., Pavesi, M., Angeli, P., Cordoba, J., Durand, F., Gustot, T., Saliba, F., Domenicali, M.*, et al.* (2013). Acute-on-chronic liver failure is a distinct syndrome that develops in patients with acute decompensation of cirrhosis. Gastroenterology *144*, 1426-1437, 1437 e1421-1429.

Muller, M., Ishikawa, T., Berger, U., Klunemann, C., Lucka, L., Schreyer, A., Kannicht, C., Reutter, W., Kurz, G., and Keppler, D. (1991). ATP-dependent transport of taurocholate across the hepatocyte canalicular membrane mediated by a 110-kDa glycoprotein binding ATP and bile salt. The Journal of biological chemistry *266*, 18920-18926.

Myant, N.B., and Mitropoulos, K.A. (1977). Cholesterol 7 alpha-hydroxylase. Journal of lipid research *18*, 135-153.

Neimark, E., Chen, F., Li, X., and Shneider, B.L. (2004). Bile acid-induced negative feedback regulation of the human ileal bile acid transporter. Hepatology *40*, 149-156.

Nelson, J.D., Denisenko, O., and Bomsztyk, K. (2006). Protocol for the fast chromatin immunoprecipitation (ChIP) method. Nature protocols *1*, 179-185.

Nishida, T., Gatmaitan, Z., Che, M., and Arias, I.M. (1991). Rat liver canalicular membrane vesicles contain an ATP-dependent bile acid transport system. Proceedings of the National Academy of Sciences of the United States of America *88*, 6590-6594.

Noe, J., Hagenbuch, B., Meier, P.J., and St-Pierre, M.V. (2001). Characterization of the mouse bile salt export pump overexpressed in the baculovirus system. Hepatology *33*, 1223-1231.

Noe, J., Stieger, B., and Meier, P.J. (2002). Functional expression of the canalicular bile salt export pump of human liver. Gastroenterology *123*, 1659-1666.

O'Brien, R.M., Noisin, E.L., Suwanichkul, A., Yamasaki, T., Lucas, P.C., Wang, J.C., Powell, D.R., and Granner, D.K. (1995). Hepatic nuclear factor 3- and hormone-regulated expression of the phosphoenolpyruvate carboxykinase and insulin-like growth factor-binding protein 1 genes. Molecular and cellular biology *15*, 1747-1758.

Okin, D., and Medzhitov, R. (2012). Evolution of inflammatory diseases. Current biology : CB *22*, R733-740.

Okin, D., and Medzhitov, R. (2016). The Effect of Sustained Inflammation on Hepatic Mevalonate Pathway Results in Hyperglycemia. Cell *165*, 343-356.

Oswald, M., Kullak-Ublick, G.A., Paumgartner, G., and Beuers, U. (2001). Expression of hepatic transporters OATP-C and MRP2 in primary sclerosing cholangitis. Liver *21*, 247-253.

Oude Elferink, R.P., Ottenhoff, R., van Wijland, M., Smit, J.J., Schinkel, A.H., and Groen, A.K. (1995). Regulation of biliary lipid secretion by mdr2 P-glycoprotein in the mouse. The Journal of clinical investigation *95*, 31-38.

Pani, L., Overdier, D.G., Porcella, A., Qian, X., Lai, E., and Costa, R.H. (1992). Hepatocyte nuclear factor 3 beta contains two transcriptional activation domains, one of which is novel and conserved with the Drosophila fork head protein. Molecular and cellular biology *12*, 3723-3732.

Pauli-Magnus, C., Kerb, R., Fattinger, K., Lang, T., Anwald, B., Kullak-Ublick, G.A., Beuers, U., and Meier, P.J. (2004). BSEP and MDR3 haplotype structure in healthy Caucasians, primary biliary cirrhosis and primary sclerosing cholangitis. Hepatology *39*, 779-791.

Pauli-Magnus, C., Stieger, B., Meier, Y., Kullak-Ublick, G.A., and Meier, P.J. (2005). Enterohepatic transport of bile salts and genetics of cholestasis. Journal of hepatology *43*, 342-357.

Paulusma, C.C., Kool, M., Bosma, P.J., Scheffer, G.L., ter Borg, F., Scheper, R.J., Tytgat, G.N., Borst, P., Baas, F., and Oude Elferink, R.P. (1997). A mutation in the human canalicular multispecific organic anion transporter gene causes the Dubin-Johnson syndrome. Hepatology *25*, 1539-1542.

Paulusma, C.C., and Oude Elferink, R.P. (1997). The canalicular multispecific organic anion transporter and conjugated hyperbilirubinemia in rat and man. J Mol Med (Berl) *75*, 420-428.

Pikuleva, I.A., Babiker, A., Waterman, M.R., and Bjorkhem, I. (1998). Activities of recombinant human cytochrome P450c27 (CYP27) which produce intermediates of alternative bile acid biosynthetic pathways. The Journal of biological chemistry *273*, 18153-18160.

Ploton, M., Mazuy, C., Gheeraert, C., Dubois, V., Berthier, A., Dubois-Chevalier, J., Marechal, X., Bantubungi, K., Diemer, H., Cianferani, S.*, et al.* (2018). The nuclear bile acid receptor FXR is a PKA- and FOXA2-sensitive activator of fasting hepatic gluconeogenesis. Journal of hepatology *69*, 1099-1109.

Qian, X., and Costa, R.H. (1995). Analysis of hepatocyte nuclear factor-3 beta protein domains required for transcriptional activation and nuclear targeting. Nucleic acids research *23*, 1184-1191.

Rui, L. (2014). Energy metabolism in the liver. Comprehensive Physiology *4*, 177-197.

Russell, D.W., and Setchell, K.D. (1992). Bile acid biosynthesis. Biochemistry *31*, 4737-4749.

Sasaki, H., and Hogan, B.L. (1993). Differential expression of multiple fork head related genes during gastrulation and axial pattern formation in the mouse embryo. Development *118*, 47-59.

Scheimann, A.O., Strautnieks, S.S., Knisely, A.S., Byrne, J.A., Thompson, R.J., and Finegold, M.J. (2007). Mutations in bile salt export pump (ABCB11) in two children with progressive familial intrahepatic cholestasis and cholangiocarcinoma. The Journal of pediatrics *150*, 556-559.

Scholmerich, J., Becher, M.S., Schmidt, K., Schubert, R., Kremer, B., Feldhaus, S., and Gerok, W. (1984). Influence of hydroxylation and conjugation of bile salts on their membrane-damaging properties--studies on isolated hepatocytes and lipid membrane vesicles. Hepatology *4*, 661-666.

Shaham, O., Wei, R., Wang, T.J., Ricciardi, C., Lewis, G.D., Vasan, R.S., Carr, S.A., Thadhani, R., Gerszten, R.E., and Mootha, V.K. (2008). Metabolic profiling of the human response to a glucose challenge reveals distinct axes of insulin sensitivity. Molecular systems biology *4*, 214.

Shih, D.Q., Navas, M.A., Kuwajima, S., Duncan, S.A., and Stoffel, M. (1999). Impaired glucose homeostasis and neonatal mortality in hepatocyte nuclear factor 3alpha-deficient mice. Proceedings of the National Academy of Sciences of the United States of America *96*, 10152-10157.

Shneider, B.L., Dawson, P.A., Christie, D.M., Hardikar, W., Wong, M.H., and Suchy, F.J. (1995). Cloning and molecular characterization of the ontogeny of a rat ileal sodium-dependent bile acid transporter. The Journal of clinical investigation *95*, 745-754.

Shneider, B.L., Fox, V.L., Schwarz, K.B., Watson, C.L., Ananthanarayanan, M., Thevananther, S., Christie, D.M., Hardikar, W., Setchell, K.D., Mieli-Vergani, G.*, et al.* (1997). Hepatic basolateral sodium-dependent-bile acid transporter expression in two unusual cases of hypercholanemia and in extrahepatic biliary atresia. Hepatology *25*, 1176-1183.

Shoelson, S.E., Lee, J., and Goldfine, A.B. (2006). Inflammation and insulin resistance. The Journal of clinical investigation *116*, 1793-1801.

Simon, F.R., Fortune, J., Iwahashi, M., Gartung, C., Wolkoff, A., and Sutherland, E. (1996). Ethinyl estradiol cholestasis involves alterations in expression of liver sinusoidal transporters. The American journal of physiology *271*, G1043-1052.

Smit, J.J., Schinkel, A.H., Oude Elferink, R.P., Groen, A.K., Wagenaar, E., van Deemter, L., Mol, C.A., Ottenhoff, R., van der Lugt, N.M., van Roon, M.A.*, et al.* (1993). Homozygous disruption of the murine mdr2 P-glycoprotein gene leads to a complete absence of phospholipid from bile and to liver disease. Cell *75*, 451-462.

Smushkin, G., Sathananthan, M., Piccinini, F., Dalla Man, C., Law, J.H., Cobelli, C., Zinsmeister, A.R., Rizza, R.A., and Vella, A. (2013). The effect of a bile acid sequestrant on glucose metabolism in subjects with type 2 diabetes. Diabetes *62*, 1094-1101.

Song, X., Kaimal, R., Yan, B., and Deng, R. (2008). Liver receptor homolog 1 transcriptionally regulates human bile salt export pump expression. Journal of lipid research *49*, 973-984.

Soroka, C.J., and Boyer, J.L. (2014). Biosynthesis and trafficking of the bile salt export pump, BSEP: therapeutic implications of BSEP mutations. Molecular aspects of medicine *37*, 3-14.

Stayrook, K.R., Bramlett, K.S., Savkur, R.S., Ficorilli, J., Cook, T., Christe, M.E., Michael, L.F., and Burris, T.P. (2005). Regulation of carbohydrate metabolism by the farnesoid X receptor. Endocrinology *146*, 984-991.

Stieger, B. (2011). The role of the sodium-taurocholate cotransporting polypeptide (NTCP) and of the bile salt export pump (BSEP) in physiology and pathophysiology of bile formation. Handbook of experimental pharmacology, 205-259.

Stieger, B., Hagenbuch, B., Landmann, L., Hochli, M., Schroeder, A., and Meier, P.J. (1994). In situ localization of the hepatocytic Na+/Taurocholate cotransporting polypeptide in rat liver. Gastroenterology *107*, 1781-1787.

Stieger, B., O'Neill, B., and Meier, P.J. (1992). ATP-dependent bile-salt transport in canalicular rat liver plasma-membrane vesicles. The Biochemical journal *284 (Pt 1)*, 67-74.

Strautnieks, S.S., Byrne, J.A., Pawlikowska, L., Cebecauerova, D., Rayner, A., Dutton, L., Meier, Y., Antoniou, A., Stieger, B., Arnell, H.*, et al.* (2008). Severe bile salt export

pump deficiency: 82 different ABCB11 mutations in 109 families. Gastroenterology *134*, 1203-1214.

Strautnieks, S.S., Kagalwalla, A.F., Tanner, M.S., Knisely, A.S., Bull, L., Freimer, N., Kocoshis, S.A., Gardiner, R.M., and Thompson, R.J. (1997). Identification of a locus for progressive familial intrahepatic cholestasis PFIC2 on chromosome 2q24. American journal of human genetics *61*, 630-633.

Sund, N.J., Ang, S.L., Sackett, S.D., Shen, W., Daigle, N., Magnuson, M.A., and Kaestner, K.H. (2000). Hepatocyte nuclear factor 3beta (Foxa2) is dispensable for maintaining the differentiated state of the adult hepatocyte. Molecular and cellular biology *20*, 5175-5183.

Takeuchi, O., and Akira, S. (2010). Pattern recognition receptors and inflammation. Cell *140*, 805-820.

Tirona, R.G., and Kim, R.B. (2002). Pharmacogenomics of organic anion-transporting polypeptides (OATP). Advanced drug delivery reviews *54*, 1343-1352.

Trauner, M., and Boyer, J.L. (2003). Bile salt transporters: molecular characterization, function, and regulation. Physiological reviews *83*, 633-671.

Van Wyngene, L., Vandewalle, J., and Libert, C. (2018). Reprogramming of basic metabolic pathways in microbial sepsis: therapeutic targets at last? EMBO molecular medicine *10*.

Vanwijngaerden, Y.M., Wauters, J., Langouche, L., Vander Perre, S., Liddle, C., Coulter, S., Vanderborght, S., Roskams, T., Wilmer, A., Van den Berghe, G.*, et al.* (2011). Critical illness evokes elevated circulating bile acids related to altered hepatic transporter and nuclear receptor expression. Hepatology *54*, 1741-1752.

Venteclef, N., Jakobsson, T., Steffensen, K.R., and Treuter, E. (2011). Metabolic nuclear receptor signaling and the inflammatory acute phase response. Trends in endocrinology and metabolism: TEM *22*, 333-343.

Vlahcevic, Z.R., Pandak, W.M., Heuman, D.M., and Hylemon, P.B. (1992). Function and regulation of hydroxylases involved in the bile acid biosynthesis pathways. Seminars in liver disease *12*, 403-419.

von Meyenn, F., Porstmann, T., Gasser, E., Selevsek, N., Schmidt, A., Aebersold, R., and Stoffel, M. (2013). Glucagon-induced acetylation of Foxa2 regulates hepatic lipid metabolism. Cell metabolism *17*, 436-447.

Wagner, M., Fickert, P., Zollner, G., Fuchsbichler, A., Silbert, D., Tsybrovskyy, O., Zatloukal, K., Guo, G.L., Schuetz, J.D., Gonzalez, F.J.*, et al.* (2003). Role of farnesoid

X receptor in determining hepatic ABC transporter expression and liver injury in bile duct-ligated mice. Gastroenterology *125*, 825-838.

Wagner, M., Zollner, G., and Trauner, M. (2011). Nuclear receptors in liver disease. Hepatology *53*, 1023-1034.

Wakabayashi, Y., Dutt, P., Lippincott-Schwartz, J., and Arias, I.M. (2005). Rab11a and myosin Vb are required for bile canalicular formation in WIF-B9 cells. Proceedings of the National Academy of Sciences of the United States of America *102*, 15087-15092.

Wakabayashi, Y., Lippincott-Schwartz, J., and Arias, I.M. (2004). Intracellular trafficking of bile salt export pump (ABCB11) in polarized hepatic cells: constitutive cycling between the canalicular membrane and rab11-positive endosomes. Molecular biology of the cell *15*, 3485-3496.

Wan, P., Xu, D., Zhang, J., Li, Q., Zhang, M., Chen, X., Luo, Y., Shen, C., Han, L., and Xia, Q. (2016). Liver transplantation for biliary atresia: A nationwide investigation from 1996 to 2013 in mainland China. Pediatr Transplant *20*, 1051-1059.

Wang, H., Chen, J., Hollister, K., Sowers, L.C., and Forman, B.M. (1999). Endogenous bile acids are ligands for the nuclear receptor FXR/BAR. Molecular cell *3*, 543-553.

Wang, L., Dong, H., Soroka, C.J., Wei, N., Boyer, J.L., and Hochstrasser, M. (2008a). Degradation of the bile salt export pump at endoplasmic reticulum in progressive familial intrahepatic cholestasis type II. Hepatology *48*, 1558-1569.

Wang, L., Lee, Y.K., Bundman, D., Han, Y., Thevananther, S., Kim, C.S., Chua, S.S., Wei, P., Heyman, R.A., Karin, M.*, et al.* (2002). Redundant pathways for negative feedback regulation of bile acid production. Developmental cell *2*, 721-731.

Wang, Y.D., Chen, W.D., Wang, M., Yu, D., Forman, B.M., and Huang, W. (2008b). Farnesoid X receptor antagonizes nuclear factor kappaB in hepatic inflammatory response. Hepatology *48*, 1632-1643.

Weigel, D., and Jackle, H. (1990). The fork head domain: a novel DNA binding motif of eukaryotic transcription factors? Cell *63*, 455-456.

Weigel, D., Jurgens, G., Kuttner, F., Seifert, E., and Jackle, H. (1989). The homeotic gene fork head encodes a nuclear protein and is expressed in the terminal regions of the Drosophila embryo. Cell *57*, 645-658.

Wolfrum, C., Asilmaz, E., Luca, E., Friedman, J.M., and Stoffel, M. (2004). Foxa2 regulates lipid metabolism and ketogenesis in the liver during fasting and in diabetes. Nature *432*, 1027-1032.

Wolfrum, C., Besser, D., Luca, E., and Stoffel, M. (2003). Insulin regulates the activity of forkhead transcription factor Hnf-3beta/Foxa-2 by Akt-mediated phosphorylation and nuclear/cytosolic localization. Proceedings of the National Academy of Sciences of the United States of America *100*, 11624-11629.

Wong, M.H., Oelkers, P., Craddock, A.L., and Dawson, P.A. (1994). Expression cloning and characterization of the hamster ileal sodium-dependent bile acid transporter. The Journal of biological chemistry *269*, 1340-1347.

Woznica, E.A., Inglot, M., Woznica, R.K., and Lysenko, L. (2018). Liver dysfunction in sepsis. Advances in clinical and experimental medicine : official organ Wroclaw Medical University *27*, 547-551.

Xie, C., Jiang, C., Shi, J., Gao, X., Sun, D., Sun, L., Wang, T., Takahashi, S., Anitha, M., Krausz, K.W*., et al.* (2017). An Intestinal Farnesoid X Receptor-Ceramide Signaling Axis Modulates Hepatic Gluconeogenesis in Mice. Diabetes *66*, 613-626.

Yamagata, K., Daitoku, H., Shimamoto, Y., Matsuzaki, H., Hirota, K., Ishida, J., and Fukamizu, A. (2004). Bile acids regulate gluconeogenic gene expression via small heterodimer partner-mediated repression of hepatocyte nuclear factor 4 and Foxo1. The Journal of biological chemistry *279*, 23158-23165.

Zhang, Y., Lee, F.Y., Barrera, G., Lee, H., Vales, C., Gonzalez, F.J., Willson, T.M., and Edwards, P.A. (2006). Activation of the nuclear receptor FXR improves hyperglycemia and hyperlipidemia in diabetic mice. Proceedings of the National Academy of Sciences of the United States of America *103*, 1006-1011.

Zimmerman, T.L., Thevananther, S., Ghose, R., Burns, A.R., and Karpen, S.J. (2006). Nuclear export of retinoid X receptor alpha in response to interleukin-1beta-mediated cell signaling: roles for JNK and SER260. The Journal of biological chemistry *281*, 15434-15440.

Zollner, G., Fickert, P., Zenz, R., Fuchsbichler, A., Stumptner, C., Kenner, L., Ferenci, P., Stauber, R.E., Krejs, G.J., Denk, H*., et al.* (2001). Hepatobiliary transporter expression in percutaneous liver biopsies of patients with cholestatic liver diseases. Hepatology *33*, 633-646.

7. LIST OF FIGURES AND TABLES

7.1 List of figures

Figure 1. Classic and alternative pathways of bile acids synthesis.
Figure 2. The hepatocytes tight junction complex.
Figure 3. Membrane transporters in hepatocytes.
Figure 4. Enterohepatic circulation of the bile acids.
Figure 5. FXR regulates the expression of kye genes involved in bile acid synthesis, conjugation and transport in hepatocyte.
Figure 6. Structure of the forkhead domain.
Figure 7. Immunohistochemistry staining depicts expression of FXR and BSEP in HBV infection patients.
Figure 8. Fxr agonist GW4064 promotes Bsep expression on bile canaliculi.
Figure 9. Fxr impacts Bsep expression in hepatocytes.
Figure 10. Immunohistochemistry staining depicts expression of BSEP in HBV infection and ACLF.
Figure 11. Immunohistochemistry staining depicts expression of FXR, FOXA2 and BSEP in HBV infection and ACLF
Figure 12. Overexpression of FOXA2 promotes BSEP expression in hepatocytes.
Figure 13. Knockdown of FOXA2 impacts BSEP expression in hepatocytes.
Figure 14. Ectopic Foxa2 expression restores Bsep expression in hepatocytes with Fxr knockdown.
Figure 15. Ectopic Foxa2 expression restores Bsep expression in AML12 cells with Fxr knockdown.
Figure 16. Bsep expression is significantly decreased in *fxr*-/- mice.
Figure 17. Ectopic Foxa2 expression restores apical Bsep expression in hepatocytes isolated from *fxr* knockout mice.
Figure 18. Ectopic Foxa2 expression restores apical Bsep expression in *fxr* knockout mice.
Figure 19. Foxa2 binds to the *bsep* gene promoter, which is impacted by Fxr.
Figure 20. Glucagon induces BSEP expression through upregulating FOXA2.
Figure 21. Glucagon induces Bsep expression through upresulating Foxa2 in AML-12 cells.
Figure 22. Insulin inhibits Foxa2 activation.

Figure 23. Glucagon restores insulin-mediated inhibition to Foxa2 and Bsep.
Figure 24. TNFα and LPS induce Foxa2-dependent Bsep expression.
Figure 25. TNFα induces insulin resistance in MPHs and HPHs.
Figure 26. LPS induces Foxa2-dependent Bsep expression through NFκB signaling.
Figure 27. High concentration of LPS induces Foxa2 nuclear exclusion in MPHs.
Figure 28. The scheme depicts two regulatory mechanisms maintaining Bsep expression on bile canaliculi in healthy and ACLF conditions.

7.2 List of tables

Table 1. List of selected membrane proteins targeted to either the canalicular or sinusoidal membrane of hepatocytes.
Table 2. Chemicals and reagents.
Table 3.Primary antibodies used for immunobloting.
Table 4. Primary antibodies used for immunohistochemistry.
Table 5. Primary antibodies used for immunofluorescence.
Tbale 6. Primary antibodies used for ChIP.
Table 7. Second antibodies.
Table 8. Buffers
Tbale 9. Cell culture materials.
Table 10. Instruments and software.
Table 11. Cells and cell culture medium.
Table 12. Primers used for qRT-PCR in this study.

8. CURRICULUM VITAE

Personal information

Name:	Sai Wang
Date of birth:	Aug. 5th, 1990
Nationality:	Chinese
Marital state:	Married
Email:	saiwang0616@outlook.com
Address:	C7-14, 68159, Mannheim

Education

Aug.2017 – present	Ph.D. student (Dr.sc.hum.) Ruprecht-Karls-University Heidelberg
Ph.D. project:	FXR and FOXA2 govern two complementary regulatory mechanisms to guarantee apical BSEP expression in hepatocytes
Sep. 2013 – Jul. 2017	Master of Biochemistry and Molecular Biology University of Chinese Academy of Sciences
Master project:	The role of samll ATPase Cdc42 in regulating bile canalicular network formation
Sep. 2009 – Jul. 2013	Bachelor of Biological Science and Biotechnology Shandong Normal University

Scholarship

Ph.D. scholarship from China Scholarship Council

Publications

Mei Han, Weronika Pioronska, **Sai Wang**, et al. Hepatocyte Caveolin - 1 Modulates Metabolic Gene Profiles and Functions in Non- Alcoholic Fatty Liver Disease. *Cell Death & Disease.*

Sai Wang, Rilu Feng, Shanshan Wang, et al. FXR and FOXA2 govern two complementary regulatory mechanisms to guarantee apical BSEP expression in hepatocytes. (In preparation for submission.)

Conference presentations and posters

2018 DGVS Oral presentation:
Polarity of liver progenitor cell-derived hepatocytes determines the clinical outcome in acute-on-chronic liver failure. Sai Wang et al.

2018 ESBRA Nordmann Award Meeting Oral presentation
Regeneration in severe Alcoholic Hepatitis patients with acute-on-chronic liver failure (ACLF)-Focused on LPC-derived-hepatocyte Polarity. Sai Wang et al.
(Won the 2018 ESBRA-Nordmann Award)

2019 GASL Poster presentation
Maintenance of functional hepatocellular polarity determines recovery in acute-on-chronic liver failure. Sai Wang et al.

2020 GASL Poster presentation
FOXA2 takes over bile salt export pump expression when farnesoid X receptor is disrupted. Sai Wang et al.

9. ACKNOWLEDGEMENT

Upon the completion of this thesis, I am grateful to those who have offered meencouragement and support during my PhD study.

Firstly, special acknowledgment is given to my respectable mentor Prof. Steven Dooley, whose patient instruction and constructive suggestions are beneficial to me a lot. I am grateful that he provides me with the opportunity of my scientific research in liver disease.

Second, I would like to express my particular heartfelt gratitude to my superviser Dr. Honglei Weng. He gives me generous support, encouragement and invaluable comments during my PhD study, which is really benifical for my career. He has given me great instructions and encouragements throughout the process of selecting the research topic, doing the research, writing the thesis, and helps me a lot in correcting the thesis. The thesis would not be finished without his patient guidance.

Then I want to say thanks to Dr. Roman Müllenbach, who helps me a lot in modification English for this thesis. Many thanks to Dr. Shanshan Wang and Prof. Huiguo Ding for providing us liver tissue and clinical data of patients. Many thanks to Dr.med. Stefan Munker for providing us human primary hepatocytes.

Many thanks to all the members of the Prof. Dooly's lab, Christoph Meyer, Shanshan Wang, Rilu Feng, Mei Han, Weronika Pioronska, Yujia Li, Kerry Gould, Vanessa Nalewaja, Xiaodong Yuan, Tao Lin, Anne Dropmann, Seddik Hammad, Samil Ayvaz and Sophie Alex. I appreciated for the help they provide to me.

Especially, I am grateful the Chinese Scholarship Council for financial support during my PhD study in Germany.

Finally, I would like to extend my deep gratefulness to my parents, my brother, my husband and my friends, for supporting me and sharing with me my worries, frustrations, and happiness.